THE POTENTIAL OF CRISPR/CAS9 TO GENERATE SPAG5 KNOCKOUT BREAST CANCER CELL LINES

Emma Duffy

A thesis submitted to
Auckland University of Technology
in partial fulfilment of the requirements for the degree of
Master of Science (MSc)

2023
Auckland University of Technology

Abstract

Breast cancer is one of the leading causes of death in women worldwide. In Aotearoa alone, more than 600 wāhine will lose their lives to breast cancer annually, despite receiving professional treatment. Breast cancer is primarily treated with chemotherapy, often in conjunction with radiation and/or surgery. While these treatments are often effective, recurrence rates remain significant, and the adverse effects experienced while undergoing treatment hugely impact patient quality of life. This is in large part due to the non-specific nature of the currently available chemotherapy drugs. Chemotherapy drugs target cancer cells efficiently, however healthy proliferating cells are also impacted. As breast cancer is a heterogeneous disease, multiple targeted treatments are necessary to address the need for increased specificity and efficacy of available treatments. It is essential that novel targets are identified to function as biomarkers and therapeutic targets that do not adversely affect healthy cells in patients with breast cancer. SPAG5 is a novel biomarker for predicting patients' chemotherapy drug response. SPAG5 is a mitotic-associated protein responsible for regulating and stabilising chromatid segregation and is often upregulated in cancer. Furthermore, SPAG5 interactions with essential cancer-associated mitotic proteins such as p53 suggest SPAG5 is a promising potential therapeutic target.

The aim of this project is to determine whether novel CRISPR/Cas9 technology may be utilised to produce SPAG5 knockout clones in cancer cell lines. By producing such cell lines, the hope is to provide further opportunities for the development of novel therapeutics in the treatment of breast and other cancers by targeting SPAG5. Triple-negative breast carcinomas have high mitotic activity, poor spindle formation and high levels of unregulated proliferative growth, all characteristics that have been linked to SPAG5 function.

CRISPR/Cas9 is rapidly becoming the most prominently utilised approach for editing cell lines. The rapid and specific nature of the technology provides an accurate and efficient approach to gene editing not previously possible. In this project, CRISPR/Cas9 technology will be utilised to create SPAG5 knockout triple-negative breast cancer cell lines MCF-7 and BT549. To determine the successful generation of SPAG5 knockout BT549 and MCF-7 cell lines, the goal of this thesis was to perform PCR, western blotting and DNA sequencing and analyse the results. Due to COVID-19 lockdowns, and extended COVID-related illness, all these confirmation techniques were performed except a second Western Blotting to confirm the disruption of SPAG5. Nonetheless, the results indicate two SPAG5-knockout cell lines were achieved within triple-negative breast cancer cell lines. The development of such lines provides opportunities for further research to determine more targeted breast cancer treatments, utilising SPAG5 as both a therapeutic target and as a biomarker for individualised treatments.

Attestation of Authorship

I hereby declare that this submission is my own work and that, to the best of my knowledge and belief, it contains no material previously published or written by another person (except where explicitly defined in the acknowledgements), nor material which to a substantial extent has been submitted for the award of any other degree or diploma of a university or other institution of higher learning.

Signed

Name Emma Duffy

Date 29 August 2023

Acknowledgments

This thesis is the result of the contribution of several individuals to whom I owe my sincerest thanks. Without the support of whom, this would not have been possible. Firstly, to my supervisor, Dr Dong-Xu Liu, I cannot thank you enough for your invaluable teaching, guidance, feedback, and time. Your input has been invaluable. I feel incredibly fortunate to have such an invested and encouraging supervisor who has guided me and shaped me into the scientist I am today. I cannot thank you enough for your support. It is a true privilege to be your student. To Dr Yan Li, thank you for your guidance, openness, and availability; I am grateful for all your advice and input. Thank you.

To Leo He and Stacey Li, thank you for assisting, teaching and guiding me in the lab. It has been a pleasure to learn from someone as dedicated to accuracy as you both have been. Thank you for your patience, willingness to answer (and re-answer) all my questions, and for supporting me throughout my research. All the hours spent in the lab wouldn't have been the same without you.

To my friends and family, thank you for your endless support, encouragement, and belief in me. Thank you for being so patient with my lack of availability over this time; your continued love means the world. To my mum, thank you for teaching me that I can do anything, no matter how hard. I did it! Thank you to Julia for constantly checking in and offering your continual love and support. Finally, to the love of my life, Cameron. Thank you for always encouraging me and for pushing me to always put my best work forward. Thank you for listening to me ramble about the cool new things I have learned and for always pumping up my hopes for future research achievements in breast cancer. With you by my side, I can be my best self and create my best work. Thank you for your endless grace and support. I am so proud to be yours. I love you.

Contents

List of Figures

List of Tables

List of Abbreviations

AKT – Protein Kinase B (PKB)

BAX – Bcl-2-Associated X Protein

bp – Base Pair(s)

BT549-12A – BT549 Clone 12, Allele "A"

BT549-12B – BT549 Clone 12, Allele "B"

BT549-14A – BT549 Clone 14, Allele "A"

BT549-14B – BT549 Clone 14, Allele "B"

BUC – Bladder Urothelial Cancer

CDK1 – Cyclin Dependent Kinase 1

CDK2 – Cyclin Dependent Kinase 2

CDK5 – Cyclin Dependent Kinase 5

CDK5RAP2 – Cyclin Dependent Kinase 5 Regulatory Subunit-Associated Protein 2

cDNA – Complementary Deoxyribonucleic Acid

CEP – Centrosomal Protein

CEP55 – Centrosome Protein 55

CLASP1 – Cytoplasmic Linker-Associated Protein

CRISPR – Clustered Regularly Interspaced Palindromic Sequences

ddNTP – Dideoxy Nucleotide Triphosphates

DFS – Disease-Free Survival

DMSO – Dimethyl Sulfoxide

DNA – Deoxyribonucleic Acid

ECM – Extracellular Matrix

EGFR – Epidermal Growth Factor Receptor

EMT – Epithelial-Mesenchymal Transition

ERE – Oestrogen Response Element

FIP200 – Focal Adhesion Kinase Interacting Protein of 200kDa

FOXM1 – Foxhead Box M1

G_0 – Resting Phase / Gap Phase 0

G_1 – Gap Phase 1

G_2 – Gap Phase 2

gRNA – Guide RNA

HER2 – Human Epidermal Growth Factor Receptor 2

HIF-1α – Hypoxia-Inducible Factor 1α

ICBMT – Intercellular Bridge Microtubule

KIF2B – Kinesin Family Member 2B

M – Mitosis Phase

MCPH – Primary Microcephaly

MID2 – Midline-2

MMP2 – Matrix Metalloproteinase-2

mRNA – Messenger Ribonucleic Acid

miRNA – Micro Ribonucleic Acid

mTOR – Mammalian Target of Rapamycin

mTORC1 – Mammalian Target of Rapamycin Complex 1

MYCBP – c-MYC Binding Protein

nt – Nucleotide(s)

OS – Overall Survival

PARP – Poly-ADP Ribose Polymerase

PCM1 – Pericentriolar Material 1

PCR – Polymerase Chain Reaction

PI3K – Phosphoinositide 3-Kinase

PLK1 – Polo-like Kinase 1

PP1 – Phosphatase 1

RNA – Ribonucleic Acid

RB – Retinoblastoma

S – Synthesis Phase

SCARA5 – Scavenger Receptor Class A Member 5

SKAP – Src Kinase-Associated Phosphoprotein

SPAG5 – Sperm-Associated Antigen 5

TCF – T Cell Factor

TSC1 – Tuberous Sclerosis Protein 1

TSC2 – Tuberous Sclerosis Protein 2

TP53 – Tumour Protein 53

ULK1 – Unc-51-Like Kinase 1

VEGF – Vascular Endothelial Growth Factor

Chapter 1: Introduction to Cancer

1.1 Cancer Biology

The human body is a complex network of cells, all maintaining functional roles within the healthy adult body to maintain structure, absorb and convert nutrients into energy, and perform many specialised functions to sustain life. Cell division is a process that allows a single cell to become two during the growth phase, whereas cell differentiation is an essential mitogenic process utilised to maintain tissues and organs, that require consistent cell turnover. Cells that can divide and differentiate for replenishment in such a manner are called stem cells. They are unspecialised cells but may differentiate into any cell of an organ in the human body, and have the ability of self-renewal (Zakrzewski et al., 2019). This is maintained in an equilibrium. Old or damaged cells are replaced by new and healthy cells, which are able to continue the integral functions required by the organ for optimal performance. Several molecular mechanistic networks maintain this intricate equilibrium between cell growth and death. Therefore, disruptions and changes to this equilibrium may result in an unhealthy number of cells in any one area of the body, sometimes resulting in tumour formation (Mitra et al., 2012; Zakrzewski et al., 2019).

1.1.1 Hallmarks of Cancer

Oncogenic properties may also be referred to as the hallmarks of cancer. Hanahan and Weinberg (2000) proposed six capabilities obtained during human cell carcinogenesis (Figure 1.1). They suggest that most cancers acquire the same functional capabilities throughout carcinogenesis, despite various mechanistic strategies. These six biological capabilities are proliferative signalling, evading growth suppressors, resisting cell death, enabling replicative immortality, inducing angiogenesis, and activating invasion and metastasis. (Hanahan & Weinberg, 2011) proposed a further two hallmarks, deregulating cellular energetics and avoiding immune destruction and tumour-promoting inflammation.

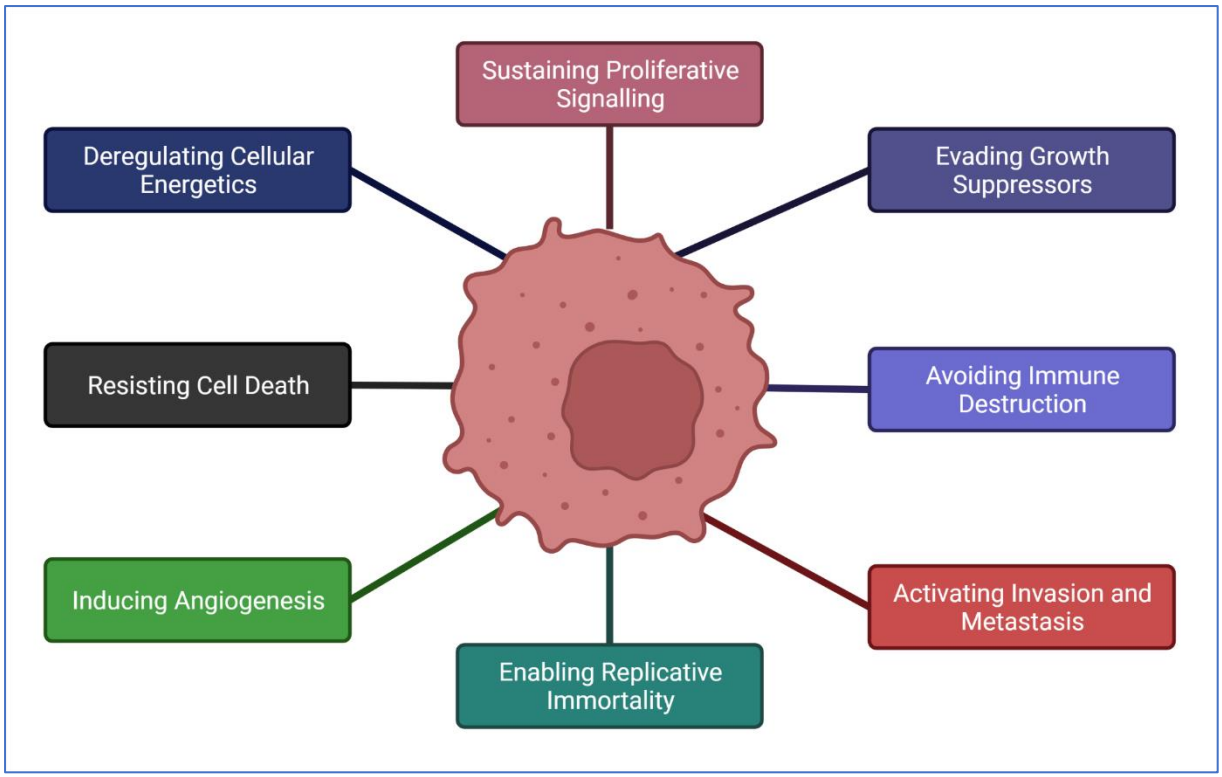

Figure 1.1: The Hallmarks of Cancer. Eight common characteristics of cancer are depicted. They include the six biological capabilities originally summarised by Hanahan & Weinberg in 2000, as well as the two proposed later by them in 2011, which are deregulating cellular energetics, and evading growth suppressors. [Adapted from Hanahan and Weinberg (2011)]

1.1.1.1 Sustaining Proliferative Signalling

This hallmark is debatably the most basal characteristic of cancer cells (Hanahan & Weinberg, 2011). The timing and rate of cell division are integral for normal growth and development. Healthy tissues meticulously regulate the production and release of growth factors. Growth factors are ligands produced by surrounding tissues, which signal cell proliferation, differentiation and regeneration

(Aaronson, 1991). Growth factors bind to specific receptors on the cell membrane, signalling the activation of various subsets of genes responsible for cell growth and proliferation (M. Zhang et al., 2021). Progression through the cell cycle requires specific cooperation between two complementary growth factor classes: CDKs and cyclins. Such regulation ensures the homeostasis of cell numbers and maintains effective tissue structure and function (M. Zhang et al., 2021).

By contrast, cancer cells can proliferate at a sustained and unregulated rate. The deregulation of growth factor signalling allows for growth-factor-independent proliferation. This may occur in several ways: cancer cells may signal stimulation of normal cells within the supporting tumour-associated stroma, providing diverse growth factors to the cancer cells (Bhowmick et al., 2004). Alternatively, cancer cells may employ the production of growth factor ligands independently, which cancer cells may then respond to via the expression of cognate receptors, resulting in autocrine proliferative stimulation (Cheng et al., 2008). Furthermore, cancer cells can increase growth factor receptor prevalence on the cell surface, inducing a hyperreactive response from otherwise limiting growth factor availability (Park & Nam, 2020). Cells may also elicit this response via structural alterations in the receptors, which facilitate ligand-independent firing. Furthermore, these processes may be bypassed altogether. A cancer cell may become independent of growth factors via the constitutive activation of downstream signalling pathway components. However, given the number of pathways directly activated by a ligand-mediated receptor, this method is less effective because only one or a subset of the pathways may be activated (Hanahan & Weinberg, 2011).

Homeostatic cell maintenance is achieved via negative feedback mechanisms that prevent proliferative signalling in the cell. Proliferative signalling can therefore be enhanced by impairment of these mechanisms (Hanahan & Weinberg, 2011). An example of this occurrence involves the mammalian target of rapamycin (mTOR) kinase, an essential regulatory kinase responsible for healthy cell growth and metabolism. mTOR kinase is located both upstream and downstream of the phosphoinositide 3-kinase (PI3K) pathway, which is responsible for cell growth, proliferation, and inhibition of apoptosis (O'Reilly et al., 2006). In some cancer cells, mTOR activation inhibits PI3K signalling via negative feedback. Therefore, when mTOR is inhibited by pharmaceuticals such as rapamycin, the loss of feedback increases PI3K activity, effectively counteracting the antiproliferative effects of mTOR inhibition (O'Reilly et al., 2006; Sudarsanam & Johnson, 2010). Furthermore, disruption of self-proliferative signalling can result in unintended adaptive drug-resistance toward mitotic-signalling targeted drugs, as has been observed in the mTOR/PI3K feedback loop when treated with rapamycin (Rozengurt et al., 2014). Compromised negative feedback loops in mitotic signalling pathways likely serve as an important mechanism by which cancer cells develop independent proliferative function.

1.1.1.2 Evading Growth Suppressors

To maintain active proliferation, cancer cells need not only to induce and sustain positively enforcing proliferation signals, but also evade cellular programmes that negatively regulate cell proliferation. In normal tissue, soluble growth inhibitors send anti-proliferative signals, which function to maintain tissue homeostasis (Hanahan & Weinberg, 2011). To allow for homeostasis, growth inhibitors function similar to, but as an inverse relationship with growth factors. Growth inhibitors activate receptors on the cell surface, signalling several intracellular molecular pathways to prevent proliferation (Hanahan & Weinberg, 2011).

Anti-proliferative signals are imperative for successful cell division (Hanahan & Weinberg, 2011). The cell cycle is composed of four stages: Gap 1 (G_1), synthesis (S), gap 2 (G_2), and mitosis (M). DNA replication and synthesis occurs during the S phase, prior to segregation by mitotic spindles and cell division in the M phase. During phase G_1 the cell grows in size, and cell cycle control genes are transcribed. Phase G_2 represents the necessary time for the cell to grow and engage proof-reading mechanisms in preparation for division (Tan et al., 2017). Anti-proliferative signals utilise two distinct mechanisms to prevent cell division. The dividing cell may be placed into cell cycle arrest, halting proliferation and entering into the resting phase, G_0. Alternatively, the cell enters a post-mitotic state, and is perpetually unable to proliferate (Hanahan & Weinberg, 2011).

The majority of such negatively acting cell proliferation programmes rely on tumour suppressor genes, which function in diverse manners to restrict cell growth and proliferation. Such tumour suppressor genes regularly encode TP53 and retinoblastoma (RB) associated proteins, serving as critical coordinators within complementary regulatory systems denoting the proliferation or apoptosis of cells (Hanahan & Weinberg, 2011).

1.1.1.3 Avoiding Immune Destruction

A newer addition to the originally proposed six hallmarks of cancer involves the immune system's role in preventing, and eradicating micro-metastases, late-stage tumours and neoplasms (Hanahan & Weinberg, 2011). This emergent hallmark is based on the time-honoured theory of immune surveillance. This process ensures cells are under constant supervision by the immune system. It is responsible for detecting and eradicating developing cancer cells and thus emerging tumours. Therefore, developed tumours that have managed to avoid detection by the immune system's various protective mechanisms have minimised immunological cell destruction, thereby evading total eradication (Hanahan & Weinberg, 2011).

Hanahan and Weinberg (2011) proposed that this new hallmark is supported by the significant increase in specific cancer incidences in immunocompromised individuals (Vajdic & van Leeuwen,

2009). This proposal has since been endorsed by various more recent studies (Reusser et al., 2015; Schoemmel et al., 2021). Critical analysis of such studies suggests this hallmark is most evident in virus-induced cancer development, indicating such prevention of cancer development may be primarily dependent upon the immune system's role in reducing the viral impact on virus-infected individuals; in part, this responsibility is achieved via the elimination of virus-infected cells. Therefore, these observations do not seem to explain the immune system's role in the >80% of tumours of non-viral emergence. A systematic analysis of cancer in primary immunodeficiency diseases found an increased cancer incidence in primary immunodeficiency diseases in some but not all tumours of non-viral aetiology (Mayor et al., 2018). Notably, there was no increased incidence in the most common solid tumour malignancies seen in the US population (Cilibrasi et al., 2021). This supports the proposal for a restricted role of immunosurveillance in some cancers while being less important for others. To date, ample preclinical and clinical evidence supports that breast cancer is under immunosurveillance (Cilibrasi et al., 2021; Kroemer et al., 2015).

1.1.1.4 Activating Invasion and Metastasis

Avoiding immune destruction is not limited only to within the original cancer site. The capacity of a cancer cell to avoid immune destruction is also a requirement when cancer cells metastasise (Hanahan & Weinberg, 2011). Metastasis is the spread of cancer cells from the original tumour (primary site) to surrounding tissues and distal organs. It is the principal cause of mortality in cancer (Guan, 2015). Metastasis is a multi-step process, which can be divided into five critical steps: 1) invasion and migration, 2) intravasation, 3) survival in circulation, 4) extravasation, and 5) colonisation (Figure 1.2). These processes collectively form the metastatic cascade. Each stage poses harsh environmental and energetically taxing conditions that the cancer cells must endure to achieve metastasis. As the cascade progresses, the number of cells that survive and complete each stage decreases significantly (Hapach et al., 2019).

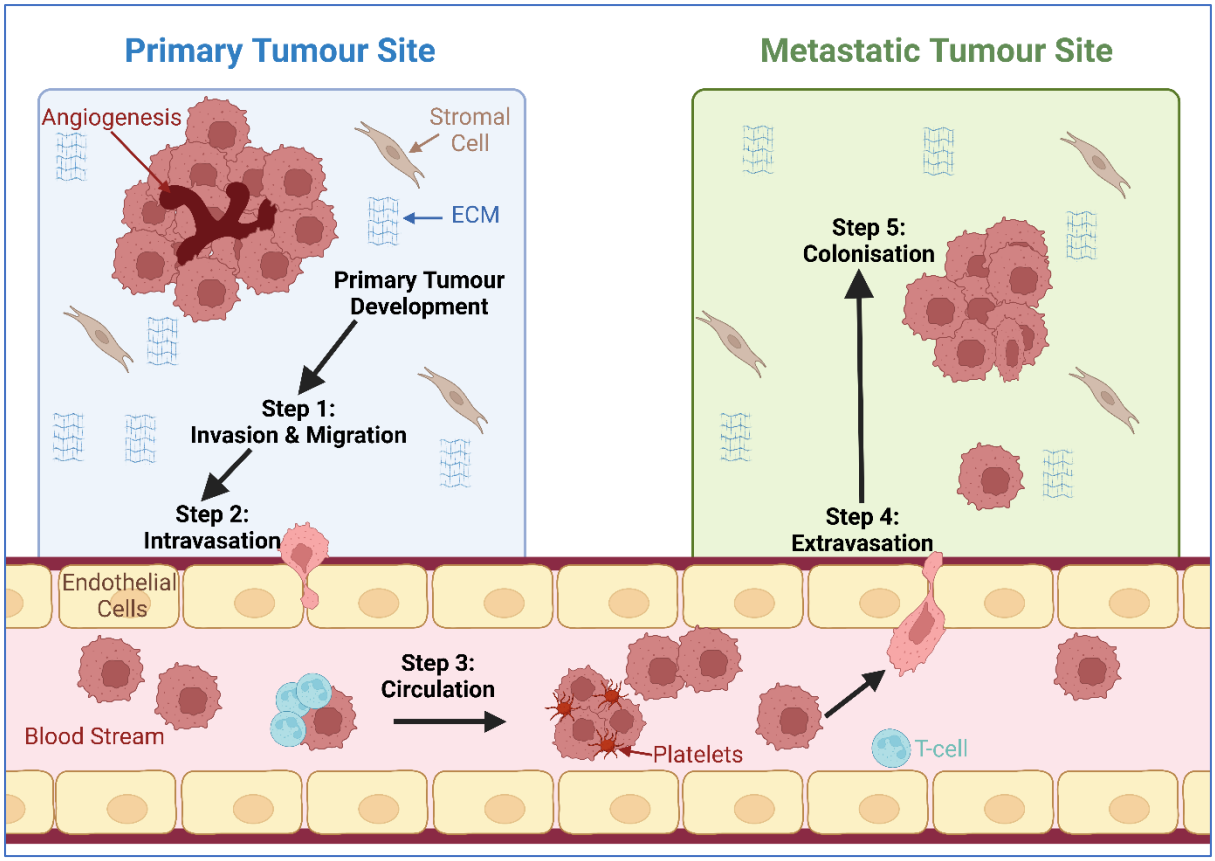

Figure 1.2: Overview of the Metastatic Cascade. Step 1: Cancer cells invade through the basement membrane and migrate through the tumour stroma; Step 2: Intravasation into the bloodstream through the endothelial barrier; Step 3: Survival in circulation. The circulation of tumour cells in the bloodstream places the cells under stress and requires the cells to avoid detection by the immune system before reaching different organs; Step 4: Extravasation from the bloodstream, into the secondary site, through the endothelial barrier. Step 5: Colonization of the tumour cells inside the metastatic target organ. (Adapted from Hapach et al. (2019)). *Created with BioRender.com*)

Invasion and migration are the initial steps of metastasis. Tumour cells must invade the direct surrounding tissue. To achieve invasion, tumour cells must alter the proteins which form cell-to-cell and cell-to-extracellular matrix (ECM) adhesion. During invasion, tumour cells must undergo epithelial-mesenchymal transitions (EMT). EMT may be characterised by the loss of epithelial traits, including cell polarity and cell-to-cell junctions (such features support the cell-to-cell adhesion), and instead acquire mesenchymal traits, such as spindle-shaped morphology to increase the mobility of the tumour cells. EMT has also been identified as the linking mechanism between metastasis and stem cell properties (Hass et al., 2019).

The loss of epithelial traits supporting the cell-to-cell adhesion required for EMT and, therefore, migration of the tumour cells is primarily monitored by the cadherin protein family. E-cadherin maintains the cell-to-cell adhesion complexes and is abundant in epithelial tissues. E-

cadherin's absence or downregulation is often observed in cancers (Petrova et al., 2016). In breast cancers, decreased E-cadherin is critical for metastatic growth (Padmanaban et al., 2019) due to its crucial role in maintaining cell-to-cell adhesions which prevent the tumour cell movement.

Integrins are cell adhesion receptors that bind to extracellular ligands and transmit signals upon cell adhesion to inside the cell. Exosomal integrins promote growth in metastatic cells. Increased expression of specific integrins increases metastasis in many cancers. Of interest, integrin-binding proteins actively increase invasion and metastasis in breast cancer (Yousefi et al., 2021). Assisted by integrin-mediated adhesion, the permeable intra-tumoral blood vessels allow the ready transfer of the cells from the ECM into the circulatory system.

Once the tumour cells have successfully absconded into the circulatory system, a biological "hide-and-seek" occurs between the tumour cells seeking to find a new organ, and the body's natural defence mechanisms, seeking to prevent further harm from the escaped tumour cells. While under stress in a new macroenvironment, the tumour cells must successfully evade the host's immune surveillance and destructive systems to survive and settle in a secondary metastatic site.

Various evasive strategies are employed by tumour cells to avoid detection while in circulation (H. Zhang et al., 2021). Notably, tumour cells will express self-antigens that T-cells have already been desensitised to, such as p53. This provides a layer of protection, preventing detection (Vinay et al., 2015). Tumour cells may also secrete immunosuppressive cytokines such as TGF-β, FoxP3, and IL-10 to evade immune surveillance via inhibition of immune cell differentiation and function (Gonzalez et al., 2018; Tauriello et al., 2018). Furthermore, physical protection of tumour cells can be achieved by binding with platelets, resulting in a protective layer to shield tumour cells from detective T cells. Combining these strategies allows a proportion of metastatic tumour cells to survive the transportation through the circulatory system to the secondary organ.

After surviving the hostile intravascular environment, the cells must extravasate into the surrounding tissue. This method is assumed to be much the same as intravasation into the systematic circulation; however, other methods have been observed (Strilic & Offermanns, 2017). At this stage, tumour cells can congregate, colonising to form a metastatic tumour in a new location or organ in the host, thus completing the metastatic cascade.

1.1.1.5 Enabling Reproductive Immortality

It is widely accepted that cancer cells require an unlimited reproductive capacity to form tumours. Cellular senescence is an essential, stable cell cycle arrest that functions in healthy cells to maintain homeostatic regulation of cell numbers (Kumari & Jat, 2021). Senescence is a typically irreversible state of the cell in which the cell remains viable but non-proliferative; in cellular crisis, it

involves cell death. In rare instances of sustained cellular stress, cells do not die but rather survive and become immortalised – a term used to describe the cells' unlimited reproductive potential. These cells may endlessly proliferate without evidence of either senescence or crisis (Kumari & Jat, 2021).

Developmental signals can trigger senescence when under stress. Dependent upon the intensity and nature of the stress, cells may induce cellular repair, apoptosis, or senescence (Hanahan & Weinberg, 2011). Healthy somatic cells have limited replicative capacity determined by telomere related processes. The telomere is a non-coding sequence at the ends of chromosomes. This protective sequence maintains chromosomal integrity and genomic stability (Hanahan & Weinberg, 2011). Human telomeres constitute approximately 5 – 15 kilobases of tandem hexanucleotide repeat TTAGGG and 12 – 400 nt of 3' G-rich single-stranded overhang (McElligott & Wellinger, 1997; Zhao et al., 2009). Telomeres on each chromosome shorten approximately 50-100 bp after each mitotic cell cycle, a phenomenon titled the End Replication Problem (Bonnell et al., 2021); this is also considered a "Hallmark of Aging" (López-Otín et al., 2013).

The reverse transcriptase, telomerase, is a specialised DNA polymerase that adds telomere repeat segments to the end of telomeric DNA (Hanahan & Weinberg, 2011). In healthy, non-immortalised cells, telomerase is functionally absent, and senescence or apoptosis is entered when the telomere shortens, preventing telomeric crisis. However, it is present at functionally significant levels in immortalised cells. Telomerase is expressed in 85-95% of all cancer cells, regardless of cancer type (Trybek et al., 2020). This considerable presence and function of telomerase effectively counteracts the progressive telomere erosion, providing a preventative mechanism against the induction of senescence and apoptosis. Such active prevention of senescence and apoptosis has been attributed to the eventual immortalisation of cancer cells, providing unrestrained reproductive potential and, thus, their ability to form macroscopic tumours (Hanahan & Weinberg, 2011).

1.1.1.6 Inducing Angiogenesis

Tissues require sustenance in the form of nutrients and oxygen to survive. Once utilised, tissues require a mechanism to discard metabolic waste and carbon dioxide (Hanahan & Weinberg, 2011). New blood vessels must be formed to ensure adequate transport of oxygen, nutrients, and wastes for any cell population to survive and proliferate. Neovasculature is the generation of new blood vessels. It is activated by angiogenesis, providing ample blood supply to the cells to fulfil their supply and waste transport mechanisms (Hanahan & Folkman, 1996). During embryogenesis, the development of new blood vessels is an active and essential requirement for healthy human

development. This process is primarily dormant in adults unless activated transiently during female reproductive cycling and wound healing and repair (Hanahan & Weinberg, 2011).

Tumours require the same nutrient and waste requirements. In contrast to healthy cells, the "angiogenic switch" is almost always turned-on during tumour development, allowing continuous development of new blood vessels to supply nutrients and dispose of metabolic wastes to the growing number of tumour cells replicating (Hanahan & Weinberg, 2011). Furthermore, the formation of new blood vessels enables cancer cells to metastasise and proliferate to distant sites due to the proximity of entry into the blood and lymphatic system for intravasation (Ravi et al., 2000). Angiogenic factors monitor the angiogenic switch, which releases tumours from a state of dormancy, and initiates prolific growth of malignant cells alongside new blood vessel formation. The switch is considered "on" when anti-angiogenic factors are more abundant than pro-angiogenic factors and "off" when anti-angiogenic factors are more abundant than pro-angiogenic factors (Hanahan & Folkman, 1996).

Tumour cells often acquire the ability to leave this switch almost always on, allowing continual aid for new cell growth (Carmeliet, 2005). Vascular endothelial growth factor (VEGF) is the primary pro-angiogenic regulator of the angiogenic switch and is upregulated in response to oncogene expression, other growth factors, and hypoxia (Carmeliet, 2005). Vascular endothelial cells are ordinarily quiescent but may sprout under signalled instruction to initiate angiogenesis by factors such as VEGF (Lugano et al., 2020). VEGF co-regulates the tip and stall cell selection process with DLL4/Notch pathways. VEGF inhibits Notch signalling, enhancing sprouting, branching, vessel migratory capacity and filopodia formation in tip cells, activating the neovascular metabolic pathway (Lugano et al., 2020). Additionally, VEGF may increase vascular permeability, as observed *in vivo*, allowing leakage of plasma proteins into the ECM, improving the capacity for further epithelial growth (Bates, 2010). The poor cell-to-cell junctions that often accompany tumour angiogenesis promote intravasation and extravasation by increasing the ease at which cells migrate through the endothelium (Reymond et al., 2013).

1.1.1.7 Resisting Cell Death

Tumour cell numbers are the resultant of a high proliferation rate and the rate of cell death (Hanahan & Weinberg, 2011). Programmed cell death by apoptosis is a natural cellular cancer prevention mechanism. In healthy tissues, cell division balances cell death. Apoptosis in healthy cells is triggered by various physiological stresses on the cells, such as overexpression of oncogenes, insufficient survival factors, hypoxia, or DNA damage. Apoptosis is mediated by intracellular

proteolytic cascade, activated by intracellular initiator procaspases, or by killer extracellular lymphocyte production of Fas ligand, which binds to the Fas receptor of the cell and initiates apoptosis (Hanahan & Weinberg, 2011).

In tumour cells, apoptosis is inhibited. Thus, the cells evade the natural cell death mechanism and can proliferate freely (Hanahan & Weinberg, 2011). Several mechanistic pathways of apoptosis inhibition have been identified. Of particular interest is tumour suppressor protein p53, which activates apoptosis by upregulation of apoptotic Bax, releasing cytochrome c, thus initiating apoptosis (Harris, 1996). Overserved in over half of human cancers, functional inactivation of the p53 protein prevents DNA damage detection, inhibiting the apoptotic proteolytic cascade and preventing apoptosis (Harris, 1996).

1.1.1.8 Autophagy Upregulation Promoting Cancer Cell Survival

Autophagy is a physiological cell response induced by specific states of the cellular arrest. By the breakdown and recycling of damaged cellular organelles, autophagy is a pro-survival mechanism of cells utilised to prevent apoptosis and maintain cell viability and homeostasis (Hanahan & Weinberg, 2011). However, this process may result in the maintenance of cancerous cells by supporting cell survival and contributing to reduced apoptosis. Human breast, ovarian and prostate cancers have all been reported with higher frequencies of allele deficiency of the autophagy gene, beclin1 (Aita et al., 1999; Liang et al., 1999).

1.2 Breast Cancer Overview

1.2.1 Epidemiology

Breast cancer is the world's most prevalent cancer (DeSantis et al., 2015). In 2022 alone, 2.3 million women were diagnosed with breast cancer, accounting for 12.5% of all newly diagnosed cancer cases, and 685,000 breast cancer deaths were recorded globally (Ferlay J, 2024). The occurrence rates of breast cancer vary significantly around the world, depending on socio-economic location, and ethnic diversity. Western developed countries tend to display significantly higher incidence rates than less developed regions such as Middle Africa (Ferlay J, 2024).

The global standardised incidence rate (ASR) in 2018 was 46.3 per 100,000 population, however in New Zealand and Australia, the ASR was 94.2 – more than double the average incidence rate (Huang et al., 2021). With the highest incidence globally, an estimated one in nine females in New Zealand will suffer from breast cancer in their lifetime, and, on average, nine women will be informed of this prognosis each day (*Breast cancer in New Zealand*).

Furthermore, a significant ethnic disparity exists within the survival rates of women with breast cancer in New Zealand. Wāhine Māori are 33% more likely to die of breast cancer than Pākehā women, and Pacific women are 52% more likely to die of breast cancer across ten years (Lawrenson et al., 2016). The World Health Organisations report suggests that this is likely due to the higher occurrence of the more aggressive subtypes of cancer, containing a higher expression of human epidermal growth factor receptor (HER2). However, there are many contributing factors to these poorer outcomes. Māori women are more likely to have increased wait times and decreased access to GP appointments, delayed specialist treatments, increased likelihood of delayed treatment, and are less likely to attend mammographic breast screening. (Lawrenson et al., 2016) Such factors significantly contribute to the inequity between Māori and non-Māori women.

1.2.2 Risk Factors

Breast cancer is an inheritable disease, and familial genetic history is known to be one of the highest contributing factors to breast cancer development (Collins & Politopoulos, 2011). Significant modifiable risk factors of breast cancer include hormonal replacement therapy, obesity, physical inactivity, consumption of high protein diet, alcohol consumption, smoking, and the use of oral contraceptive pills (Łukasiewicz et al., 2021).

1.2.3 Breast Cancer Subtypes

Breast cancer is a heterogeneous complex of diseases. The array of several subtypes with distinct physiological and molecular features leads to variable responses to treatment and clinical outcomes (Yersal & Barutca, 2014). Therefore, it is necessary to identify and understand the subtype of breast cancer before determining effective therapies. The classifications of each subtype are traditionally defined by the oestrogen receptors (ER), progesterone receptors (PR), and HER2 status. Table 1.1 summarises the basic characteristics of breast cancer molecular subtypes.

Table 1.1: Basic Characteristics of Breast Cancer Molecular Subtypes (Badowska-Kozakiewicz & Budzik, 2016)

Breast Cancer Subtype	Steroid Receptors, HER2 and Cytokeratin Expression
Luminal A	ER+ and/or PR+, HER2-, CK5 / 6-
Luminal B	ER+ and/or PR+, HER2+, CK5 / 6-
HER2 Positive (HER2+)	ER-, PR-, HER2+, CK5 / 6-
Basal-like	ER-, PR-, HER2-, CK5 / 6+
Normal-like	Cancers not classified in above subtypes

1.2.3.1 Luminal A Subtype

Overall, Luminal A breast cancer is the least aggressive and most prominent subtype, representing around 50 - 60% of all breast cancers (Acheampong et al., 2020; Yersal & Barutca, 2014). Luminal A tumours tend to have a low histological grade, low levels of mitotic activity, good prognosis, and lower relapse occurrence. Characterised by high levels of oestrogen receptor activity and lower levels of proliferation-related genes, luminal A tumours are distinguished by the expression of luminal epithelial cytokeratins (CK) 8 and 18, and other luminal-associated markers and genes associated with ER function. Luminal A tumours may be positive for ER or PR, or both, but are always negative for HER2.

1.2.3.2 Luminal B Subtype

Luminal B tumours account for around 15 - 20% of all women diagnosed with breast cancer (Yersal & Barutca, 2014). This luminal subtype tends to be more aggressive, have a higher histological grade, and has a poorer prognosis. Furthermore, this subtype has a higher recurrence rate and lower overall survival than luminal A. The primary distinction between these luminal subtypes is the increased expression of proliferation-related genes in luminal B tumours. Luminal B tumours also tend to have higher expression levels of growth receptor signalling genes – including HER2. These factors all contribute to the increased probability of a poorer prognosis (Yersal & Barutca, 2014).

1.2.3.3 HER2-positive Subtype

HER2-positive breast cancer accounts for 15 - 20% of breast cancer subtypes (Yersal & Barutca, 2014). It is distinguished by the absence of both ER and PR, alongside the overexpression of HER2. HER2 is a 185 kDa transmembrane protein belonging to the ERBB class of receptor tyrosine kinases consisting of four homologous proteins: HER1, HER2, HER3, and HER4. These receptor kinases are essential contributors to several signal transduction pathways that regulate cell growth and differentiation processes. Overexpression of HER2 leads to the increased interaction of numerous intracellular signalling molecules, resulting in the activation of downstream messenger pathways. Transcription factors activated by these signalling pathways are responsible for regulating many genes involved in mitotic activity, proliferation, differentiation, survival, angiogenesis, invasion and metastasis. These interactions result in highly proliferative tumours with high histological grades and an overall poorer prognosis (Yersal & Barutca, 2014).

1.2.3.4 Basal-like Subtype

The basal-like subtype is often referred to as triple-negative breast cancer due to the lack of ER, PR, and HER2 expression. Basal-like tumours overexpress basal myoepithelial markers such as cytokeratins (CK5/6+), epidermal growth factor receptor (EGFR), SMA, P-cadherin, p63 or c-kit antigen (Yersal & Barutca, 2014). They contain frequent mutations in the tumour protein 53 (TP53) gene and

have evidence of genomic instability and inactivation of the retinoblastoma (Rb) pathway. Basal-like breast carcinomas have high mitotic activity, poor spindle formation and high levels of unregulated proliferative growth. They have aggressive growth and invasion rates, often metastasising to the brain and lung within 5 years of initial occurrence (Heitz et al., 2009). As such, the basal-like subtype is highly associated with high histological grades and poor clinical outcomes.

1.2.3.5 Normal-like Subtype

The normal-like breast cancer subtype consists of just 5 - 10% of tumours, and to date is poorly characterized and understood (Weigelt et al., 2010). Although lacking the expression of ER, PR, HER2 and CDK5/6, they are not considered basal-like, as they are negative for EGFR. The clinical significance of this subtype remains poorly understood. Furthermore, some researchers believe this subtype may not truly exist distinct from other subtypes, but rather may be the result of high levels of contamination of normal breast cells in the determining microarrays (Weigelt et al., 2010).

1.3 Current Treatments and Therapies

The survival outcomes of patients with breast cancer can be attributed to two main aspects: stage of detection and efficacy of post-diagnostic treatment (Bhushan et al., 2021). The following section will briefly discuss current preventative and treatment methods.

1.3.1 Detection

Consistent enhancement of mammography and screening technologies for early detection has significantly decreased mortality due to breast cancer in developed countries (Trieu et al., 2022). This remains the foundation of breast cancer regulations. Regular public drives for awareness of common signs and symptoms may also contribute to the increased incidence of early detection. Preventative medical therapy such as antioestrogens like tamoxifen can be prescribed to decrease the probability of breast cancer development for high-risk individuals. Surgical treatment as a double mastectomy is an additional preventative measure for females with an increased risk of breast cancer development.

Different treatments and management strategies are implemented for individuals identified with an existing breast tumour, such as targeted therapy, radiation therapy, hormonal therapy and chemotherapy.

1.3.2 Surgical Treatments

The primary treatment of early breast cancer in New Zealand is surgically removing the tumour from the breast (*Breast cancer treatment*, 2023). Surgical treatment aims to maximise control of the disease in the breast, obtain tissue for diagnostic testing and further treatment, and maximise the quality of life, including the cosmetic outcome. The surgical treatment varies depending on the

size and location of the tumour. For tumours larger than 4 cm in diameter, chemotherapy is often administered before surgery to shrink the tumour before a mastectomy. Removing the whole breast, with or without reconstruction, in these larger tumours is generally the recommended treatment option. For tumours less than 4cm in diameter, the patient may undergo a partial mastectomy (lumpectomy), where only the tumour is removed. Often, postoperative radiation therapy is performed for these non-metastatic tumours (Waks & Winer, 2019).

1.3.3 Radiation Therapy

Radiation therapy may be delivered to the whole breast, a portion of the breast, the chest wall and the regional lymph nodes. Radiation therapy is the standard treatment after a partial mastectomy, although it is often utilised in other cases. Radiation therapy is given after the chemotherapy treatment is completed if chemotherapy is also utilised. It is associated with reduced recurrence of breast cancer and mortality, and the proportional benefit of radiation is generally constant regardless of the overall diagnostic risk (Darby et al., 2011; Guidolin et al., 2019). Radiation therapy is typically delivered to the breast with a linear accelerator, which delivers the beam externally. It is a localised treatment specifically targeted to terminate any malignant or cancerous cells in the breast. The regional lymph nodes in the underarm, above the collar bone and internal mammary chain may also be treated if necessary. While patients do not feel the radiation waves, skin irritation, fatigue, and breast heaviness, tenderness, itchiness, and swelling are common short-term side effects. Long-term side effects can include changes to the look and feel of the breast and heart disease resulting from radiation field exposure when treating the left breast (Belzile-Dugas & Eisenberg, 2021; *Radiation Therapy*, 2022).

1.3.4 Chemotherapy

Chemotherapy treatment is the administration of cytotoxic drugs orally or intravenously, and is used as neoadjuvant prior to surgery, as adjuvant therapy to kill remaining non-visible cancer cells post-surgery, and as palliative therapy (McLaughlin et al., 2021). Unlike surgery and radiation therapy, chemotherapy drugs are non-specific and target all rapidly dividing cells, so they are not specific to cancer cells. As such, healthy rapidly dividing cells in the digestive system, hair follicles and nails are also damaged during chemotherapy. Unlike cancer cells, however, these healthy cells maintain their repair mechanisms and can generally repair themselves. Despite this, common adverse effects include alopecia, bone marrow suppression and gastrointestinal complications. Furthermore, chemotherapy dose, duration and cycles can be severely limited due to drug-specific toxicities such as cardiotoxicity and vascular toxicity in breast cancer (McLaughlin et al., 2021; Montisci et al., 2021).

Perhaps the most notable of these adverse effects is cardiovascular disease due to cardiotoxicity. To date, cardiovascular disease remains one of the leading causes of mortality in breast

cancer survivors, accounting for 35% of non-cancer-related deaths in breast cancer survivors aged 50 or over (Montisci et al., 2021). Commonly used breast cancer chemotherapy drug types, for example, anthracyclines such as doxorubicin, and anti-HER2 agents such as trastuzumab and lapatinib, are most associated with cardiotoxicity due to their specific molecular pathways utilised for treatment (Montisci et al., 2021).

Anthracyclines prevent DNA synthesis and repair by disrupting topoisomerase-II, an isomerase necessary for cell function (Marinello et al., 2018; Saha & Das, 2021). Free radicals generated by anthracyclines cause lipid peroxidation and disrupt mitochondrial electron transport mechanisms, resulting in cell membrane and protein damage, and induce apoptosis (Saha & Das, 2021).

Taxanes, such as paclitaxel prevent cell division. Paclitaxel prevents microtubule depolymerization and regulates apoptosis-mediation proteins such as the Bcl-2 family and the BAX proteins (Lim et al., 2022). At high concentrations, paclitaxel targets microtubules resulting in mitotic arrest at G_2/M phase. In lower dosages, apoptosis is induced at G_0 and G_1/S phase by activation of Raf-1 kinase or P53/P21 (Kampan et al., 2015).

However, like all current chemotherapies, paclitaxel is not fool-proof, and further developments in cancer treatments are required to improve the risk of recurrence and overall survival rate. Furthermore, anticancer drug resistance is a complex process in which cancer cell will become resistant to the drug(s) by such mechanisms as inactivation of the drug, apoptosis suppression, epigenetic changes, changes in the drug targets, drug metabolism, alteration DNA, enhanced DNA repair and target gene amplification. Cancer drug resistance is a common phenomenon; thus, combination therapies are often utilised (Mansoori et al., 2017). Ineffective treatment by many chemotherapy drugs is one of the many battles that research has yet to win, and so, more personalised, adaptable treatments are needed to help improve the outcomes of cancer patients worldwide.

1.3.5 Targeted Therapy

While chemotherapy remains the optimum treatment of choice for triple-negative breast cancer, patients who are ER+, PR+ and HER2+ are frequently eligible for targeted therapies (*Breast cancer treatment*, 2023). Targeted therapy has a higher drug specificity and therefore higher efficacy with less adverse effects when compared to chemotherapy (Joo et al., 2013).

ER+ breast cancer accounts for approximately 75% of all diagnosed breast cancers (Patel & Bihani, 2018). Oestrogen promotes the growth and differentiation of ER+ breast cancer cells. Hormone therapy inhibits the growth of ER+ tumours by preventing hormone production or interfering with the

metabolic pathways that hormones affect in breast cancer cells. This can be performed by blocking the production of oestrogens, or by blocking the action of oestrogens on breast cancer cells. Prevention of oestrogen production within the body can be achieved surgically, by performing an oophorectomy, radiologically, chemically, or via aromatase inhibitors (Patel & Bihani, 2018). Aromatase inhibitors are included in adjuvant settings singularly, and in conjunction with tamoxifen for both pre- and post-menopausal women. Blocking the oestrogen-dependent pathways can also be performed through selective oestrogen receptor modulators (SERMs) and selective oestrogen receptor degraders (SERDs). SERMs are antioestrogens that prevent ER activity by binding with ER in place of its cofactor associates. This, in turn, prevents the oestrogen receptor pathway from proceeding and acting as a transcription factor and binding oestrogen receptor elements present in target DNA promotor regions active in ER+ breast cancers. In contrast, SERDs are antioestrogens that destabilise the Helix 12 component in ER (Patel & Bihani, 2018). Helix 12 is essential for ER function (Gu, 2002); thus, SERD destabilisation of this component results in proteasomal degradation and inhibition of the ER pathway (Patel & Bihani, 2018). These interactions are summarised in Figure 1.3 below.

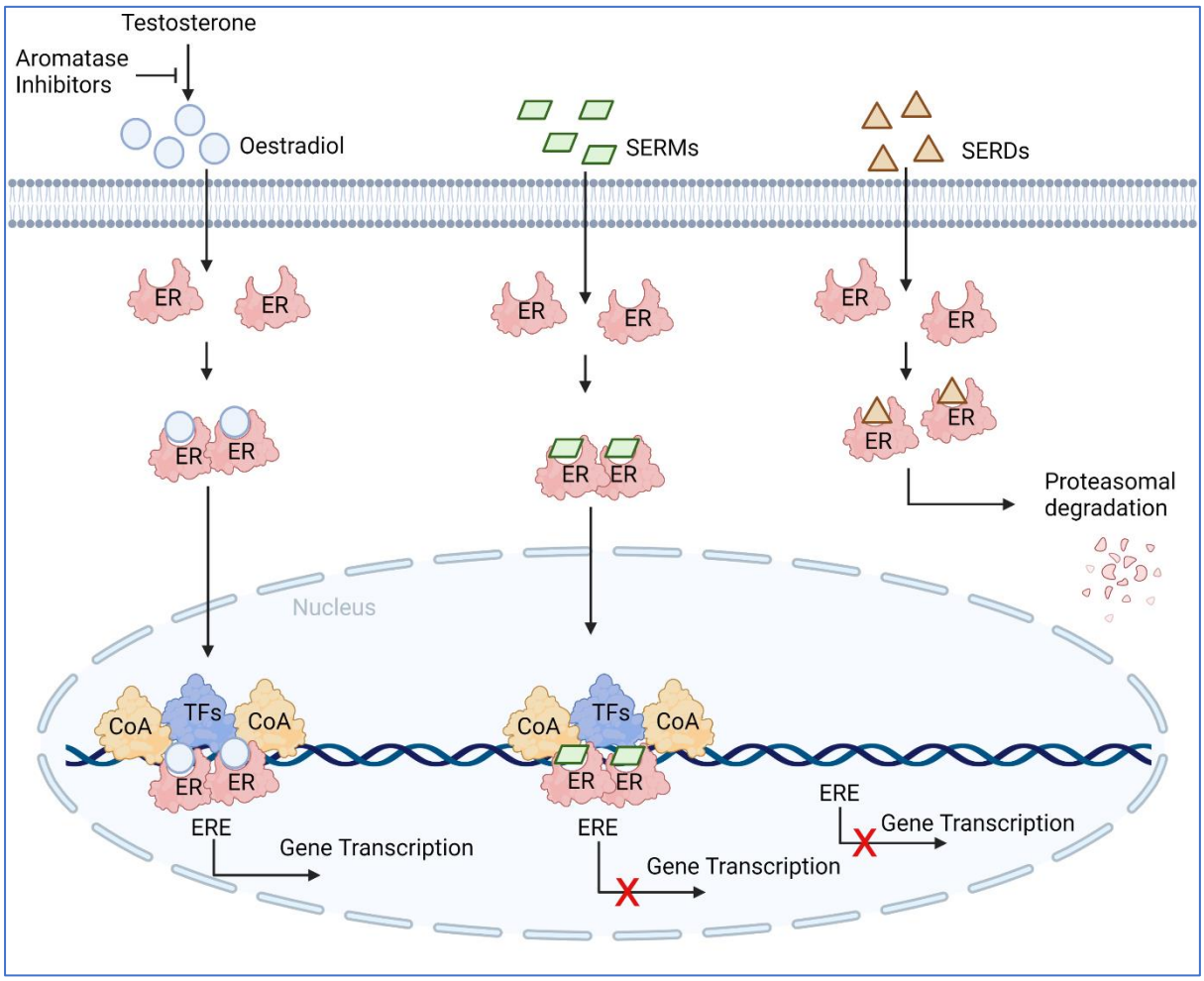

Figure 1.3: The Effects of Endocrine Therapies on the Oestrogen Receptor Pathway. Aromatase Inhibitors inhibit oestradiol synthesis, thereby preventing the ER signalling pathway. SERMs bind to ERs, causing an inactive complex preventing the ER signalling pathway continuation and subsequent gene transcription. SERDs bind to ERs, resulting in proteasomal degradation and inhibiting the ER pathway. (Adapted from Patel and Bihani (2018). *Created with Biorender.com*).

Tamoxifen is an extremely effective, and most utilised SERM prescribed to treat breast cancer (Patel & Bihani, 2018). Tamoxifen has anti-proliferative effects in breast tissue; however, some agonistic effects can occur in the uterus, bone and cardiovascular system (Gu, 2002). These risks are significant limiting factors in the utilisation of tamoxifen. Moving forward, new drugs should continue to be manufactured and trialled to assist in the treatment of breast cancer without the increased risks of developing other carcinomas.

In addition to ER status, breast tumours often overexpress HER2, another key therapeutic target. HER2 overexpression inhibits apoptosis and encourages proliferative activity. Trastuzumab is a monoclonal antibody that inhibits HER2 homodimerization, preventing HER2 signalling and therefore overexpression in HER2 positive breast cancer. Trastuzumab may also facilitate cellular cytotoxicity,

eliminating HER2 expressing cells. Trastuzumab may be administered in conjunction with paclitaxel, an antimicrotubular agent with cytotoxic properties, to increase the efficiency of treatment in later stage metastatic breast cancer when required (Klos et al., 2003; Tolaney et al., 2021).

While current treatments offer a range of potential options for breast cancer patients, clinical outcomes are not wholly positive. In 2022, 685,000 breast cancer deaths were recorded globally (Ferlay J, 2024). Targeted therapy has a higher efficacy with less adverse effects when compared to other treatments (Joo et al., 2013), and thus, identifying potential targets is a critical step in improving treatment options, and thus, patient outcomes. One such potential target is SPAG5.

Chapter 2: SPAG5

2.1. SPAG5

Understanding the roles and mechanisms of genes with oncogenic properties is essential to determining the development and growth of any cancer. Importantly, the insights provided by understanding the molecular workings of any oncogene quintessential to the development of new treatments and personalised therapies for cancer patients. Sperm-associated antigen 5 (SPAG5), also known as astrin, is a relatively novel oncogene promising significant potential as a target for personalised therapy (Abdel-Fatah et al., 2016). SPAG5 conducts several vital functions that help to maintain healthy cell growth and mitotic activity (Conti et al., 2019). Before considering the adverse outcomes associated with an imbalance in SPAG5 activity, it is essential to first understand the structure and function of SPAG5 in healthy human cells.

2.1.1 Structure

Studies have been conducted to characterise the molecular structure of SPAG5 (Chang et al., 2001; Gruber et al., 2002; Mack & Compton, 2001). Chang et al. (2001) denoted the cDNA sequence of 4.1 kb, containing a 3,360 bp open reading frame encoding a 1,120 amino acid-forming protein of approximately 126 kDa. In the same year, Mack and Compton (2001) published similar work, with sequencing analysis determining a longer, alternative open reading frame of 3,843 bp encoding a protein of 1,193 amino acids and a predicted molecular mass of 134 kDa.

The SPAG5 sequence can best be characterised into three distinct domains (Figure 2.1). Namely, a proline-rich N-terminal head domain and two coiled-coil domains connected by a proline-rich linker region (Gruber et al., 2002). The prevalence of such abundant proline in the N-terminal head accompanied by serine and threonine residues suggests a probable key site of phosphorylation, an observation confirmed by *in vitro* studies determining the substrate function of the SPAG5 N-terminal for Cyclin Dependant Kinase 1 (CDK1) (Chang et al., 2001; Gruber et al., 2002).

SPAG5 is shaped in a 'lollipop' structure via the formation of parallel dimers, totalling approximately 80nm in length. The N-terminus regions form a globular head, notable for interaction with kinetochore-associated protein Ndc80. The parallel coiled-coil regions form a rod-liked shape, connected by the proline-rich linking region. A portion of coiled-coil 1 is notable for its SKAP binding region, a significant structure denoting the role of SPAG5 in the stabilisation of kinetochore attachments during mitosis: a significant observation indicated by the localised expression of SPAG5. The C terminal has a key structure containing a structural 70 amino acid tail motif responsible for SPAG5 interaction with phosphatase 1 (PP1), a critical binding site in the kinetochore-stabilisation role of SPAG5.

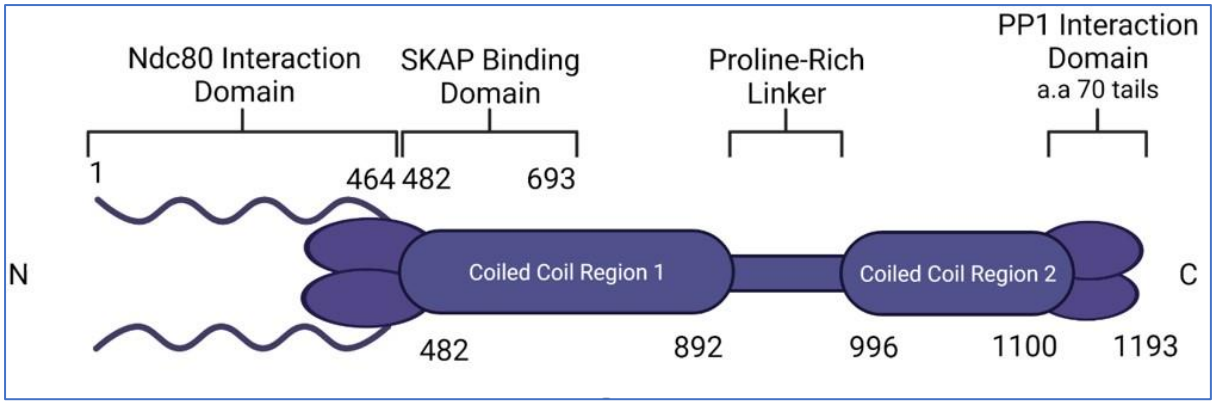

Figure 2.1: A Schematic of SPAG5 Indicating the Relative Shape and Regions of Significance. SPAG5 is constructed of three distinct domains. The N-terminal head domain, and two coiled coil regions connected by a proline-rich linker region. The globular head at the N terminus contains the Ndc80 interaction domain, followed by rod-like coiled coil regions, including the SKAP binding domain. At the C-terminus, a 70 amino acid motif is a critical binding site for PP1.
(Adapted from Ying et al. (2020). *Created with BioRender.com*)

2.1.2 Subcellular Location

The subcellular location of any protein is an invaluable indicator in determining the potential functions in human cells. Analysis of the subcellular location of SPAG5 throughout the cell cycle provides us with significant understandings of the key roles of SPAG5, and therefore its potential oncogenic properties. During interphase, SPAG5 diffuses into the cytoplasm and colocalizes with pericentriolar material (PCM1) at the centrosome (Mack & Compton, 2001). When the cells enter mitosis and spindle formation is completed, SPAG5 is evident on the spindle and kinetochores, indicating a mitosis-specific role in spindle formation and alignment. This was confirmed via an *in vitro* knockdown of SPAG5 resultant in defective chromosome segregation and alignment (Gruber et al., 2002; Thein et al., 2007).

2.1.3 Introduction to SPAG5 in Mitosis

Cell division represents the essence of cell growth, reproduction, and genetic inheritance, with mitosis providing an accurate replication of the organism's genome and equal division of daughter cells at metaphase (Thein et al., 2007). As suggested in sections 2.1.1 and 2.1.2, SPAG5 plays an integral role in mitosis; SPAG5 is most critically involved in spindle structure formation, further assisting in kinetochore and microtubule attachments which ensure the correct alignment and segregation of chromosomes during anaphase and telophase. In healthy cells, incorrect attachment of kinetochore and microtubules results in a halt of further division at the spindle assembly checkpoint, preventing continuation into anaphase without the correct kinetochore-microtubule attachment. On achieving correct attachment, the chromosomes aligned at the metaphase plate undergo cleavage of sister chromatids, and the cell enters anaphase. Maintaining such checkpoints is essential to the production of healthy new cells (Gruber et al., 2002).

SPAG5 is associated with microtubule attachments, making it an essential component of healthy cell division. SPAG5 colocalises at the centrosome during interphase with the pericentriolar material (PCM1). Assisting in the alignment of chromosomes, SPAG5 is also prevalent on the mitotic spindle and kinetochores. Following these essential roles, SPAG5 continues to contribute to several critical tasks in metaphase.

2.1.3.1 SPAG5 "Lock" Function in End-on Kinetochore-Microtubule Attachment Stability

SPAG5 performs an integral role as a "lock" to increase the stability of end-on kinetochore-microtubule attachments during metaphase (Conti et al., 2019) through its complexation with small kinetochore associated protein (SKAP) (Figure 2.2). The SPAG5-SKAP complex, also known as the astrin-SKAP complex, utilises the plus-end tracking ability of SKAP and the N-terminus of SPAG5 to bind to the plus end of microtubules. The complex also interacts with the Ndc80 complex, an integral kinetochore component in attaching microtubules to chromosomes. The interaction between the complexes may be responsible for the stable binding of chromosomes to microtubules. Furthermore, since the C-terminal structural motif of SPAG5 in the SPAG5-SKAP complex interacts with phosphatase 1 (PP1), it is theorised to deliver PP1 to Ndc80. Recruitment of PP1 by the kinetochores results in increased SPAG5 expression, initiating anaphase by facilitating end-on kinetochores and microtubule pulling. Thus, the SPAG5-Phosphatase-1 complex has been described as a "lock", stabilising the kinetochore-microtubule bridges generated by Ndc80 at end-on kinetochores, enabling kinetochores to tolerate pulling from spindle microtubules. Furthermore, PP1 interaction under dynamic regulation results in stability of end-on attachments. This suggests a potential disruption resulting in chromosomal alignment delay, and this may prevent the onset of anaphase (Conti et al., 2019). Anaphase may errantly proceed in some instances, resulting in defective chromosome segregation from constitutive artificial interaction of PP1 with SPAG5.

The timing of SPAG5 localisation to end-on kinetochores is essential to correct chromosome segregation (Liu et al., 2009). One such complex mechanism is engineered by the regulating molecular switch Aurora B. This serine/threonine kinase recognises incorrect kinetochore-microtubule attachments by recognising kinetochore tension, ultimately regulating the bi-orientation of chromosomes (Liu et al., 2009). Incorrect kinetochore localisation mediated by SPAG5 is also prevented by Aurora B, resulting in the bi-orientation of kinetochores. While this process may initially be supported in prophase by Aurora-B recruitment of KIF2B and CLASP1 due to low inter-kinetochore tension, inter-kinetochore tension increases by metaphase, decreasing Aurora B. As such, the KIF2B-CLASP1 complex is supplanted by the SPAG5-CLASP1 complex, allowing SPAG5 recruitment to end-on kinetochores (Manning et al., 2010) and bi-oriented chromosomes. Such regulation of end-on

attachment stability depends highly on both Aurora B and SPAG5-PP1 interactions, as the two regulators have an inverse relationship in regulation management (Conti et al., 2019).

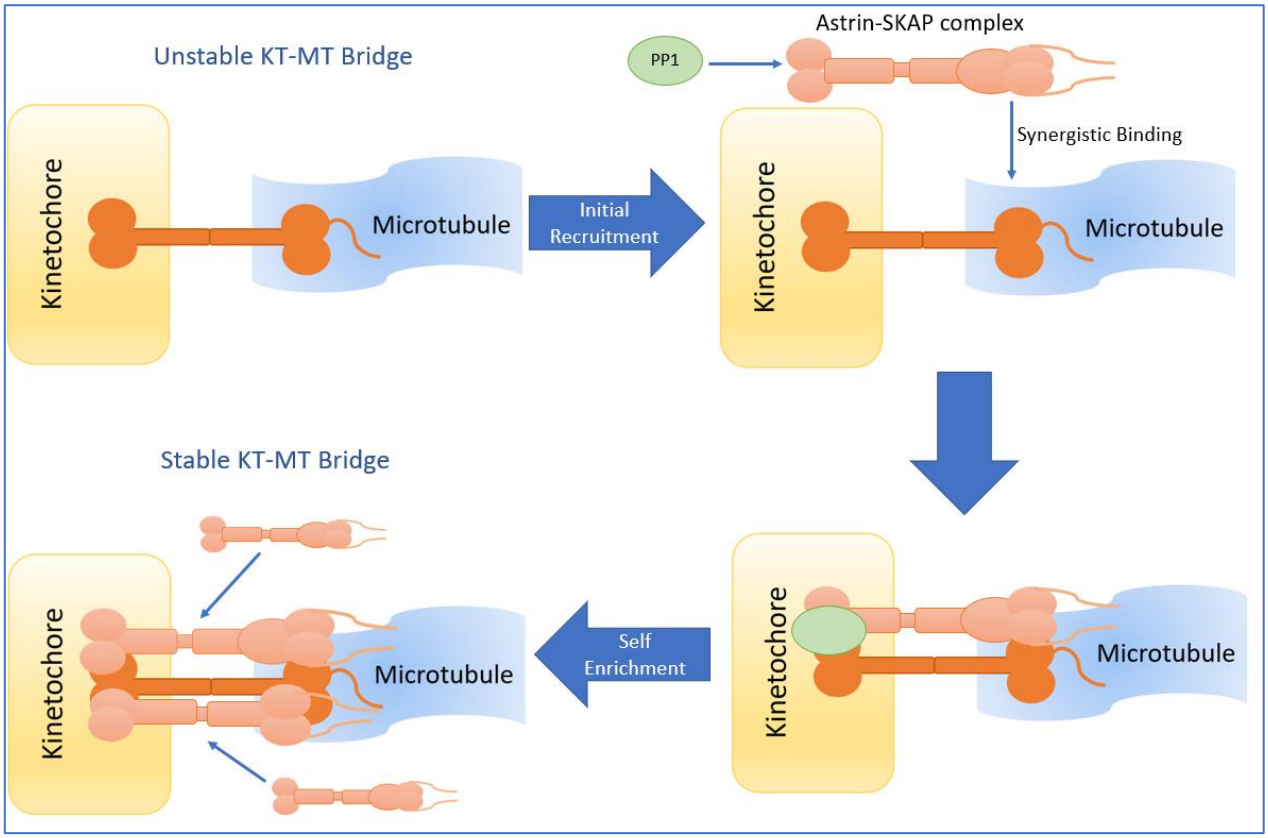

Figure 2.2: Stabilization Process of Kinetochore-Microtubule Attachments via SPAG5 Binding. An unstable kinetochore-microtubule bridge recruits PP1. Kinetochore recruitment of PP1 increases SPAG5 expression. The SPAG5-SKAP complex is guided to the KT-MT by the plus-end tracking ability of SKAP, and the N terminus of SPAG5 binds with the plus end of the microtubules. PP1 binding with the SPAG5-SKAP complex stabilises the KT-MT bridges. This process continues as several SPAG5-SKAP complexes secure the previously unstable KT-MT interaction.

2.1.3.2 Summary

SPAG5 plays an integral role in the selective stability of kinetochore-microtubule attachments. Reduction of Aurora B allows SPAG5 binding to end-on kinetochores. SPAG5-PP1 interaction near the C-terminus of Ndc80 increases SPAG5 recruitment and binding at end-on kinetochores. Synergistic microtubule binding of SPAG5-SKAP and Ndc80 results in the rapid increase of stability of end-on kinetochore attachments. However, this tension-sensing model remains hypothetical and has received some criticism; de Regt et al. (2018) suggests the tension on kinetochores is insufficient for Aurora B differentiation of kinetochore-microtubule attachment. The mitotic kinases polo-like kinase 1 (PLK1) and cyclin-dependent kinase 1 (CDK1) may play a role in regulating SPAG5 localisation to kinetochores; a secondary regulatory pathway proposed is through PLK1 activation of CDK1, which phosphorylates SPAG5 at Ser135 and Ser249 resulting in phosphorylated-SPAG5 localisation of

kinetochores (Chung et al., 2016). Supporting this secondary pathway is the finding that SPAG5 recruitment to kinetochores can occur prior to chromosome bi-orientation, so the tension-sensing activity of Aurora B may not be solely responsible for SPAG5-PP1 kinetochore localisation (Conti et al., 2019). Xue et al. (2002) further found that knock-out models of SPAG5 did not impact spermatogenesis or fertility, indicating a secondary mechanism must function to support kinetochore-microtubule stability.

2.1.4 Localization of SPAG5 to Chromosomes Promotes Centriole Replication During Interphase and Maintains Chromosome Integrity During Mitosis

SPAG5 localises to centrosomes with pericentriolar material (PMC1) throughout mitosis and contributes to centriole duplication (Ying et al., 2020). During interphase, SPAG5 and centrosomal protein (CEP) 72 play an essential role in centrosomal localisation of primary microcephaly (MCPH) and associated protein CDK5 regulatory subunit protein 2 (CDK5RAP2). Such localisation results in the assembly at the centrosome of an MCPH complex which promotes centrosomal localisation of an essential centriole duplication kinase, CDK2. A decrease in SPAG5 reduces CDK5RAP2 localisation at the centrosome, resulting in lower stability and extent of CDK2 centrosome localisation, reducing centriole numbers during the S-phase of the cell cycle (Ying et al., 2020).

SPAG5 localises to the spindle pole during pro-metaphase to metaphase, significantly increasing chromosome integrity throughout mitosis. Downregulation of SPAG5 results in centriole disengagement during metaphase, resulting in unaligned chromosomes and ultimately prolonged spindle checkpoint arrest (Ying et al., 2020).

2.1.5 Downregulation of SPAG5 at the End of Mitosis

SPAG5 localises to intercellular bridge microtubules (ICBMTs) during telophase in which SPAG5 downregulation is critical for healthy cytokinesis (Mack & Compton, 2001). Ubiquitin ligase midline 2 (MID2) ubiquitinates Lys409 of SPAG5 at intercellular bridge microtubules, downregulating SPAG5 by enabling its degradation. Expression of SPAG5 K409A mutant results in cytokinesis defects, indicating that the lack of a ubiquitination site for MID2 results in an accumulation of SPAG5 at the ICBMTs and ultimately leads to incorrectly disconnected daughter cells (Gholkar et al., 2016). Failure of cytokinesis is sometimes associated with cancer development due to incorrect chromosome numbers and the commonly resultant DNA damage (Hayashi & Karlseder, 2013).

2.2 SPAG5 and Cancer

The integral role of mitotic spindle protein SPAG5 is a novel and significant focus in recent cancer research. Recent research has regularly found SPAG5 is overexpressed in several human

cancers, functioning as an oncogene. Furthermore, SPAG5 performs critical roles throughout mitosis, modulates proliferation, migration, and metastasis, impacts cell growth and apoptosis, and increases resistance to chemotherapy drugs (Huang & Li, 2020; Li et al., 2021; Liu et al., 2021; Wang et al., 2020; Yang et al., 2020; Ying et al., 2020; Zhang et al., 2020).

2.2.1 Key Signalling Pathways of SPAG5 in Cancer.

2.2.1.1 p53

The p53 pathway regulates cellular responses to DNA damage, abnormal oncogene amplification, redox stress and upregulates several apoptotic genes, including Bcl-2-associated X protein (BAX) (Vousden & Lane, 2007). SPAG5 inhibits apoptosis via the p53-mediated DNA damage pathway. Under genotoxic stress, depleted SPAG5 expression coupled with upregulated p53 increases caspase-3 activity by inducing BAX expression (Yang et al., 2006). Furthermore, p53 upregulation inhibits mTORC1 activity through the tuberous sclerosis proteins 1 and 2 (TSC1-TSC2) complex preventing protein synthesis (Yang et al., 2006). Evidently, SPAG5 overexpression in conjunction with p53 downregulation results in favourable cell growth and proliferation conditions under cytotoxic stress.

2.2.1.2 mTORC1

The mammalian target of rapamycin complex 1 (mTORC1) is activated by TSC1-TSC2 when a cell experiences oxidative stress, promoting the genesis of stress response proteins. Under such conditions, TSC1-TSC2 also upregulates SPAG5 expression. SPAG5 inhibits the association of mTOR-raptor and recruits raptor to stress granules, preventing mTORC1 activity (Thedieck et al., 2013). In this manner, TSC1-TSC2 coupled with SPAG5 maintain mTORC1 cellular levels, enabling cell survival responses to stress, preventing mTORC1 hyperactivation-induced apoptosis. However, SPAG5-induced mTORC1 activation may generate hypoxia-inducible factor 1α (HIF-1α), increasing cancer cell hypoxia tolerance (Saxton & Sabatini, 2017). SPAG5-induced mTORC1 activation may also phosphorylate autophagy regulatory complex containing unc-51-like kinase 1 (ULK1), mammalian ATG13 protein, and focal adhesion kinase interacting protein of 200 kDa (FIP200) (Chen et al., 2014). The role of SPAG5-mediated mTORC1 in both autophagy and hypoxia tolerance is yet to be further investigated.

2.2.1.3 WNT3

Compelling evidence suggests WNT3, a proto-oncogenic signalling protein, contributes to the development of several cancers, including breast (Jiang et al., 2019), rectal (Nie et al., 2020), lung (Nakashima et al., 2012) and gastric (Wang et al., 2016) cancer. SPAG5 upregulates WNT3 via activating the AKT/mTOR signalling pathway (Liu, Q. H. Zeng, et al., 2018). Thus, overexpression of SPAG5 in cancer cells expressing WNT3 increases cell proliferation, invasion, and chemotherapy

resistance; such events continue even in the presence of cell cycle arrest inducing agents (Wu et al., 2012). Ligand binding of WNT3 results in dephosphorylation of β-catenin, and subsequent translation of β-catenin into the nucleus and the formation of a complex with T cell factor (TCF). Because TCF is partially responsible for the activation of gene transcription, this process initiates the transcription of oncogenes. Furthermore, the WNT3/β-catenin signalling pathway transactivates EGFR expression, which is associated with trastuzumab chemoresistance HER2 positive breast cancer cells (Wu et al., 2012). The WNT3/β-catenin signalling pathway can also provide chemoresistance to cisplatin in bladder cancer (Liu, Q. H. Zeng, et al., 2018). Additionally, β-catenin translocation regulates EMT, a key trastuzumab resistance mechanism, and potentially increases tumour invasion and metastases in HER2-overexpressing breast cancer cells (Wu et al., 2012). SPAG5 is a chemotherapy sensitivity predictor in breast cancer (Abdel-Fatah et al., 2016). Given that WNT3/β-catenin signalling pathway is associated with chemoresistance, research should be conducted to determine whether SPAG5 may also be an effective chemosensitivity predictor in cancer.

2.2.1.4 CEP55

Centrosome Protein 55 (CEP55) is a crucial contributor to the separation of cells during cytokinesis. CEP55 activates the PI3K/AKT/mTOR pathway, promoting cell proliferation and migration. In healthy cells, SPAG5 mediates CEP55, controlling cell division and proliferation in a manageable manner. In cancer cells, overexpression of SPAG5 results in a detrimental rate of SPAG5-CEP55 interaction, stimulating downstream activation of cell proliferation and survival factors (Yang et al., 2018). Expression of miR-363-3p can suppress SPAG5 by inhibiting SPAG5 mRNA promotor activity, reducing SPAG5-CEP55 binding, and ultimately reducing cell proliferation (Figure 2.3); Thus, miR-363-3p/SPAG5/CEP55 axis may prove an effective therapeutic target in some cancers (Yang et al., 2018).

2.2.1.5 SCARA5

Tumour suppressor gene scavenger receptor class A member 5 (SCARA5) suppresses the progression and metastasis of cancer. SCARA5 is regularly downregulated in cancer cells; SPAG5 suppression increases SCARA5 activity, slowing cell progression and increasing apoptosis. SPAG5 downregulates SCARA5 expression occurs via β-catenin/TCF4 pathway activation. SPAG5 interaction with β-catenin can dephosphorylate and translocate β-catenin in the aforementioned AKT/mTOR/WNT axis. When coupled with TCF4, degraded β-catenin downregulates SCARA5 expression (Table 2.1). Therefore, SPAG5 overexpression accelerates the uncontrolled proliferation of cancer cells by decreasing SCARA5 activity (Liu, Hu, et al., 2018)

2.2.1.6 c-MYC

The oncogenic transcription factor c-MYC is often referred to as a “master regulator” (Miller et al., 2012). It is a critical factor in cancer development and progression, being responsible for

sustaining several cellular mechanisms, including cell cycle regulation, proliferation, apoptosis, and DNA repair. Olaparib is a poly-ADP ribose polymerase (PARP) inhibitor; it prevents DNA repair, increasing the likelihood of cancer cell death. SPAG5 may incite Olaparib resistance in triple-negative breast cancer by increasing c-MYC transcriptional activity. SPAG5 binds with c-MYC binding protein (MYCBP), promoting c-MYC transcription activity, thereby upregulating homologous repair (HR) proteins. Increased expression of HR DNA repair proteins, such as BRCA1, BRCA2 and RAD51, inhibit PARP activity, allowing for DNA lesion repairs, counteracting the PARP inhibitory functions of Olaparib, and providing resistance to the cancerous cells (Table 2.1; Figure 2.3). Furthermore, SPAG5 promotion of the S/G_2 phase transition during mitosis decreases the duration of the S phase, during which Olaparib functions. This indicates the probable effectiveness of SPAG5 as a biomarker for Olaparib resistance in cancer patients.

2.3 The Oncogenic Properties of SPAG5

SPAG5 has various cellular regulatory processes that account for four significant oncogenic properties: sustaining proliferative signalling, inhibition of apoptosis, mediation of autophagy, and supporting metastasis (Li et al., 2019; Liu, Q. H. Zeng, et al., 2018; Wang et al., 2021; Wang et al., 2020; Yang et al., 2020). A more recent study has suggested that SPAG5 may also support cancer cell survival through a previously unobserved role in regulating autophagy (Huang & Li, 2020). The following section will review the known oncogenic functions of SPAG5 in several prominent human cancers including liver, breast, prostate and cervical cancers. The following sections will summarise the role of SPAG5 in various cancers (Table 2.1; Figure 2.3)

2.3.1 Oncogenic Properties of SPAG5 in Lung Adenocarcinoma

SPAG5 is involved in the tumorigenesis of lung cancer. SPAG5 upregulation can occur in a range of cancers and is often associated with poor prognosis. SPAG5 is particularly often implicated in lung cancers, in which it may act as a biomarker and likely also has an oncogenic role in promoting proliferation, migration, invasion, autophagy, and finally, in inhibiting apoptosis (Huang & Li, 2020).

2.3.1.1 Sustaining Proliferative Signalling and SPAG5 in Lung Adenocarcinoma

AKT-regulated pathway disruptions are associated with cancer development and progression (Nitulescu et al., 2018), as AKT has an integral role in cell signalling and apoptosis suppression (Zhao et al., 2015), and proliferation stimulation in several cancers (Johnson et al., 2009; Mitra et al., 2012; Toulany et al., 2017). SPAG5 knockdown can suppress AKT signalling activation in human non-small cell lung cancer, with Song et al. (2018) further finding the potential role of miR-1179 in AKT signalling inhibition, as upregulation of miR-1179, which targets SPAG5, also results in AKT signalling inhibition. Supporting this observation is a study published by Wang et al. (2020), which found that the oncogene

long non-coding RNA (lncRNA) LINC00857 regulated cell proliferation, glycolysis and apoptosis of lung adenocarcinoma cells by targeting the miR-1179/SPAG5 axis. While its exact molecular mechanisms remain to be understood, the developments in the knowledge of miR-1179 are promising and may lead to a therapeutic target within the SPAG5/AKT axis for lung cancer patients (Figure 2.3).

SPAG5 may inhibit the effectiveness of gefitinib, a treatment used for non-small cell lung carcinomas with EGFR mutations, because sensitivity to the agent is mediated by miR-133a-3p, of which SPAG5 is a critical target (Li et al., 2021). Since gefitinib is a central agent in the treatment of non-small cell lung carcinomas with EGFR mutations, the miR-133a-3p/SPAG5 axis could be an important therapeutic target to improve therapeutic efficiency in these patients.

2.3.1.2 Apoptosis Evasion and SPAG5 in Lung Adenocarcinoma

The p53 protein has an inverse relationship with SPAG5 in lung cancer. SPAG5 expression in lung adenocarcinomas is regulated by the MDM2-p53-p21 pathway. Repression of p53 and p21. p53 is essential for oncogenic SPAG5 upregulation in lung cancer (Wang et al., 2019). However, the detailed mechanism for this relationship yet remains to be determined, and further evidence is needed to confirm if the relationship is direct. Wang et al. (2019) suggest that SPAG5 suppression may be achieved via downstream targets of the p53 pathway due to the suppression of SPAG5 by Nutlin-3a after p21 knockdown.

2.3.1.3 SPAG5 and Autophagy Upregulation in Lung Adenocarcinoma

Knockdown of SPAG5 in lung cancer cell line A549 resulted in induction of apoptosis, inhibition of autophagy, and suppression of proliferation, migration, and invasion of cancer cells. Huang and Li (2020) presented results supporting a previous hypothesis that SPAG5 inhibits mTORC1 activity via interaction with raptor to inhibit mTORC1 assembly in HeLa cells, thus preventing mTORC1 from suppressing autophagy (Figure 2.3) (Thedieck et al., 2013). The promotion of autophagy may enhance cancer cell survival by maintaining the cell microenvironment via the recycling of cellular components. The results of Huang and Li (2020) are limited by the singular use of one cell line A549, so further research is required to confirm the conclusions reached. Given the consistency of the results with those observed in other cancers, however, it is probable that SPAG5 has an integral oncogenic role in lung cancer, so its expression and mechanical mechanisms should be studied for further understanding and treatment of lung cancer.

2.3.2 Oncogenic Properties of SPAG5 in Cervical Cancer

SPAG5 is an independent biomarker for the prognosis of cervical cancer patients (Yuan et al., 2014). The oncogenic roles of SPAG5 in cervical cancer are thus far identified within the hallmarks of

uninhibited cell proliferation and inhibition of apoptosis. While the molecular pathway for the processes observed is well understood, further research is required to determine whether the reported mechanism is consistent across cervical cancer subtypes.

SPAG5 is upregulated in pelvic lymph node metastasis-positive cervical cancer, and conversely, Yuan et al. (2014) report that downregulation of SPAG5 inhibits cell proliferation. Insufficient SPAG5 levels interrupt cell migration and invasion, and lead to cell cycle arrest at G_2/M, inducing apoptosis. However, when cells are under stress, SPAG5 prevents apoptosis by inhibiting mTORC1 association, with the mTORC1 component raptor instead binding to stress granules (table 2.1) (Thedieck et al., 2013). Also interacting with mTOR is paclitaxel, which constitutes a critical first-line cervical cancer chemotherapy (Yan et al., 2013). Paclitaxel causes p53-independent apoptosis in cervical cancer, inhibiting mitosis via cell spindle assembly disruption and ultimately inducing apoptosis in harmful cells. Yuan et al. (2014) hypothesised that this is resultant of SPAG5 downregulation, with similar observations of this interaction, observed in the lung (Spoerke et al., 2012; Sun et al., 2013), gastric (Zhang et al., 2013), liver (Yan et al., 2013), oesophageal (Qu et al., 2021), ovarian (Ho et al., 2015), breast (Dastmalchi et al., 2021), and nasopharyngeal cancers (Wong et al., 2013). Furthermore, AKT/PI3K activity and SPAG5 expression are suppressed during treatment with trastuzumab and paclitaxel (Le et al., 2005). Thus, Yuan et al. (2014)concluded that SPAG5 likely influences the therapeutic effect of paclitaxel by altering the activity of mTOR.

SPAG5 promotes apoptosis in cervical cancer cells treated with low-dose paclitaxel but prevents apoptosis at higher doses. Related is the observation that downregulation of SPAG5 increases mTOR activity, inducing cell death as mTOR leads the cell to apoptosis (Table 2.1); however, mTOR activation also protects cells under paclitaxel, so SPAG5 consequently has a lessened impact on cells treated with paclitaxel (Yuan et al., 2014). Its significant role in chemotherapy effectiveness leads to suggest that inhibition of the mTOR pathway constitutes a therapeutic target in cervical cancer treatment, and the relative expression of SPAG5 could serve as a potential therapeutic marker for this treatment.

Since 2014, further research has been completed to confirm these suggestions. Notably, analogues of the highly selective mTORC1 inhibitor rapamycin are approved for clinical use in cancer treatment, with other mTOR inhibitors possessing variable mechanisms of action since developed and undergoing clinical trials in various human cancers. However, no conclusions have been reached regarding the potential use of SPAG5 as a predictor for the therapeutic success of mTOR pathway inhibitors.

2.3.3 Oncogenic Properties of SPAG5 in Prostate Cancer

Several papers have reported the vital roles of SPAG5 in several cancers, with earlier studies showing that SPAG5 binds to microtubules, regulating spindle arrangement timing and sister chromatid separation (Thein et al., 2007). Thedieck et al. (2013) suggested the potential of SPAG5 as a promoter in tumorigenesis and cancer progression, with its overexpression, presented as a valuable biomarker in predicting the prognosis of several cancers (Thedieck et al., 2013; Välk et al., 2010; Yuan et al., 2014). SPAG5 potentially also plays a role in drug resistance of cancers, with its overexpression shown to alter the sensitivity of cervical cancer cells to paclitaxel treatment via the mTOR signalling pathway (Yuan et al., 2014). (Zhang et al., 2016) investigated the SPAG5 expression pattern associated with prostate cancer prognosis, progression, and carcinogenesis, identifying a correlation between SPAG5 expression levels and cancer progression. High SPAG5 expression was independently associated with unfavourable outcomes, and multivariate analysis suggested that SPAG5 can be utilised as a molecular marker to predict prostate cancer prognosis.

Zhang et al. (2016) proposed a novel progression-driving role of SPAG5 in prostate cancer. That miRNA miR-549 can successfully regulate SPAG5 indicates that the miR-539/SPAG5 pathway may serve as a therapeutic target for prostate cancer. SPAG5 plays an active role in prostate cancer progression, and SPAG5 knockdown can significantly impair tumour progression and metastasis in vivo (Zhang et al., 2016). Considering the relationship between miRNA miR-539 and osteosarcoma and thyroid cancer (Gu & Sun, 2015), research by Zhang et al. (2016) identified an inverse relationship between miR-549 and SPAG5 mRNA levels, miR-539 targeting of SPAG5, and the ectopic overexpression of SPAG5 resulting in the reversal miR-539 tumour suppressor effects (Table 2.1). The summary of these results suggests that SPAG5 plays an essential role in prostate cancer development and metastasis. Similar results were obtained when comparing the xenograft tumour volumes of miR-539 overexpression and SPAG5 knockdown: a decreased volume compared to control groups and reduced metastasis. Zhang et al. (2016) conclude their study with suggestions that SPAG5 has a progression-inducing function in prostate cancer, of which miR-539 can inhibit prostate growth and metastasis by inhibiting SPAG5 (Figure 2.3).

2.3.4 Oncogenic Properties of SPAG5 in Hepatocellular Cancer

SPAG5 functions as an oncogene in hepatocellular cancer. As observed in other cancers, increased SPAG5 expression in hepatocellular cancer is associated with poor prognosis (Liu, Hu, et al., 2018; Yang et al., 2018).

Overexpression of SPAG5 in hepatocellular cancer promotes tumour growth and metastasis, whereas the knockdown of SPAG5, inversely, results in inhibited growth and metastasis (Liu, Hu, et al., 2018; Yang et al., 2018). SPAG5 overexpression significantly impacts the AKT pathway in

hepatocellular cancer, perhaps unsurprisingly, given the role of SPAG5 in microtubule regulation and spindle integrity. Two key pathways are observed to explain the phenotypic effects of SPAG5 overexpression in hepatocellular cancer.

Yang et al. (2018) report SPAG5 interaction with centrosomal protein CEP55, resulting in AKT phosphorylation at Ser47, associated with cell proliferation in several cancers (Cicenas, 2008; Itoh et al., 2002; Kreisberg et al., 2004; Kunter et al., 2014). Interestingly, SPAG5-mediated growth was significantly decreased by inhibiting PI3K/AKT signalling, and miR-363-3p could suppress SPAG5 by inhibiting the activity of SPAG5 mRNA 3'UTR (Table 2.1; Figure 2.3). Furthermore, abnormal SPAG5 expression reduced miR-363-3p dependent cell cycle arrest and promoted cell proliferation.

As with many cancers, the predominant mechanisms for cell progression may vary within the cancer type. SPAG5 may promote the proliferation of cancer cells by downregulating cytoplasmic protein SCARA5 in hepatocellular cancer, and (H. Liu et al., 2018)report a negatively correlated relationship between SPAG5 and cytoplasmic protein SCARA5 in prostate hepatocellular cancer tissues. SPAG5 actively promotes cell progression in hepatocellular carcinoma by downregulating SCARA5 via modulation of β-catenin degradation (Table 2.1; Figure 2.3). Thus, several pathways in which SPAG5 may promote cell proliferation have been observed in hepatocellular cancer (Figure 2.3).

2.3.5 Oncogenic Properties of SPAG5 in Bladder Urothelial Cancer

As observed in breast, cervical, liver, and prostate cancer, SPAG5 may be a valuable prognostic biomarker of bladder urothelial carcinoma (BUC) patients (J. Y. Liu et al., 2018). SPAG5 promotes proliferation and suppresses apoptosis in BUC. It is also suggested that SPAG5 may be an effective therapeutic target in BUC.

SPAG5 promotes proliferation and suppresses apoptosis in BUC through upregulating signalling protein Wnt3 via activation of the AKT/mTOR pathway (Table 2.1; Figure 2.3) (Liu, Q. H. Zeng, et al., 2018). The AKT/mTOR pathway is a critical mitogenic process frequently activated in carcinogenesis (Slomovitz & Coleman, 2012) and functions as an oncogenic driver in many tumour types (Samarin et al., 2016; Siu et al., 2015; Slomovitz & Coleman, 2012). The AKT kinase promotes cell survival, growth and motility, further suppressing apoptosis (Liu et al., 2014), while mTOR kinase regulates protein translation, ribosome biogenesis and metabolism (Easton & Houghton, 2006). In 2013, Thedieck et al. (2013) published findings describing the downregulation of the mTOR signalling pathway by SPAG5 in response to oxidative stress and the ultimate prevention of apoptosis in breast cancer. Subsequently, the role of SPAG5 in the suppression of apoptosis and promotion of proliferation in BUC was mechanically investigated by Liu, Q. H. Zeng, et al. (2018). They presented that SPAG5 at least partially suppressed apoptosis and promoted proliferation by upregulating Wnt3

via activation of the AKT/mTOR signalling pathway, which is integral in cell cycle regulation (Table 2.1; Figure 2.3). The AKT/mTOR signalling pathway is a critical oncogenic pathway frequently activated during carcinogenesis due to its essential roles in apoptosis, survival, and growth (Guertin & Sabatini, 2007; Liu et al., 2014; Manning & Cantley, 2007; Slomovitz & Coleman, 2012). Liu, Q. H. Zeng, et al. (2018) analysed the expression of SPAG5 in BUC cell lines with Western blotting and qRT-PCR analysis. They found that tumour tissues had a statistically significant higher mRNA expression and protein levels of SPAG5 than normal tissues, providing evidence that SPAG5 levels correlate with tumour size and tumour multiplicity. The regulatory role of SPAG5 in BUC proliferation and apoptosis was investigated in both *in vitro* and *in vivo* assays; Knockout of SPAG5 in BUC cells resulted in reduced proliferation and increased rate of apoptosis, whereas SPAG5 overexpression in BIU87 BUC cells inversely increased proliferation and decreased cell death. The results of this study provide evidence that SPAG5 has an integral role in the regulation of proliferation and apoptosis, and therefore functions as an oncogene in BUC. However, this study focused solely on BUC cell line BIU87 cells, and further experiments should be conducted to confirm the oncogenic properties of SPAG5 in bladder urothelial cancer. Furthermore, the molecular mechanisms involved in the pathway of this relationship remain unclear and should be determined to understand the potential of SPAG5 as a therapeutic target in BUC treatment.

2.3.6 Oncogenic Properties of SPAG5 in Gastric Cancer

SPAG5 is frequently upregulated in gastric cancer tissues (Liu et al., 2019) and could be used as an effective biomarker for malignant phenotype and overall survival of patients with gastric cancer. Moreover, knockdown of SPAG5 in gastric cancer significantly inhibits the proliferation of gastric cancer cells, simultaneously increasing apoptosis (Liu et al., 2019). Recent studies conclude that Survivin is an apoptosis inhibitor associated with poor prognosis in several human cancers (Gunaldi et al., 2018; Jaiswal et al., 2015). With the evidence of the oncogenic properties of SPAG5 and its upregulation and biomarker potential for poor patient prognosis in various previously discussed cancers, this is likely also the case for SPAG5 in gastric cancer. Liu et al. (2019) report that SPAG5 promotes proliferation and inhibits apoptosis in gastric cancer through regulating the oncogenic protein Survivin via the Wnt/β-catenin pathway (Table 2.1). However, the molecular mechanism of this suggested pathway is not yet fully understood, and further research to determine this should be conducted. Nonetheless, these results show the promising potential of SPAG5 as a therapeutic target to halt or prevent progression in gastric cancer patients.

2.3.7 Oncogenic Properties of SPAG5 in Ovarian Cancer

SPAG5 is noted to be overexpressed in ovarian cancers (Zhang et al., 2020). Its increased expression in cancerous ovarian tissues is related to lower survival rates and constituting an

independent prognostic factor for disease-free survival in ovarian cancer patients. In a study published by Zhang et al. (2020), multiple ciliopathic characteristics of ovarian cancers were correlated with SPAG5 overexpression, such as distant and lymph node metastases, histological type, TNM staging, and prognosis. Although these results present a highly significant correlation and are consistent with the results found in the many cancers discussed above, the small sample size and lack of confirmation in either *in vitro* or *in vivo* models demonstrate a need for further large-scale investigations to confirm these conclusions. Furthermore, the biological pathways should be determined to understand better the impact of SPAG5 expression in ovarian cancer development and metastasis. Such research would be an invaluable contribution to understanding SPAG5 pathways and thus towards the potential utilisation of SPAG5 as a prognostic marker and therapeutic target.

2.3.8 Oncogenic Properties of SPAG5 in Breast Cancer

Several studies have found potential use for SPAG5 as a biomarker. Bertucci et al. (2016) identified SPAG5 as a proliferation marker in breast cancer, while Abdel-Fatah et al. (2016) identified SPAG5 as a serviceable biomarker for determining sensitivity to chemotherapy of breast cancers. SPAG5 also functions as an oncogene in breast cancer, preventing apoptosis in breast cancer cell lines.

Thedieck et al. (2013) found that in breast cancer cells, oxidative stress results in downregulation of the mTOR signalling pathway by SPAG5, preventing apoptosis. The study presents SPAG5-raptor binding when the raptor is not bound within an mTOR complex, with a positive correlation between SPAG5-protein levels and AKT activity. The negative correlation between SPAG5 and phosphorylation of mTORC1 substrates PRAS40-S183 and S6K1-T389 suggests that SPAG5 exerts an inhibitory effect on the mammalian target of rapamycin complex 1, mTORC1. This protein complex controls growth and survival in response to metabolic signals. Furthermore, SPAG5 protein specifically interacts with the mTORC1 component raptor, mediated by the SPAG5-terminal head domain. Due to competition with mTOR for raptor binding, mTORC1 formation increases in the absence of SPAG5, ultimately inhibiting mTORC1 signalling independent of the mitotic functions of SPAG5. Thedieck et al. (2013) also determined SPAG5's inhibitory effect on mTOR substrate S6K1-pT389 to be mTORC1 dependent, ultimately determining that the mTORC network interaction is accelerated in the absence of SPAG5 protein, alongside the increased association of mTOR and raptor. This confirms the requirement of stress granule presence for SPAG5 to prevent hyperactivation.

Hyperactive mTORC1 signalling increases apoptosis rate (Sosa et al., 2013), while decreased SPAG5 also aids to facilitates apoptosis (Gruber et al., 2002; J. Y. Liu et al., 2018), as apoptosis in cells with reduced SPAG5 is mediated by mTORC1 hyperactivation induced by decreased SPAG5 levels (Thedieck et al., 2013). Overexpression of SPAG5 would therefore prevent apoptosis through the prevention of mTORC1 hyperactivation. The results were consistent when tested using siAstrin

facilitated PARP cleavage in breast cancer cell line MCF-7, although results were not reported for the several other breast cancer cell lines tested. The reported results confirm that SPAG5 may inhibit apoptosis in some cancer cells by preventing mTORC1 hyperactivation upon oxidative stress, but further research should be conducted to determine whether this mechanism is consistent across breast cancer subtypes.

2.3.9 Summary of Properties of SPAG5 in Various Cancers

Table 2.1 and Figure 2.3 below outline the summary of SPAG5 expression, effects and known pathways in various cancers discussed above.

Table 2.1: Summary of SPAG5 Expression and Affects in Cancers

Type of Cancer	SPAG5 Expression	Result	Oncogenic Properties (+, promotion; -, inhibition)	Downstream Pathways	Possible Upstream Suppressor (-) and Promoter (+)	Model	References
Non-small Cell Lung Cancer (NSCLC)	Upregulated	• Poor Prognosis • Resistance to gefitinib	Growth^{+} Invasion^{+}	PI3K/AKT	p53-p21 axis^{-} miR1179^{-} miR-133a-3P^{-}	NSCLC specimen PC9, NCI-H1581 and NCI-H2122 NSCLC cells	(Li et al., 2021; Song et al., 2018; Välk et al., 2010)
Cervical Cancer	Upregulated	• Poor survival rate • Poor DFS • Resistance to Taxol	Proliferation^{+} Growth^{+} Migration^{+} Invasion^{+}	mTOR pathway Wnt/ β-catenin	miR-367-3p^{-}	Cervical cancer specimen HeLa and SiHa cervical cancer cells	(Yang et al., 2020; Yuan et al., 2014)
Breast Cancer (BC)	Upregulated	• Poor prognosis • Local recurrence • Poor OS and DFS • Resistance to olaparib • Resistance to endocrine therapy	Proliferation^{+} Growth^{+} Migration^{+} Invasion^{+} Lymph node metastasis^{+}	Wnt3/β-catenin/TCF4 MYCBP/c-MYC	miR-10b-3p^{-} YAP/TAZ/TEAD^{+}	BC specimen BC patients MDA-MB-231, MDA-MB-468, Hs-578t, BT20, BT549, and MCF-7 BC cells	(Abdel-Fatah et al., 2016; Hanahan & Folkman, 1996)
Prostate Cancer (PC)	Upregulated	• Poor prognosis • Clinical stage • Gleason score • Recurrence	Proliferation^{+} Migration^{+} Invasion^{+} Lymph node metastasis^{+}	-	miR-549^{-}	PC specimen PC-3 and LNCaP cells Xenograft mice	(Zhang et al., 2016)
Hepatocellular Cancer (HCC)	Upregulated	• Poor survival rates • Poor OS and DFS • Poor tumour differentiation • Large tumour size • TNM stage	Proliferation^{+} Growth^{+} Apoptosis^{-} Migration^{+} Invasion^{+} Lymph node metastasis^{+}	β-catenin/TCF4/ SCARA5 CEP55/PI3K/ AKT	miR-363-3p^{-} miR1179^{-} circFOXM1^{+}	HCC specimen Huh7, HCCLM3, SMCC7721, HepG2, Hep3B, PLC8024, MHCC97-H, and QGY-7703 HCC cells Xenograft mice	(H. Liu et al., 2018; J. Y. Liu et al., 2018; Wang et al., 2021; Yang et al., 2018)
Bladder Urothelial Cancer (BUC)	Upregulated	• Poor prognosis • Poor OS • Large tumour size • Tumour multiplicity • Worse survival	Proliferation^{+} Growth^{+} Apoptosis^{-} Migration^{+} Invasion^{+} Apoptosis^{-}	PI3K/AKT/mTOR/WNT3	-	BUC specimen BIU-87, 5637, T24, EJ, and RT4 BUC cells Xenograft mice	(Liu, Q. H. Zeng, et al., 2018; Liu et al., 2021)

Gastric Cancer (GC)	Upregulated	• Poor prognosis • Poor OS and DFS • Large tumour size • TNM stage • Invasion depth	Proliferation^{+}	Wnt/β-catenin/Survivin	-	GC specimen MKN28, MGC803, BGC823, and SGC7901 GC cells	(Liu et al., 2019)
Ovarian Cancer (OC)	Upregulated	• Poor prognosis • Histological type • TNM stage • Poor OS and DFS	Lymph node metastasis^{+} Distant metastasis^{+}	-	-	OC specimen	(Zhang et al., 2020)
Osteosarcoma (OS)	Upregulated	• Poor prognosis • Malignant phenotype • Poor OS and DFS • Clinical stage	Migration^{+} Invasion^{+} Lymph node metastasis^{+} Distant metastasis^{+}	FOXM1/MMP2	-	OS specimen MG-63, Saos-2, 143B, and U2OS OS cells	(Li et al., 2020)

Abbr., DFS; disease-free survival; FOXM1, Forkhead box M1; MMP2, matrix metalloproteinase-2; OS, overall survival;

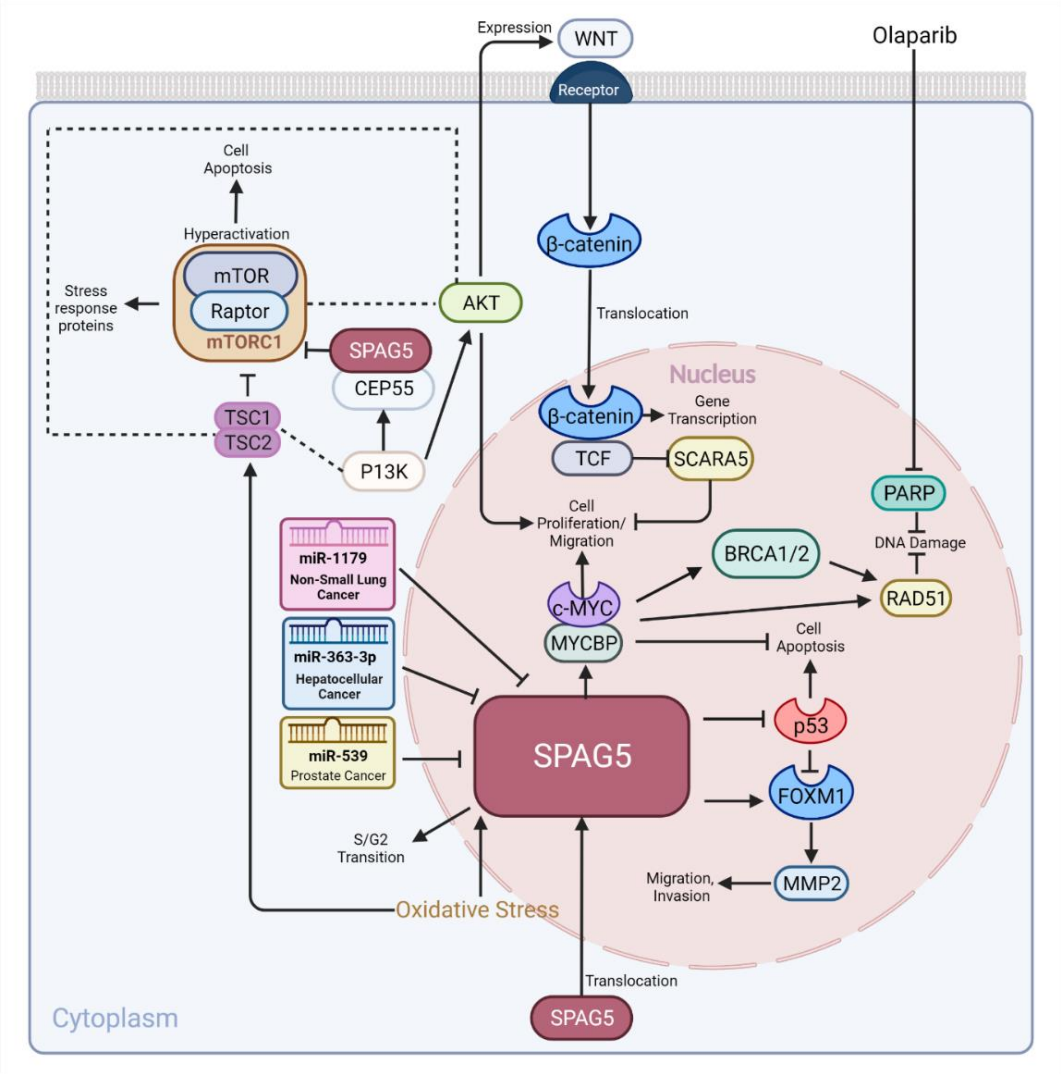

Figure 2.3: Summary of the Known Signalling Pathways of SPAG5 in Cancer.
SPAG5 inhibits apoptosis via interaction with MYCBP, which increases c-MCP activity, thereby inhibiting apoptosis and enhancing cell proliferation. Furthermore, c-MYC inhibits Olaparib effectiveness. SPAG5 upregulation of c-MCP promotes the expression of DNA repair proteins RAD51, BRCA1, and BRCA2. SPAG5 can also confer resistance to Olaparib by promoting the S/G2 phase transition, shortening the S phase in which Olaparib lesions occur. SPAG5 also inhibits apoptosis by p53 inhibition. This prevents p53 inhibition of the Forkhead box transcription factor, FOXM1. SPAG5 upregulates FOXM1, promoting MMP2 expression, resulting in increased cell invasion and migration. When the cell undergoes cytotoxic stress, SPAG5 regulates mTORC1, upregulating TSC1-TSC2, inhibiting mTORC1 activity and thereby apoptosis, promoting cell survival under stress. SPAG5 upregulates WNT3 via activation of the AKT/mTOR pathway. WNT3 upregulates β-catenin, which interacts with TCF, promoting oncogene transcription. SPAG5 also inhibits antioncogene SCARA5 through the WNT/β-catenin/TCF pathway, promoting proliferation and metastasis. SPAG5/CEP55 binding activates the PI3K/AKT/mTOR signalling pathway, associated with chemoresistance, cell progression, and metastasis. SPAG5 inhibits Olaparib effectiveness by upregulating DNA repair proteins RAD51, BRCA1, and BRCA2. SPAG5 further confers resistance to Olaparib by promoting the S/G2 phase transition, shortening the S phase where Olaparib lesions occur. miRNA molecules miR-1179, miR-363-3p, and miR-539 may inhibit cancer progression via SPAG5 in particular cancers. (*Created with BioRender.com*)

2.4 CRISPR/Cas9

Clustered regularly interspaced palindromic repeats (CRISPR)/Cas9 is a relatively novel gene editing technique that can be utilised to activate or silence genes (Redman et al., 2016). The concept is relatively simple: an 18-20 nucleotide guide RNA is designed to match the sequence of the desired target gene, and endonuclease CRISPR-Associated Protein 9 (Cas9), cuts the double-sided DNA, allowing modifications to the genome during the repair process. A homologous section of DNA containing a new sequence can be delivered alongside the guide RNA and Cas9 nuclease, replacing the removed section of unwanted sequence (Redman et al., 2016).

Utilising this method, a defective gene can be "knocked down", or disrupted, and another sequence may be inserted in its stead. Such could theoretically be as precise as a single base-pair (Redman et al., 2016).

2.5 Research Aims

SPAG5 is a novel oncogene with possibly unprecedented potential as a therapeutic target and biomarker. SPAG5 has significant roles in the several mechanistic pathways of oncogenic properties across cancer subtypes. Understanding the promising applications of targeting SPAG5 for therapeutic benefit could result in significantly improved clinical outcomes and overall survival in cancer patients worldwide. The overexpression of SPAG5 negatively affects the efficacy of several chemotherapies, and yet there are still many cancers treated by targeting the same pathways for which the impact of SPAG5 overexpression has not yet been determined. Thus, it is important that we have the correct tools to conduct the necessary research to determine this seemingly limitless potential of SPAG5 as a therapeutic target, and as a predictive biomarker.

This research aims to generate several breast cancer cell lines, namely BT549 and MCF-7, with disrupted knock-down SPAG5 function by utilising novel CRISPR/Cas9 technology. The successful establishment of such cell lines would deliver a necessary tool for further research to determine the potential of SPAG5 in breast cancer. Furthermore, as SPAG5 plays an integral role across several cancers, the generation of such cell lines would provide a framework of successful methodology that could be utilised to create potential tools in other cancers.

Chapter 3: Materials and Methodology

3.1 Materials

3.1.1 Chemicals, Reagents, Buffers and Solutions

The chemicals, reagents, buffers, solutions and kits used in this thesis are provided in Table 3.1.

Table 3.1: List of Chemicals, Reagents, Kits, Buffers and Solutions.

Product	Supplier
1kb Plus DNA Ladder	New England Biolabs, Ipswich, MA, USA
Agarose	Life Technologies, Carlsband. CA. USA
ab-241581 (anti-SPAG5 antibody)	ABCAM, Cambridge, UK
ab-184142 (anti-SPAG5 antibody)	ABCAM, Cambridge, UK
Blocking Buffer	Bio-Rad Laboratories, Hercules, CA, USA
Bovine Serum Albumin (BSA)	Sigma-Aldrich, St Louis, MO, USA
BT549 Human Breast Cancer Cell Line	American Type Culture Collection, Manassas, VA, USA
CutSmart Buffer	New England Biolabs, Ipswich, MA, USA
DMEM	Thermo Fisher Scientific, Waltham, MA, USA
DMSO	Sigma-Aldrich, St Louis, MO, USA
dNTPs	Thermo Fisher Scientific, Waltham, MA, USA
Eco RI	New England Biolabs, Ipswich, MA, USA
Fetal Bovine Serum	Thermo Fisher Scientific, Waltham, MA, USA
Hind III	New England Biolabs, Ipswich, MA, USA
L-Glutamine	Thermo Fisher Scientific, Waltham, MA, USA
Lipofectamine	Thermo Fisher Scientific, Waltham, MA, USA
Loading (2 × Laemmli) Buffer	Bio-Rad Laboratories, Hercules, CA, USA
Magnesium Carbonate ($MgCl_2$)	Sigma-Aldrich, St Louis, MO, USA
MDA-MB-231 Human Breast Cancer Cell Line	Sigma-Aldrich, St Louis, MO, USA
Microtiter Plate	Thermo Fisher Scientific, Waltham, MA, USA
Microtiter Plate Filters	Thermo Fisher Scientific, Waltham, MA, USA
MTT Cell Proliferation Assay 30-1010K	ATCC, Manassas, VA, USA
Neomycin G418	InvivoGen, San Diago, CA, USA
Opti-MEM™ I	Thermo Fisher Scientific, Waltham, MA, USA
pCasGuide RNA Vectors	Origene, Rockville, MD, USA
P3000™	Thermo Fisher Scientific, Waltham, MA, USA
PBS	Thermo Fisher Scientific, Waltham, MA, USA
Penicillin / Streptomycin	Life Technologies, Carlsbad, CA, USA
Proteinase K	Thermo Fisher Scientific, Waltham, MA, USA
Puromycin	InvivoGen, San Diago, CA, USA
RedSafe™ N	Sigma-Aldrich, St Louis, MO, USA
RIPA Buffer	Bio-Rad Laboratories, Hercules, CA, USA
RPMI 1640 Medium	Merck, Auckland, New Zealand
Running (Tris/Glycine/SDS) Buffer	Bio-Rad Laboratories, Hercules, CA, USA
SPAG5-Donor Plasmids	Blue Heron Biotech, Bothell, WA, USA
TA810452 (anti-SPAG5 antibody)	Thermo Fisher Scientific, Waltham, MA, USA
TAE Buffer	Thermo Fisher Scientific, Waltham, MA, USA
Taq Polymerase	Thermo Fisher Scientific, Waltham, MA, USA
TB Buffer	Thermo Fisher Scientific, Waltham, MA, USA
TBE Buffer	Thermo Fisher Scientific, Waltham, MA, USA
TE Buffer	Thermo Fisher Scientific, Waltham, MA, USA

Transfer Buffer	Bio-Rad Laboratories, Hercules, CA, USA
Tris-Buffered Saline with Tween 20 (TBST) Buffer	Bio-Rad Laboratories, Hercules, CA, USA
Trypsin	Life Technologies, Carlsbad, CA, USA
Turbofectin 8.0	Thermo Fisher Scientific, Waltham, MA, USA
Tween 20	Bio-Rad Laboratories, Hercules, CA, USA

3.2 DNA Preparation and Detection

3.2.1 Guide RNA and Donor RNA Plasmid Design

For successful and accurate knockout of the desired *SPAG5* gene sequence, specially designed guide RNA and donor sequences were obtained from commercial supplier Origene. For a guide RNA expression, the pCas-Guide (Origene) vector was used. This vector contains the cDNA sequence encoding a codon-optimised Cas9 protein and the ampicillin resistance (AMP^r) gene. The pCas-Guide RNA vector is displayed in Figure 3.1 below. Two target sequences KN201783G1: 5'-CCTTCGCCCCAGACGGTAAG-3' and KN201783G2: 5'-AGATCTCCCGCTTACCGTCT-3', were previously cloned into the pCas-Guide vector by PhD Candidate Leo He. The resultant pCasG-SPAG5-guide-RNA1 and pCasG-SPAG5-guide-RNA2 plasmids both are the 7,998 bp long and were used in our experiment.

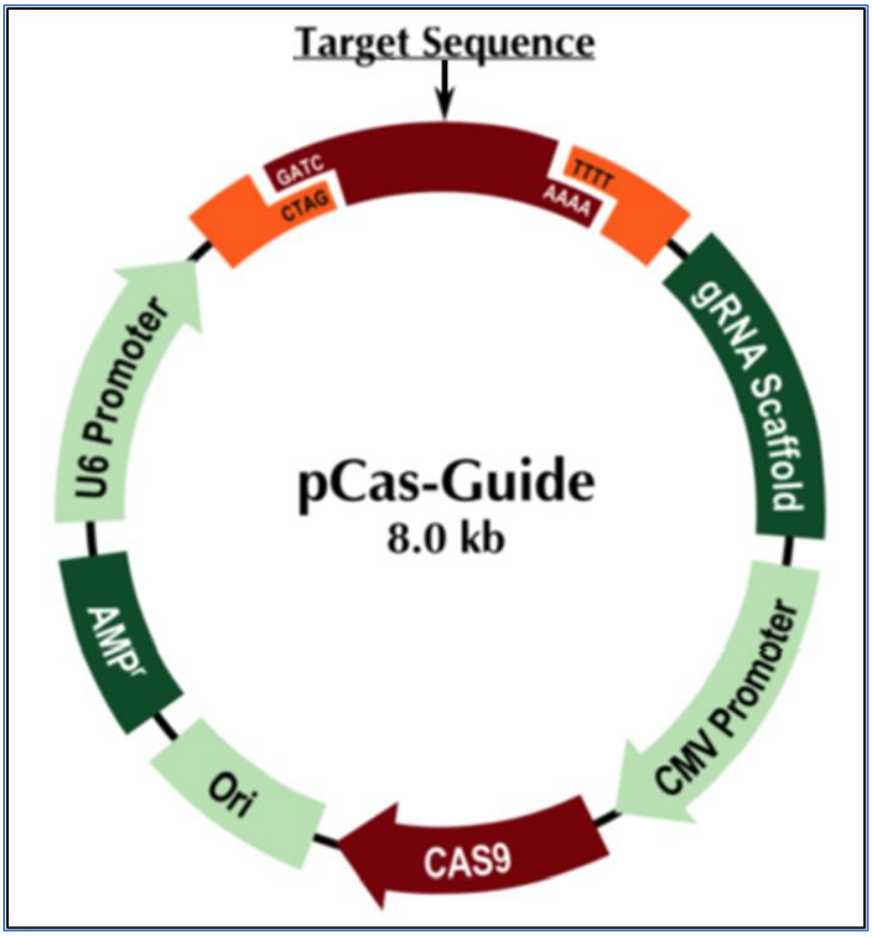

Figure 3.1: pCas-Guide RNA Vector (Origene). Figure displays the location of the target sequence of SPAG5 guideRNA, the gRNA scaffold, CMV promoter, Cas9, Ori, AMP^r, and U6 promoter.

3.2.2 Guide RNA and Donor RNA Plasmid Confirmation

Successful transfection of breast cancer cells relies on correctly identifying the guide RNA and donor RNA plasmids. To achieve this guide RNA plasmid pCasGuide-SPAG5-RNA and donor DNA plasmid pUC-SPAG5DonorLuc were digested using restriction enzymes *Eco* RI and *Hind* III, respectively. The restriction digestion was carried out as follows: 2.0 µL of 10 x CutSmart buffer, 0.5 µL BSA, 0.5 µL DNA sample, 0.5 µL of the respective enzyme, and 16.5 µL of Milli-Q water were combined to create our digestion solution. The components were then centrifuged for 2 minutes at 2000g and incubated in a 37°C water bath for 90 minutes. PCR conditions were as outlined in Table 3.4.

3.2.2.1 Gel Electrophoresis

Gel electrophoresis was performed to confirm DNA fragments visually; therefore, the plasmids were utilised in the experiment. A 1% agarose gel was prepared by dissolving 1.0g of agarose in 100mL of TAE buffer in the microwave for 2.5 minutes on high. After 3 minutes of cooling at room temperature, 5 µL 1x Cybrsafe™ nucleic acid staining solution was added. The agarose medium was then poured into a casting tray with the sample comb and allowed to set for 25 minutes. The tank was filled with TB buffer.

Each 25 µL PCR product had 5 µL of 6x loading dye added and mixed thoroughly before loaded into the 1% agarose gel wells. Finally, 5 µL of the 1 kb Plus DNA Ladder (Life Technologies, Carlsbad, CA, USA) was loaded as the standard molecular weight marker. Gel electrophoresis was then performed, running at 80 V for 10 minutes, followed by 120 V for 50 minutes. Images of the resultant gel were taken under UV light. The expected results are outlined in Table 3.2 below.

Table 3.2: Expected Results of Enzyme Digestion of Guide and Donor Plasmids

Plasmid Name	Plasmid Size	Restriction Enzyme Used	Expected Digested Band Sizes	Target Sequence (5' to 3')
pCasGuide-SPAG5-RNA1	7998 bp	*Eco* RI	1123 bp, 6875 bp	TGAGGCCCGTTTAGATACCA
pCasGuide-SPAG5-RNA2	7998 bp	*Eco* RI	1123 bp, 6875 bp	ACCTTTGAGAACAGACGATC
pUC-SPAG5DonorLuc	8014 bp	*Hind* III	566 bp, 7448 bp	-
pUC-SPAG5DonorGFPneo	7261 bp	*Hind* III	3040 bp, 3601 bp	-

3.3 Cell Maintenance

Regular maintenance of the cancer cell culture is required to allow consistent growth and survival of the wild-type breast cancer cell lines BT549 and MCF-7. All cell maintenance was performed in a sterile laminar flow hood. Cells were cultured in a 37°C humidified incubator with 5% CO_2. Complete media was prepared for the cells, comprising Dulbecco's Modified Eagle Medium (DMEM), 10% heat-inactivated FBS, 1% L-glutamine, 100 U/mL Penicillin and 100 U/mL streptomycin.

3.3.1 Passaging Cells

The maintenance of cells requires regular passaging to provide adequate media and space within plates for cells to survive and divide. Human breast cancer cell lines MCF-7 and BT549 were sub-cultured every seven days throughout this experiment using the following procedure for a total of 10-25 passages. Cells were maintained within a T25 flask, and before sub-culturing, the used media would be removed from the cells. Cells were washed with 2 mL 1 x PBS. 1mL of trypsin was added to the cells, and they were incubated for 4 minutes at 37°C, enabling the cells to detach from the surface of the T25 flask. The cells were then transferred into a 15mL conical tube thoroughly in 2 mL of the complete media and centrifuged at 200 × g for 5 to 10 minutes. The resultant supernatant was removed, and the pellet of cells was resuspended in 1mL of complete media. A new T25 flask containing 6 mL of complete media was prepared, and 200 µL of the resuspended cells were transferred into the new flask.

3.3.2 Regular Media Changes

Cells require consistent access to nutrients to survive and proliferate. Media changes were performed every 3-4 days to maintain a stable growth of wild-type cells in between passages. The 6mL of used media was removed utilising a 10mL electrical pipette and discarded. The cells were then washed with 2mL 1 x PBS to remove cellular debris. Finally, another 6mL of complete media was added to the flask to provide fresh nutrients to the cells before returning them to the 37°C incubator.

3.3.3 Reviving Cells

Breast cancer BT549 and MCF-7 cells in cryogenic vials frozen in liquid nitrogen were thawed swiftly in a 37°C water bath with slight agitation. The cell stock was then transferred into a 15 mL conical tube containing 10mL of pre-warmed complete media to reduce the concentration of dimethyl sulfoxide (DMSO), which is toxic to unfrozen cells, and centrifuged for 2 minutes at 200 × g. The supernatant was then discarded, and the cells were resuspended in 6mL of complete media, cultured in a 25cm^2 culture flask, and placed in the 37°C incubator for recovery and replication. For two weeks following cell revival, media was changed every 2-3 days and passaged twice before performing transfection.

3.3.4 Freezing Cells

Cells were grown to 85% confluency in 25cm^2 culture flasks before being frozen. Cells were washed with 2mL 1 x PBS before trypsinisation and centrifuged as described in 3.2.1. After centrifugation, the supernatant was discarded, and the pellet was resuspended in 6mL of media containing 70% complete DMEM, 20% Fetal Bovine Serum (FBS), and 10% DMSO. The cell culture was then aliquoted into six cryovials, and chilled in the -80°C freezer overnight, before transferred into the liquid nitrogen tank for long-term storage.

3.4 Establishing Stable SPAG5-Knock Out Cell Lines

3.4.1 Stable Transfection

To achieve effective transfection of the cells, the confluence of 3.5 x 10^5 cells/mL for BT549 and 1.0 x 10^6 cells/mL for MCF-7 was pre-determined. Twenty-four hours before transfection, cell cultures were washed with 1 x PBS before trypsinisation, and centrifugation as described in 3.2.1. After centrifugation, the supernatant was discarded, and the cells were resuspended in 1mL complete media and mixed thoroughly. The cell cultures of BT549 and MCF-7 were manually counted using a haemocytometer. The cells were then seeded into a six-well plate to the desired concentration to reach 70% plating density at transfection.

To disrupt the SPAG5 gene within the BT549 breast cancer cells, transfection reagents were prepared in the following order: 250 µL Opti-MEM™ I; 1 µg pCasGuide-SPAG5-RNA1 or 1 µg pCasGuide-SPAG5-RNA2; 1 µg pUC-SPAG5DonorLuc or pUC-SPAG5DonorGFPneo; 6 µL Turbofectin 8.0. The solution was thoroughly mixed between each added reagent. The transfection reagents were incubated at room temperature for 15 minutes before the solution was added dropwise to the cells and incubated for 36 hours at 37°C.

Initial attempts to disrupt MCF-7 were unsuccessful, as the transfection efficiency of Turbofectin 8.0 was too low for effective transfection in breast cancer cell line MCF-7. Therefore, MCF-7 cells were transfected utilising Lipofectamine 3000 reagent, which yields a superior transfection efficiency. Transfection reagents for MCF-7 cells were prepared in 1.5mL centrifuge tubes: In tube 1, 7.5 µL Lipofectamine 3000 reagent was added to 125 µL of Opti-MEM™ I medium. In tube 2, 5 µL of P3000™ reagent, 1.25 µg of the gRNA plasmid, and 1.25 µg of the donor plasmid were added to 125 µL of Opti-MEM™ I medium and mixed thoroughly. Tube 2 was then combined thoroughly with tube 1 and was incubated at room temperature for 15 minutes. Finally, the solution was added dropwise to the cells and swirled gently in the plate to ensure homogenous distribution and incubated for 36 hours at 37°C.

Thirty-six hours after transfection, both cell lines were washed with 1 mL PBS before trypsinisation, and centrifugation as described in 3.2.1. The supernatant was removed, and the cells were resuspended in 4 mL of complete media. Finally, 1 mL of each cell culture was added to four Petri dishes containing 9 mL complete media. The cells were washed with 2 mL PBS and had media changes every 2 to 3 days for seven days following subculture to allow for time for the expression of the inserted drug-resistance genes.

3.4.2 Stable Cell Selection

After one week of transfection recovery, the existing media was removed and replaced with complete media containing the relevant antibiotic for selection. Cells transfected with pUC-SPAG5-DonorLuc were selected using a gradually increasing puromycin concentration to 1µg/mL for both cell lines. Cells transfected with pUC-SPAG5DonorGFPNeo were selected with progressively increasing neomycin (G418) concentration up to 700 µg/mL for BT549 cells and 500 µg/mL for MCF-7 cells. The media containing a selective antibiotic was changed every 2 to 3 days for 4 to 5 weeks until the antibiotic-resistant colonies were visible on the Petri dish without magnification.

Once the colonies were visible on the plate, the individual colonies were transferred into a 96-well plate. The colonies were viewed under a microscope inside the sterile laminar flow hood to achieve this. The cells were then gently removed from the bottom of the plate with a 10 µL pipette tip, allowing the colony to be pipetted into the tip with 10 µL of surrounding media and transferred into a single well containing 10 µL complete media. The cells were allowed to grow for one week with regular media changes before subculturing the cells into a second 96-well plate for confirmation of *SPAG5* gene disruption.

3.5 Confirmation of Successful Disruption of SPAG5

3.5.1 Cell Lysis and DNA Extraction

The transfected BT549 and MCF-7 cells were lysed in a lysate solution comprising 3 mL 1 x TE buffer, 300 µL 0.1% Tween 20, and 150 µL Proteinase K. The complete media was removed from the 96-well plates, and 40µL of the lysate solution was transferred into each well. The cells were then placed in the Eppendorf Master Cycler PCR Machine. The cycle was constructed at 56°C for 15 minutes, allowing proteinase K to digest contaminating proteins and protect DNA from nuclease digestion, followed by 95°C for 10 minutes, denaturing all proteins, including proteinase K. This process was also repeated for the wild-type of each cell line to be utilised as a negative control.

3.5.2 PCR

The PCR reaction solution was prepared in a 96-well PCR plate. Each well contained the PCR reaction solution comprised of 2 µL $MgCl_2$, 2.5 µL 10x PCR buffer, 2 µL dNTPs, 12.5 µl deionised water,

1µL Taq polymerase, 0.5 µL forward primer Puro5, and 0.5 µL reverse primer SPAG5-R3. SPAG5 primer sequences can be found in Table 3.3. Finally, 4 µL of each single colony DNA lysate solution was transferred into the PCR plate and mixed well before the plate was sealed and placed into the Master Cycler Pro PCR System under the conditions outlined in Table 3.4 below.

Table 3.3: Primer Sequences used in Genomic PCR Screening for *SPAG5* Gene Knockout Clones.

Primer	Sequence (5' to 3')
Forward Primer Puro5	TTGAATGGAAGGATTGGAGCTAC
Reverse Primer SPAG5-R3	GACTGACCTTTCCGTAAGTGAC

Table 3.4: List of PCR Stages and Conditions

PCR Step	Temperature	Time Elapsed	Cycles
Initialisation	95°C	10 minutes	1
Denaturation	95°C	30 seconds	40
Annealing	62°C	30 seconds	40
Elongation	74°C	90 seconds	40
Final Elongation	74°C	7 minutes	1
Final Hold	4°C	-	-

A 1% agarose gel was prepared as described in section 3.1.2.1, and the electrophoresis tank was filled with TB buffer, covering the 1% agarose gel. Each single colony PCR product was thoroughly mixed with 5 µL of loading dye before loading into the gel. A confirmed SPAG5 knockout product was provided by PhD candidate Ji He (Auckland University of Technology) as a positive control. The negative controls and 10 µL of 1 kb DNA ladder were loaded into the gel. Gel electrophoresis was performed at 50 V for 10 minutes, followed by 100 V for 30 minutes. Finally, the gel was removed from the electrophoresis tank, and a UV image was recorded.

3.5.3 DNA Sequencing

DNA sequencing was conducted by Massey Genome Service at Massey University to confirm the successful disruption of the *SPAG5* gene in BT549 and MCF-7. This was performed using Sanger Sequencing technology, which is outlined in 5.3.2.

3.5.4 Western Blotting

3.5.4.1 Sample Preparation

To isolate the proteins for western blotting, the cells must first be lysed. The cells were grown to 80% confluence in a 25 mm^2 flask before cell lysing. The cells were washed with PBS and an aliquot of 500 µL lysis buffercomprised of dithiothreitol-containing Laemmli sample buffer [62.5 mM, tris-HCl (pH 6.8), 2% SDS, 10% glycerol, 100 mM dithiothreitol, and 0.01% bromophenol blue] was added into each 25 mm^2 flask. . The cell lysates were collected after shaking each flask for 5 minutes. Viscosity of these lysates was reduced by passing them vigorously through a 27.5-gauge needle 10 times.

3.5.4.2 Gel Preparation

The 10% polyacrylamide gels were cast in a casting stand, 1.0 mm glass spacer plates and 10 well combs. Running and stacking gel solutions were prepared separately immediately before the respective gel was poured. The compositions for these gels are listed in Table 3.5 below.

Table 3.5: Protein Gel Composition for Western Blot

Gel Components	Running Gel	Stacking Gel
40% Acrylamide/Bis Solution	2.5 mL	0.5 mL
1.5M Tris-HCl buffer pH 8.8	2.5 mL	1.25 mL
H_2O	4.85 mL	3.2 mL
10% SDS	100 µL	50 µL
10% APS	100 µL	50 µL
TEMED	10 µL	5 µL

The running gel was poured slowly into the gel plates and overlayed with Milli-Q water to level a straight line at the surface of the gel and remove bubbles due to the variation in the solution densities. The running gel was left to set for 30 minutes. The Milli-Q water was then removed, the stacking gel was poured, and the 10-well comb was inserted. The stacking gel was left to set for 30 minutes.

3.5.4.3 SDS-PAGE

Once the stacking gel was completely set, the gel was placed in the cell, and the cell was filled with 1 x SDS running buffer. The 10 mm comb was extradited, and the gel debris was removed. Once the gel was ready, 40 µL of each sample was loaded into the wells beside 10 µL of the protein standard. The gel was run at 50 V for 10 minutes, followed by 100 V for 1 hour.

3.5.4.4. Wet Transfer

Wet transfers are ideal for protein transfers due to their higher efficiency rate when compared to semi-dry transfers and are especially recommended for large proteins, such as SPAG5 (135 kDa). The gel was placed in 1 x transfer buffer for 15 minutes. The iron reservoir stack with the anode stack

was laid in the cassette base. The gel was aligned on the membrane, and any air bubbles were removed utilising the blotting roller. The cathode stack was then placed above the gel, and the blotting roller was again used to ensure consistent contact between the layers. The lid was then fitted to complete the transfer pack, and the cassette was inserted into the Trans-Blot^{R} Turbo^{TM} Transfer System and run at 100V for 90 minutes, transferring the proteins from the gel to the membrane.

3.5.4.5 Antibody Staining and Incubation

The membrane with transferred proteins was then blocked in 1 µg/mL blocking buffer with agitation for 1 hour at room temperature to prevent non-specific binding. It was then washed in TBST five times for 5 minutes on a rotator. The blot was then incubated in the antibody solution at 4˚C overnight. The blot was then rinsed five times for 5 minutes in TBST before incubating the 0.5 µg/mL HRP-conjugated secondary antibody for 1 hour at room temperature. The blot was then rinsed five times for 5 minutes with TBST and Milli-Q water before visualising the membrane.

3.5.4.6 Imaging and Data Analysis

The chemiluminescent substrate was applied to the blot, and the chemiluminescent signals were captured using the CCD camera-based imager, and digital analysis was performed to determine the signal density.

Chapter 4: Results

4.0 SPAG5 Knock Out by CRISPR/Cas9 Technology

To determine the role of SPAG5 in chemotherapy drug response in breast cancer, I used the CRISPR/Cas9 gene editing technology. Figure 4.1 illustrates the strategy to knock out *SPAG5* gene in breast cancer cell lines.

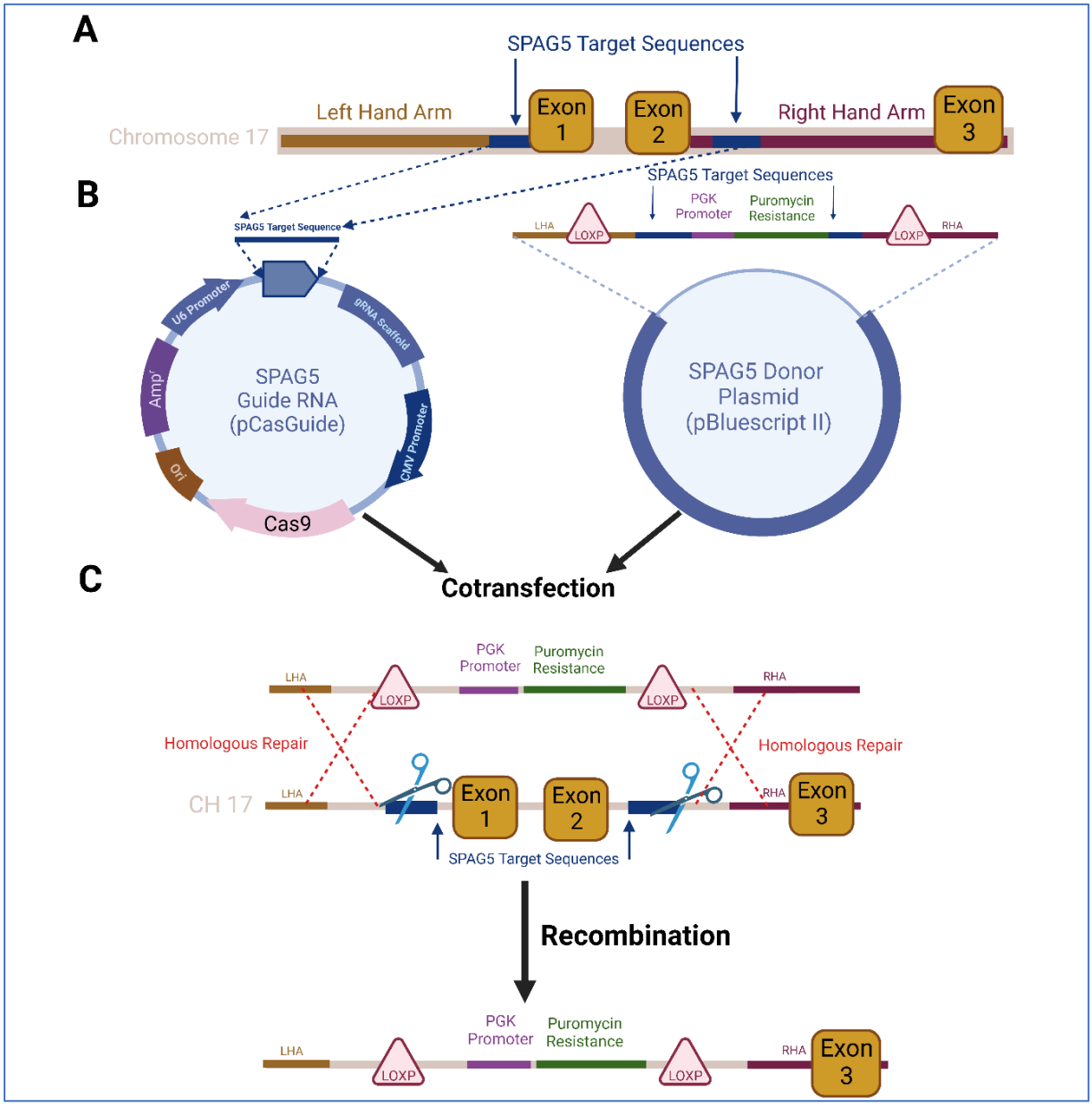

Figure 4.1: SPAG5 Knockout by CRISPR/Cas9 **A)** The original SPAG5 sequence on Chromosome 19. Fully functional exons 1, 2 and 3 are displayed, with target sequences KN201783G1 and KN201783G2 up and downstream of exons 1 and 2, respectively. **B)** Guide plasmid pCasGuide-SPAG5-RNA1/2 containing SPAG5 target sequences is displayed alongside donor plasmid SPAG5-DonorLuc, containing SPAG5 target sequences, PGK promotor, puromycin resistance gene and LoxP target sites. **C)** CRISPR/Cas9 cuts the double-stranded DNA at the SPAG5 target sites, while donor template DNA provides the template for the homologous repair. The functional cassette containing PGK promotor and puromycin resistance gene is incorporated into the genome, replacing exons 1 and 2 of the SPAG5

gene. The result after recombination is a sequence in which SPAG5 has been disrupted, instead containing the puromycin resistance gene controlled by the PGK promotor. *Created with BioRender.com*

Through CRISPR / Cas9 gene editing tool, the *SPAG5* gene on chromosome 17 was disrupted by knocking in a functional cassette of puromycin resistance gene. In this project, two *SPAG5* specific target sequences, KN201783G1 (5'-CCTTCGCCCCAGACGGTAAG-3') and KN201783G2 (5'-AGATCTCCCGCTTACCGTCT-3') were chosen to disrupt exons 1 and 2 of *SPAG5*. They were cloned into the pCasGuide (Origene) vector to express the guide RNAs, which direct the Cas9 to cut the SPAG5 gene. The knock-in sequences were cloned in the donor plasmid pUC-SPAG5-DonorLuc, flanking with the left and right hand arm sequences of SPAG5 gene. They were then inserted into SPAG5 gene when the DNA lesions were repaired by homologous repair systems. The puromycin resistance gene, which is under the control of the donor PGK promotor, served as a selection marker for knock-in clones. The SPAG5 target sequences KN201783G1 and KN201783G2 provide sites for which CRISPR/Cas will cut the double-stranded DNA while the donor template DNA provides the template for the homologous repair system. The functional cassette is then incorporated into the genome when the guide and donor DNA are co-transfected.

4.1 Confirmation of SPAG5 Expression in Wild-Type Cell Lines

To determine the successful disruption of SPAG5 expression in these cell lines, a western blot was conducted to confirm the expression of SPAG5 in the wild-type cell lines BT549, MDA-MB-231 and T47D. The results are presented in Figure 4.2.

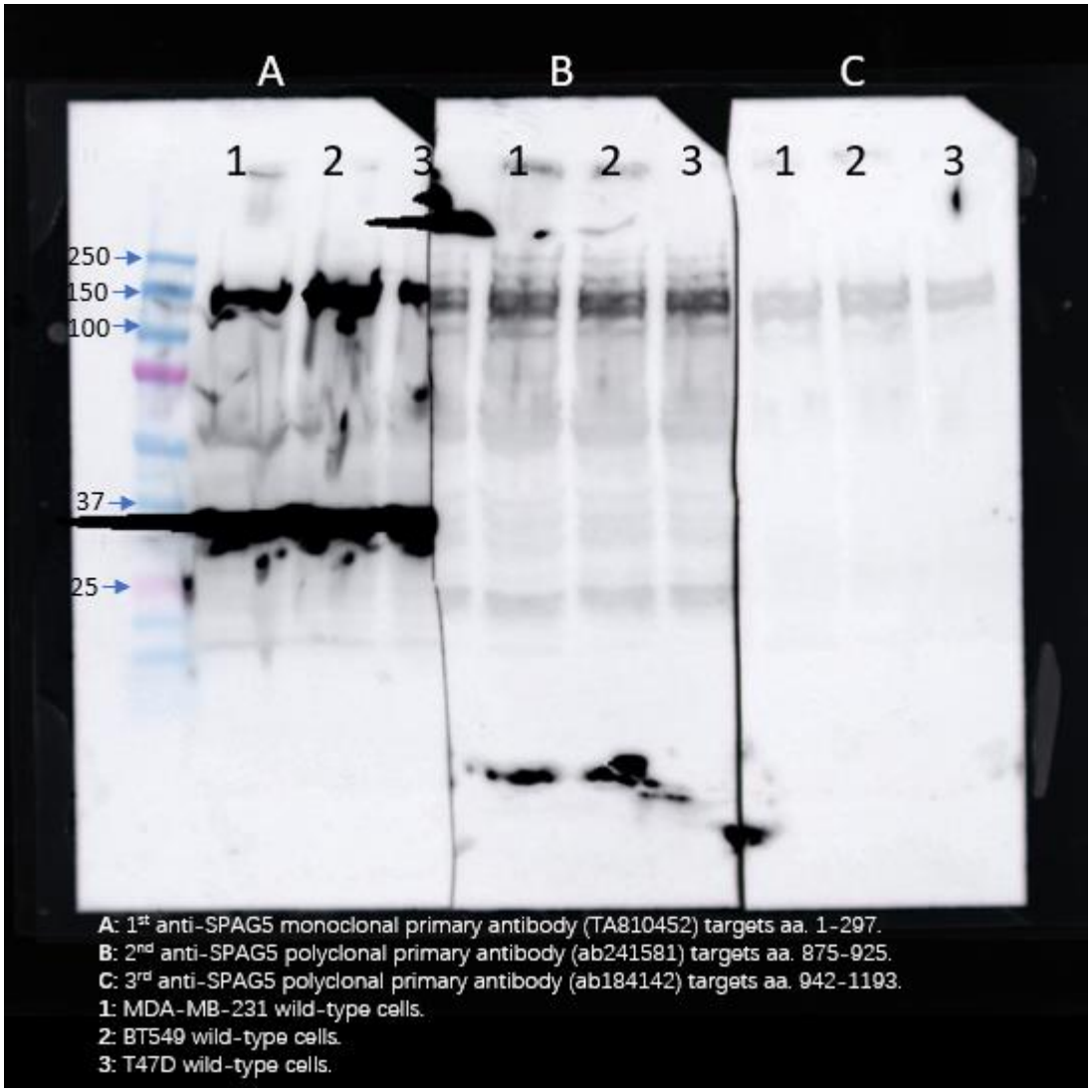

Figure 4.2: Western Blot of SPAG5 in Wild-Type Breast Cancer Cell Lines. MDA-MB-231 (1), BT549 (2) and T47D (3) confirm the expression of SPAG5 in each cell line. SPAG5 expression is detected in all wild-type cell lines examined by utilising anti-SPAG5 monoclonal primary antibodies TA810452 targeting aa. 1-297 (A), and polyclonal primary antibodies ab241581 targeting aa. 875-925 (B), and ab184142 targeting aa. 942-1193 (C).

The SPAG5 protein was present in triple-negative cell lines MDA-MB-231 and BT549 and an ER+/HER+ cell line T47. SPAG5 expression is indicated by the expected band size of approximately 170kDA. The first anti-SPAG5 monoclonal primary antibody T810452 is the most used anti-SPAG5 antibody. The second band at approximately 35kDa present in all cell lines is to be expected when using this antibody, due to a higher recognition of degraded sequences when compared to anti-SPAG5 polyclonal antibodies ab241581 and ab184142. This western blot confirms the expression of SPAG5 protein in all wild-type cell lines utilised in this thesis. A second western blot conducted under the same conditions could therefore be conducted on suspected SPAG5-knockout clones in all cell lines to confirm that SPAG5 expression has been disrupted.

4.2 DNA Preparation and Detection

Correct identification of guide and donor RNA plasmids is quintessential for the successful knockout of SPAG5 from breast cancer cell lines. The guide RNA plasmid was digested with the restriction enzyme *Eco*RI. The expected sizes of the bands with *Eco*RI digestion are displayed in Table 4.1. As demonstrated in Figure 4.3 and Figure 4.4, the guide plasmid gave a band size of 1123 bp and 6875 bp, as expected. The donor plasmid was digested with *Hind*III. The expected sizes of the bands with *Hind*III digestion are displayed in Table 4.1. As demonstrated in Figure 4.3 and Figure 4.4, the donor plasmid also gave a band size of 566 bp and 7448 bp, as expected.

Table 4.1: Expected Digested Band Sizes of Plasmids by Restriction Enzymes

Plasmid	Plasmid Size	Restriction Enzyme	Expected Digested Band Sizes
pCasGuide-SPAG5-1	7998 bp	*Eco*RI	1123 bp, 6875 bp
pUC-SPAG5-DonorLuc	8014 bp	*Hind*III	566 bp, 7448 bp

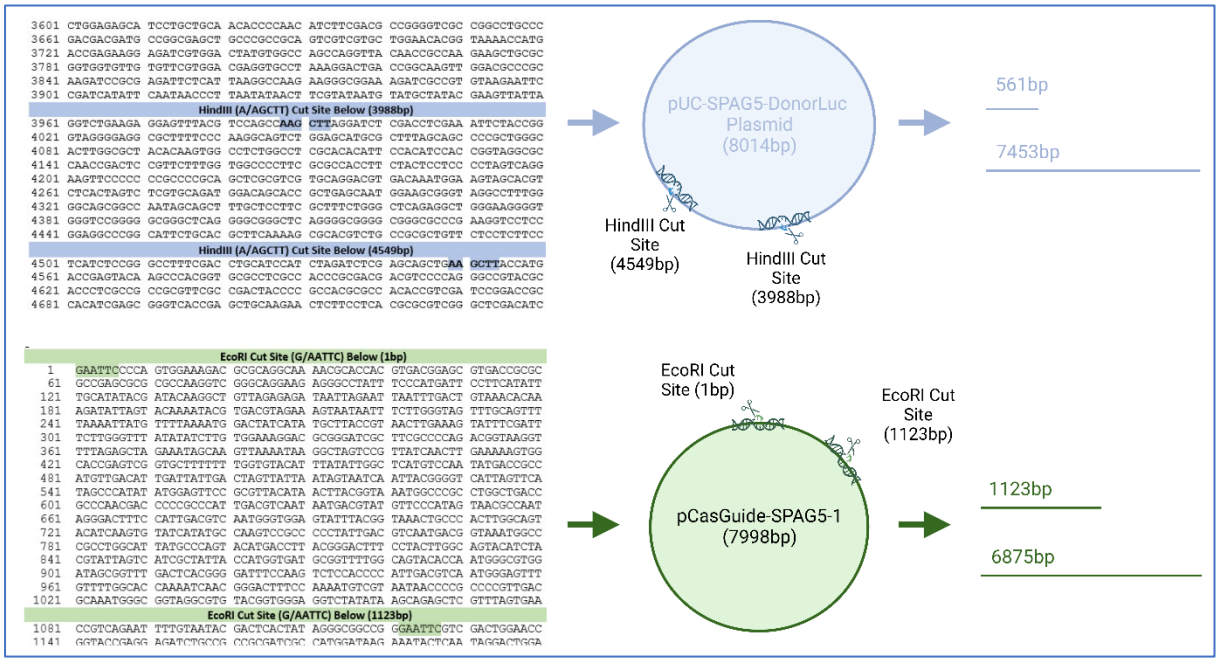

Figure 4.3: Illustrative Examples of pUC-SPAG5-DonorLuc and pCasGuide-SPAG5-RNA1 Restriction Enzyme Digestion into Measurable Band Sizes. The 8014 bp SPAG5 donor sequence contains *Hind*III cut sites located at positions 3988 and 4549 bp. When digested, two linear DNA sequences of 561bp and 7453 bp remain. The 7998 bp SPAG5 guide DNA sequence contains *Eco*RI cut sites at 1 bp and

1123bp. When digested, two linear DNA sequences of 1123bp and 6875bp remain. Created *with BioRender.com*

The restriction enzyme digestion of guide plasmids pCasGuide-SPAG5-RNA1 and donor plasmids pUC-SPAG5-DonorLuc successfully confirmed that the correct plasmids had been identified. Figure 4.3 depicts how we determine the expected band sizes when the relative restriction enzyme digests each plasmid. When digested with *Hin*dIII, 8014 bp donor plasmid pUC-SPAG5-DonorLuc is cleaved in two locations where the palindromic DNA sequence A/AGCCT is present: at 3988 bp and 4549 bp; This results in two linear DNA strands of 561 bp and 7453 bp. Similarly, when digested with *Eco*RI, 7998 bp pCasGuide-SPAG5-RNA1 is cleaved in two locations wherein the palindromic DNA sequence G/TTAAC at nt 1 and nt 1123; This results in two linear DNA strands of 1123 bp and 6875 bp.

The two expected band sizes for each digestion were present in the electrophoresis gel (Figure 4.4), indicating that guide plasmid pCasGuide-SPAG5-RNA1 and donor plasmid pUC-SPAG5-DonorLuc were correctly identified.

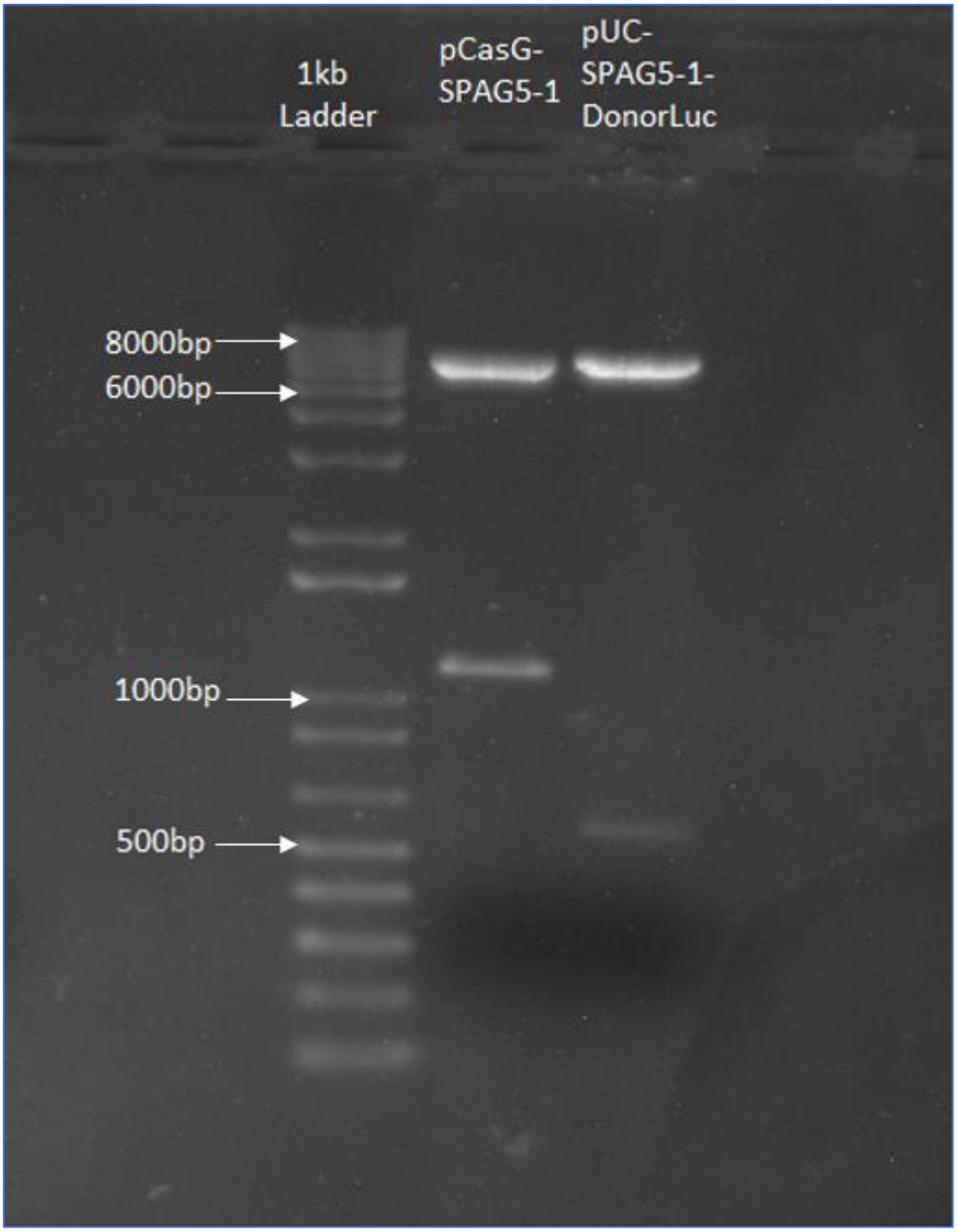

Figure 4.4: Confirmation of Guide and Donor Plasmid by Restriction Enzyme Digestion. Restriction digestion is separated by agarose gel. Gel electrophoresis displays a 1 kb DNA ladder indicating band size, and two digested plasmids: pCasGuide-RNA1 and pUC-SPAG5-DonorLuc. Digested plasmid pCasGuide-1 displays two RNA bands present, sized 1123 bp and 6875 bp, as expected. Digested plasmid SPAG5-DonorLuc is digested into two RNA bands sized approximately 566 bp and 7448 bp as expected.

4.3 Establishing Stable SPAG5-Knock Out Cell Lines

4.3.1 Stable Transfection and Cell Clone Selection

Post-transfection of two breast cancer cell lines BT549 and MCF-7 with the guide and donor plasmids, the cells recovered and were allowed to grow for between two and three months in media containing puromycin antibiotics.

The replication time for both cell lines was significantly slower than previously observed in their relative wild-type cell lines. Cell line BT549 grew into single colonies large enough to collect within seven weeks. Comparatively, MCF-7 required 12 weeks before the single-cell colonies were able to be picked up and transferred into 96-well plates. A total of 15 BT549 and 21 MCF-7 single-cell colonies were selected and seeded in a 96-well plate.

4.4 Confirmation of Successful Disruption of SPAG5

4.4.1 PCR

Potential SPAG5 knockout clones were screened by genomic PCR. As shown in Figure 4.5, the PCR screening of genomic DNA identified three BT549 clones (#8, 12, and 14), and eight MCF-7 clones (# 1, 3, 6, 11, 13, 19, 20 and 21) were potential *SPAG5* gene knockouts. They all displayed a band at the expected size of approximately 1071bp, indicating a successful SPAG5 knockout of at least on allele.

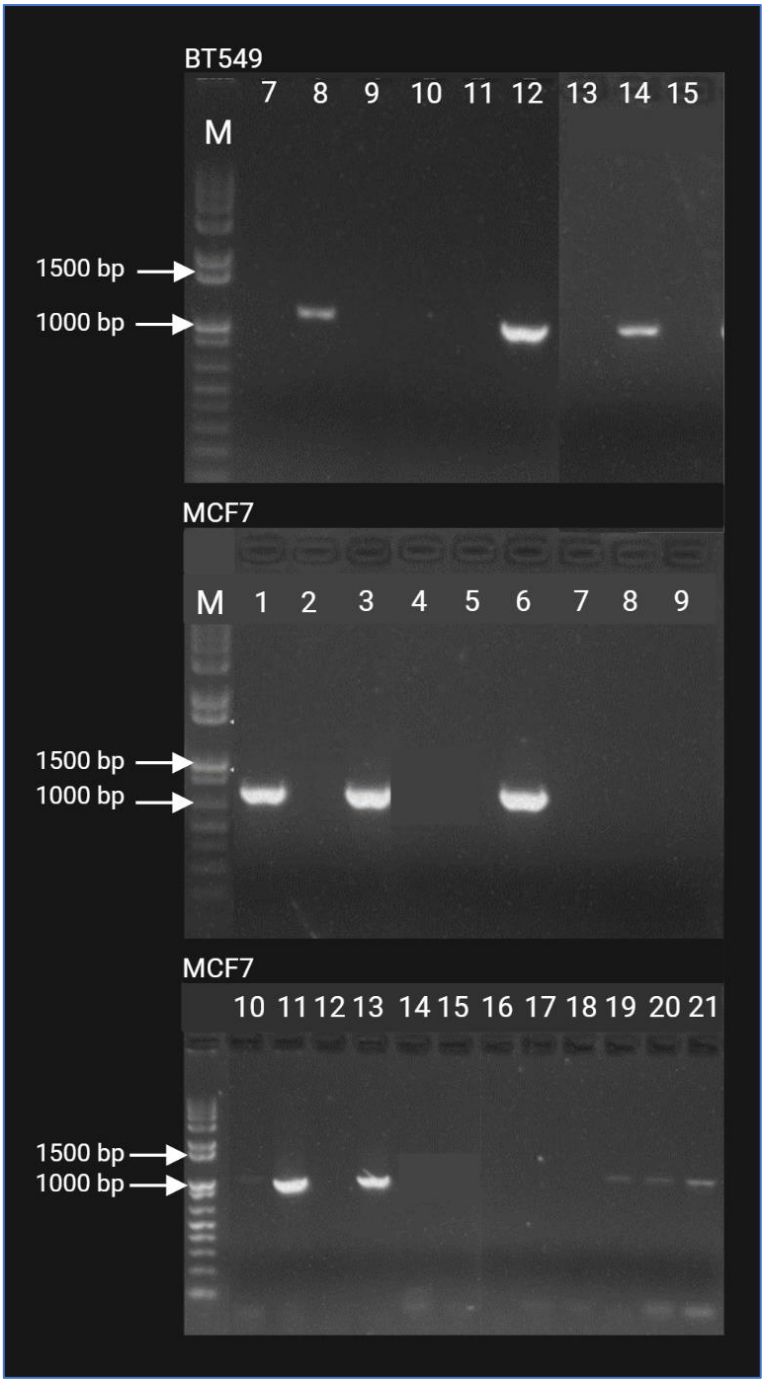

Figure 4.5: Electrophoresis Gel of BT549 and MCF-7 Clone PCR Products. Genomic DNAs were isolated from cell clones and subjected to PCR screening for potential SPAG5 gene knockout in BT549 and MCF-7 cells. The PCR products were resolved on agarose gels. Clone numbers are labelled on the top of the wells. The key size of the DNA ladder is marked on the left.

4.4.2 DNA Sequencing

To determine the sequence deleted in the positive clones obtained in the PCR screening the sequence of SPAG5 loci were analysed by DNA sequencing. Unfortunately, the clones previously identified were lost due to COVID-19 lockdown requirements. PCR confirmation was conducted on the day of a level 4 lockdown and were not able to be frozen down and were unable to be maintained throughout the lockdown. Due to time restraints, to further this project, *SPAG5* knockout clones - five BT549 cells and five MDA-MB-231 cells, were provided by PhD candidate Leo He, and sequencing was conducted on these potential knock-out clones to determine the status of *SPAG5* gene knockout homozygous (*SPAG5*$^{-/-}$) or heterozygous (*SPAG5*$^{+/-}$).

Above genomic PCR analysis of these clones confirmed that these stable knockout of SPAG5 had at least one *SPAG5* allele, i.e., allele A, deleted. The included three BT549 clones (Clones #1, 2 and 3) and five MDA-MB-231 clones (#1, 2, 3, 4, and 5). Figure 4.6 below displays the sequencing alignment of BT549 clones #1 conducted via BLASTn (*BLASTn*), in which the 589 bp of the 805 bp BT549 sequence aligned with the 8014 bp original SPAG5DonorLuc donor sequence. Within this alignment, two gaps in the sequence were recorded, and 8 bases were mis-matched. These locations are highlighted in yellow.

To determine the status of the other *SPAG5* allele, *e.g.*, allele B, a specific genomic PCR spanning the *SPAG5* gene locus was conducted. The sequence of the PCR products was determined by DNA sequencing. As shown in Figure 4.7, the allele B in this clone was interrupted by an insertion of one nucleotide (S) although the sequencing signal was not clear. There was also a nucleotide replacement of G with A.

For BT549 clone #2, allele A was interrupted by the knock-in sequence (Figure 4.8) and the allele B in this clone was interrupted by an insertion of one nucleotide (T) as clearly shown in Figure 4.9.

I also analysed the MDA-MB-231 clones by DNA sequencing. As shown in Figures 4.12-4.14, both *SPAG5* gene alleles in MDA-MB-231 Clone #3 were similarly disrupted as for BT549 clones #2

In all cases, an insertion disrupted the mRNA splicing and resulted in a reading frame shift of the allele B. Therefore, both alleles of SPAG5 gene in these clones were interrupted, they were homozygous (*SPAG5*$^{-/-}$).

BT549 Clone 1 Allele A

Sequence ID: Query_43343 Length: 8014 Number of Matches: 1

Range 1: 1648 to 2236 Graphics

Score	Expect	Identities	Gaps	Strand
1053 bits(570)	0.0	581/589(99%)	2/589(0%)	Plus/Plus

```
BT549 Clone 1      19    AGG-AAAGCCCAG-AACTCTGGAGACATTACAGCCCAGGTCGAGAACCACGGCCCGGGCC  76
                         ||| |||||||||| ||||||||||||||||||||||||||||||||||||||||||||
SPAG5DonorLuc      1648  AGGAAAAGCCCAGAAACTCTGGAGACATTACAGCCCAGGTCGAGAACCACGGCCCGGGCC  1707

BT549 Clone 1      77    GTCCCSGACGCGGGCCCACCAAGCCTAGGGAAGCCGCTCGGCACCGCTTCGGYTTCTARA  136
                         ||||| ||||||||||||||||||||||||||||||||||||||||||||| |||||| |
SPAG5DonorLuc      1708  GTCCCGGACGCGGGCCCACCAAGCCTAGGGAAGCCGCTCGGCACCGCTTCGGCTTCTAGA  1767

BT549 Clone 1      137   CTCCCTGGCCGGYTCTTTCCCGTCAAGGYTGCGGCTGGAGAGGACTGAGGGAGACCTAGG  196
                         |||||||||||| |||||||||||||| ||||||||||||||||||||||||||||||||
SPAG5DonorLuc      1768  CTCCCTGGCCGGCTCTTTCCCGTCAAGGCTGCGGCTGGAGAGGACTGAGGGAGACCTAGG  1827

BT549 Clone 1      197   GAGAGGATTCCTCTTCTCCATCCACGGAGACAACTTGGATATGAACACCATGGATGTGAG  256
                         ||||||||||||||||||||||||||||||||||||||||||||||||||||||||||||
SPAG5DonorLuc      1828  GAGAGGATTCCTCTTCTCCATCCACGGAGACAACTTGGATATGAACACCATGGATGTGAG  1887

BT549 Clone 1      257   GAGGTCCGCTGGAAGCAGGAGGGATGGACTCCTGGACTCTCCAGCTACCTGCGTGGTCCT  316
                         ||||||||||||||||||||||||||||||||||||||||||||||||||||||||||||
SPAG5DonorLuc      1888  GAGGTCCGCTGGAAGCAGGAGGGATGGACTCCTGGACTCTCCAGCTACCTGCGTGGTCCT  1947

BT549 Clone 1      317   CCCCGGTGTGAGGACAGAAGACCGGTCCTGGGCCGGGCCCGCATCCAGCCCTACCGCCGG  376
                         ||||||||||||||||||||||||||||||||||||||||||||||||||||||||||||
SPAG5DonorLuc      1948  CCCCGGTGTGAGGACAGAAGACCGGTCCTGGGCCGGGCCCGCATCCAGCCCTACCGCCGG  2007

BT549 Clone 1      377   KGTCTGAGGTGAGGGCTCCGTCAGCGGAAAACGCTCGACAACGGAGGGGCAGGCAGGGCC  436
                         |||||||||||||||||||||||||||||||||||||||||||||||||||||||||||||
SPAG5DonorLuc      2008  TGTCTGAGGTGAGGGCTCCGTCAGCGGAAAACGCTCGACAACGGAGGGGCAGGCAGGGCC  2067

BT549 Clone 1      437   GGGGGCGTGGTCAACGCGGGCCCCGCCCCCCGGGCTCTACCCCCGAGCGTACGCGCGCGC  496
                         ||||||||||||||||||||||||||||||||||||||||||||||||||||||||||||
SPAG5DonorLuc      2068  GGGGGCGTGGTCAACGCGGGCCCCGCCCCCCGGGCTCTACCCCCGAGCGTACGCGCGCGC  2127

BT549 Clone 1      497   CTGAAGCAGCCAACCAGGAAGCGCAGAGCAGGTTCAAACACAGACGGCGGGTGAACATGG  556
                         ||||||||||||||||||||||||||||||||||||||||||||||||||||||||||||
SPAG5DonorLuc      2128  CTGAAGCAGCCAACCAGGAAGCGCAGAGCAGGTTCAAACACAGACGGCGGGTGAACATGG  2187

BT549 Clone 1      557   CGTCCTCGACTTGGTCTGAGACGTGATAGGCCTGCCTTCTGGTTGAAGA 605
                         ||||||||||||||||||||||||||||||||||||||||||||||||||
SPAG5DonorLuc      2188  CGTCCTCGACTTGGTCTGAGACGTGATAGGCCTGCCTTCTGGTTGAAGA 2236
```

Key:

A: Adenine
C: Cystosine
G: Guanine
T: Thymine

S: Guanine or Cytosine
Y: Cytosine or Thymine
R: Guanine or Adenine
K: Guanine or Thymine

- : No nucleotide / gap in alignment

Figure 4.6: Sequencing Confirmation of BT549 Clone 1 SPAG5 Knockout, Allele A: Figure displays an alignment of clone BT549 allele A sequence (805 bp) with the SPAG5DonorLuc Sequence (8014 bp). The sequencing data is a 99% match of 605 bp, indicating SPAG5DonorLuc incorporation into BT549 Clone 1 and successful disruption of SPAG5. Two gaps are identified at positions 22 and 31 of BT549 clone sequence. Six positions were not identified, and were instead assigned S, Y, R, or K.

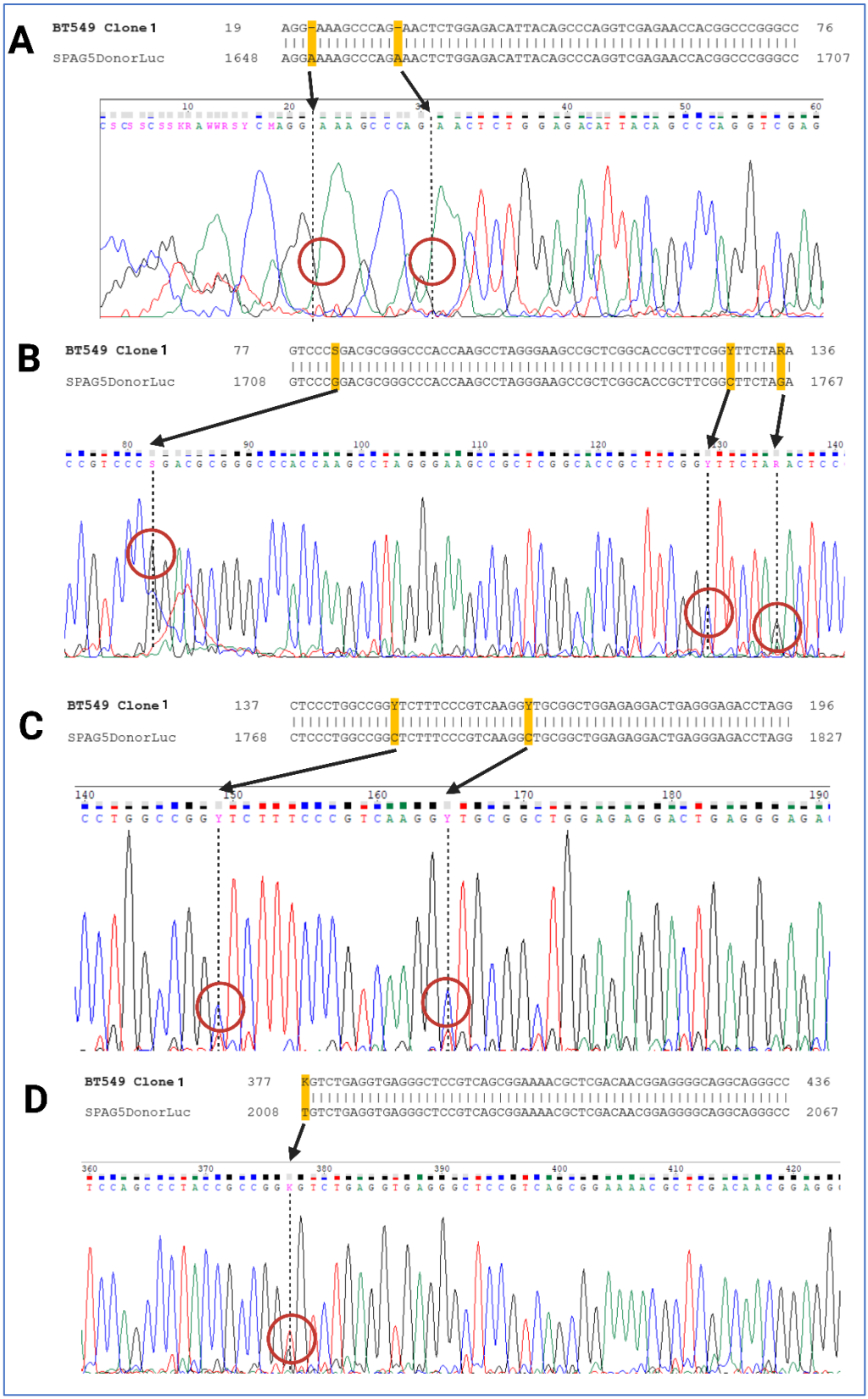

Figure 4.7: Chromatogram Analysis of Mismatches within BT549 Clone 1, Allele A and SPAG5DonorLuc Sequence. A) Gaps identified at positions 21 and 31 are circled on the histogram. **B)** Unmatched base calls "S", "Y" and "R" at locations 82, 129, and 135 are highlighted and circled on the histogram. **C)** Unmatched base calls "Y" at locations 149 and 165 are highlighted and circled on the histogram. **D)** Unmatched base call "K" at location 377 is highlighted and circled on the histogram.

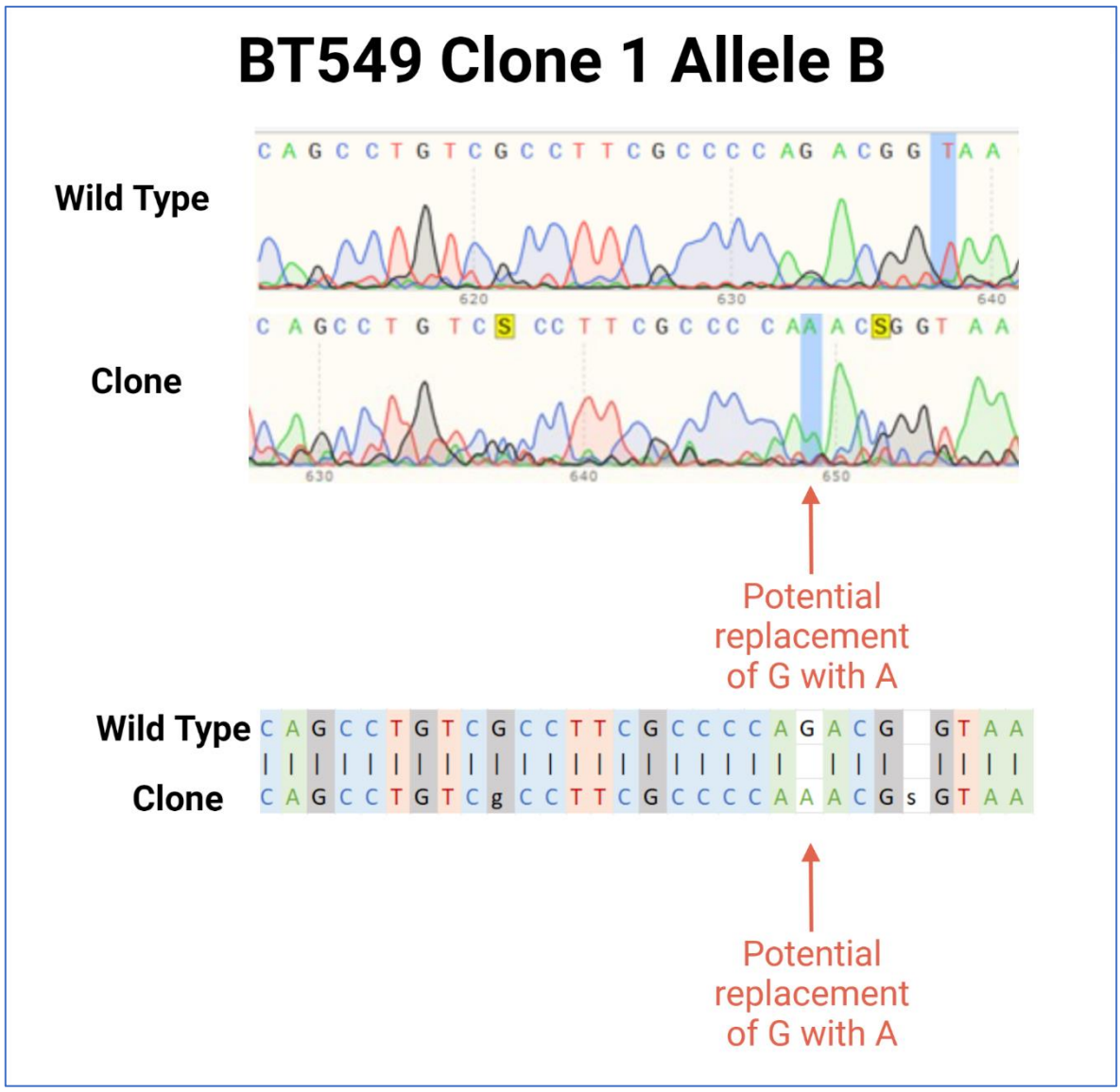

Figure 4.8: BT549 Clone 1 Allele B Histogram Sequencing and Alignment with SPAG5 Wild-Type: Figure displays a comparison of BT549 wildtype sequence and BT549 clone 1 sequence histogram. A G to A substitution is highlighted in BT549 clone 1, at position 649. The relative sequences are displayed in text.

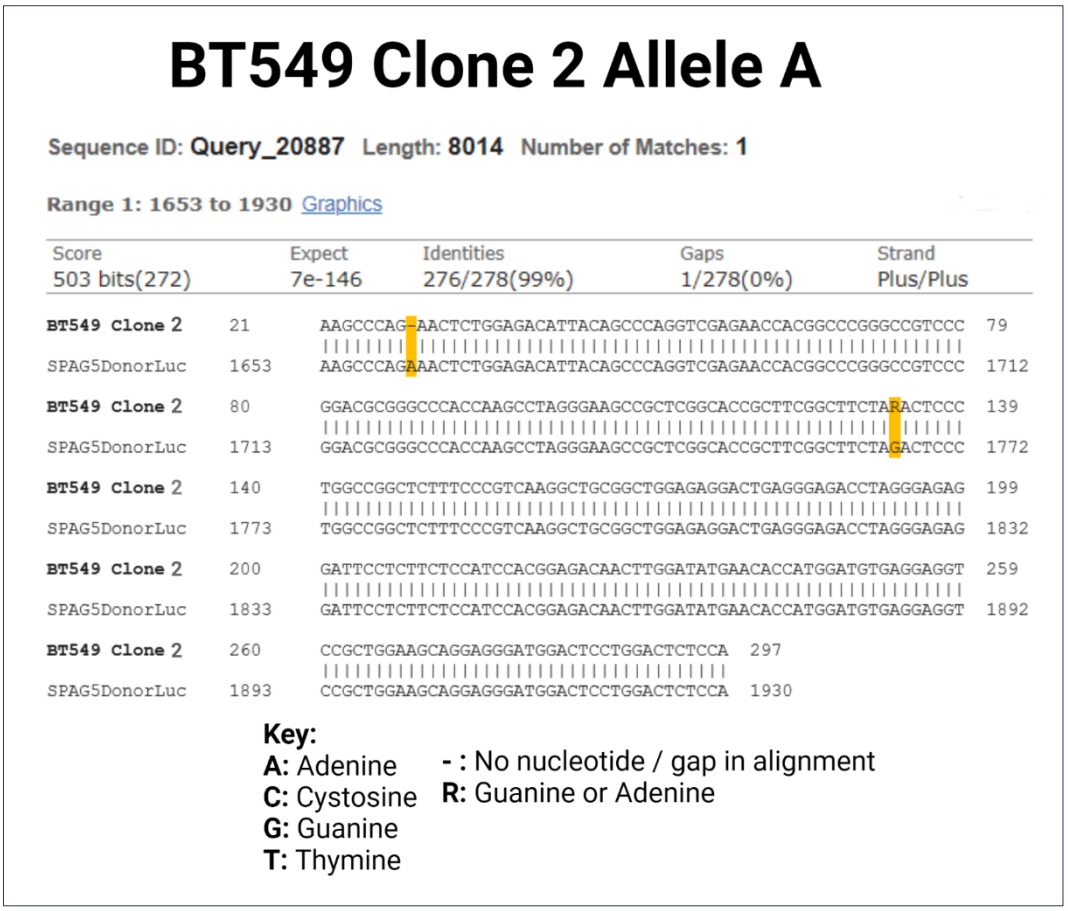

Figure 4.9: Sequencing Confirmation of BT549 Clone 2 SPAG5 Knockout, Allele A: Figure displays an alignment of clone 14 BT549 allele sequence (297 bp) with the SPAG5DonorLuc Sequence (8014 bp). The sequencing data is a 99% match of 278 bp, indicating SPAG5DonorLuc incorporation into BT549 Clone 12 and successful disruption of SPAG5. A gap is identified at position 29 of BT549 Clone 14 sequence. One unconfirmed base pair "R" is identified at position 133.

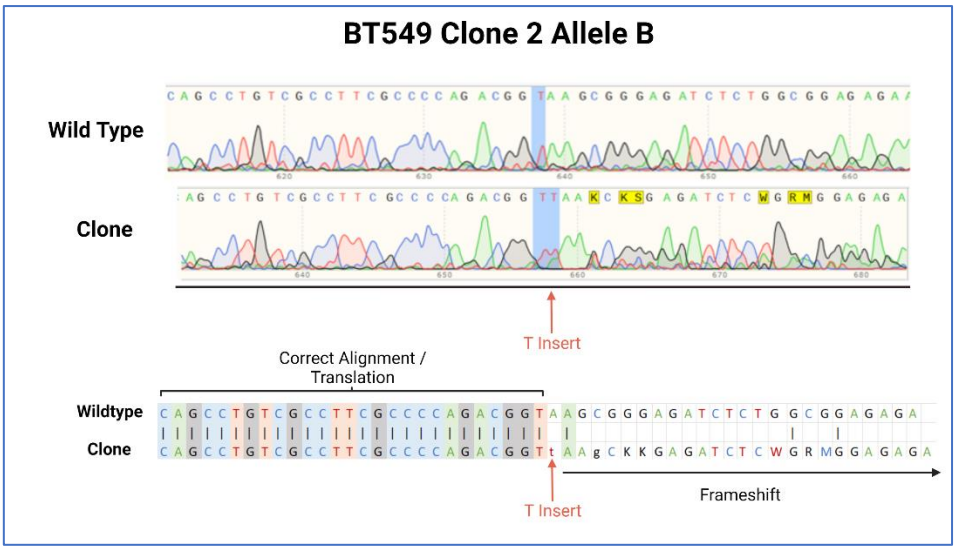

Figure 4.10: BT549 Clone 2 Allele B Histogram Sequencing and Alignment with SPAG5 Wild-Type: Figure displays a comparison of BT549 wildtype sequence and BT549 clone #1 sequence histogram. A T indel is highlighted in BT549 clone #1, at position 658. The relative sequences are displayed in text, identifying the frameshift effect downstream from the T insert.

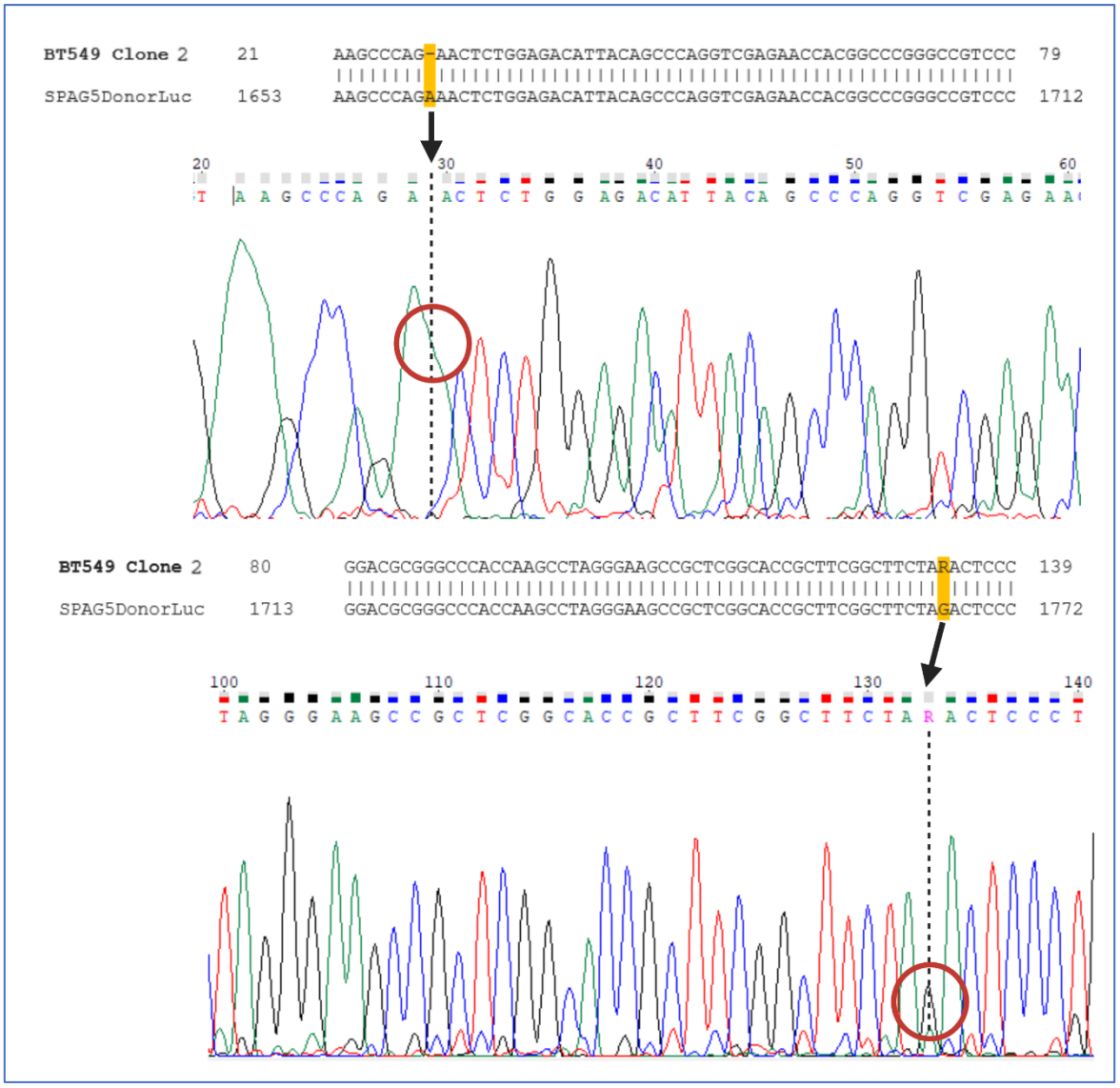

Figure 4.11: Chromatogram Analysis of Mismatches within BT549 Clone 2, Allele A and SPAG5DonorLuc Sequence. Gap identified at positions 29 is circled on the histogram. Unmatched base call "R" at position 133 is circled on the histogram.

Figure 4.12: Sequencing Confirmation of MDA-MB-231 SPAG5 Knockout, Allele A: Figure displays an alignment of MDA-MB-231 allele sequence (603 bp) with the SPAG5DonorLuc Sequence (8014 bp). The sequencing data is a 98% match of 593 bp, indicating SPAG5DonorLuc incorporation into MDA-MB-231 Clone 3 and successful disruption of SPAG5. An additional G is inserted at position 16. Two gaps are located at positions 24 and 29. Undetermined base "Y" are identified at locations 126, 146, 168, and 310. Undetermined bases "R" are identified at locations 132, 222 and 233. Undetermined base "S" is identified at locations 297. Unconfirmed base "K" us identified at location 320. Unconfirmed base W is identified at location 356. Soft-masked cytosine sequence is identified at positions 459-455, with an additional cytosine recorded at position 459.

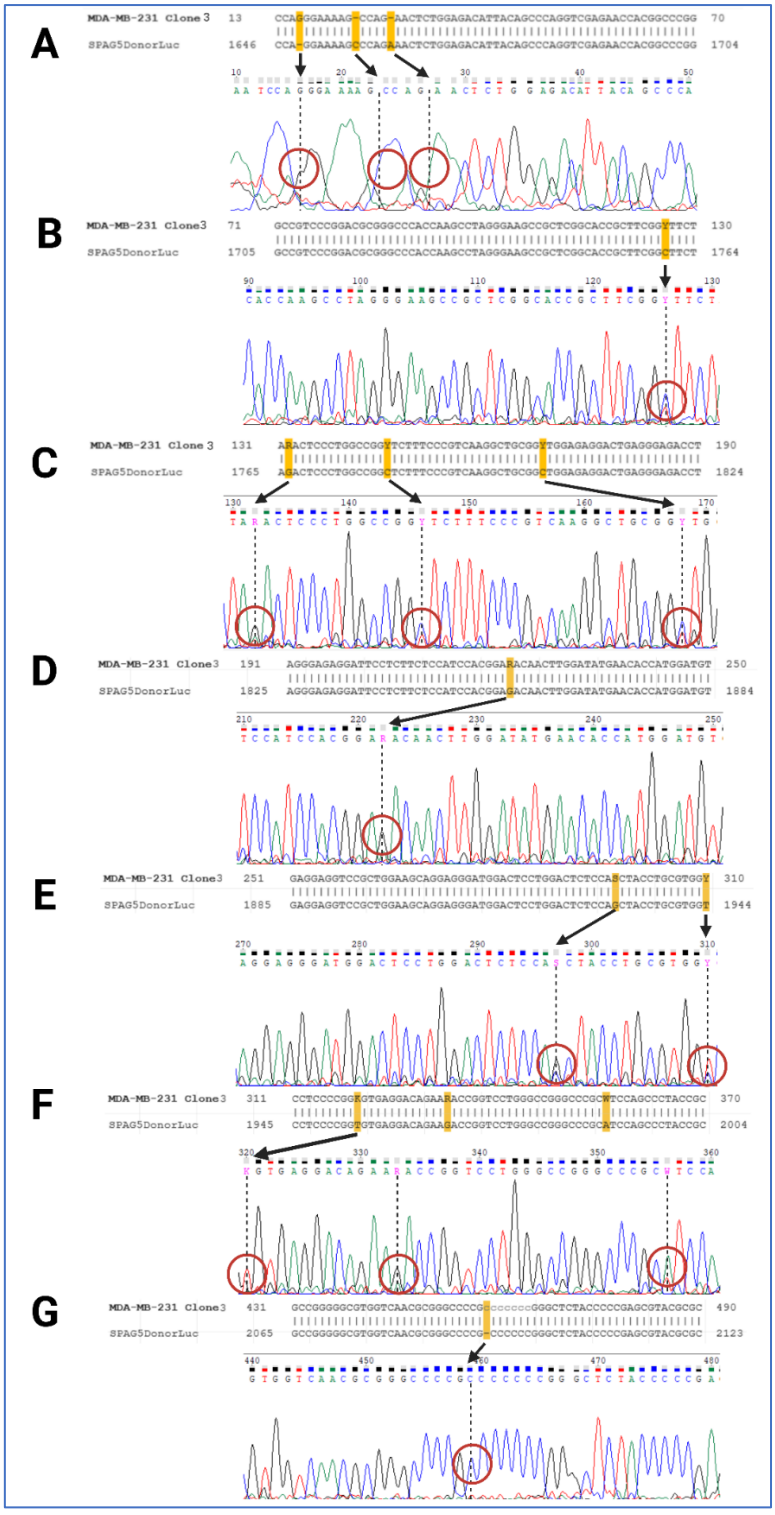

Figure 4.13: Chromatogram Analysis of Mismatches within MDA-MB-231 Clone 3, Allele A and SPAG5DonorLuc Sequence: Figure displays an alignment of MDA-MB-231 allele sequence (603 bp) with the SPAG5DonorLuc Sequence (8014 bp). SPAG5DonorLuc incorporation into MDA-MB-231 Clone 3 and successful disruption of SPAG5. An additional G is inserted at position 16. Two gaps are located at positions 24 and 29. Undetermined base "Y" are identified at locations 126, 146, 168, and 310. Undetermined bases "R" are identified at locations 132, 222 and 233. Undetermined base "S" is identified at locations 297. Unconfirmed base "K" us identified at location 320. Unconfirmed base W is identified at location 356. Soft-masked cytosine sequence is identified at positions 459-455, with an additional cytosine recorded at position 459.

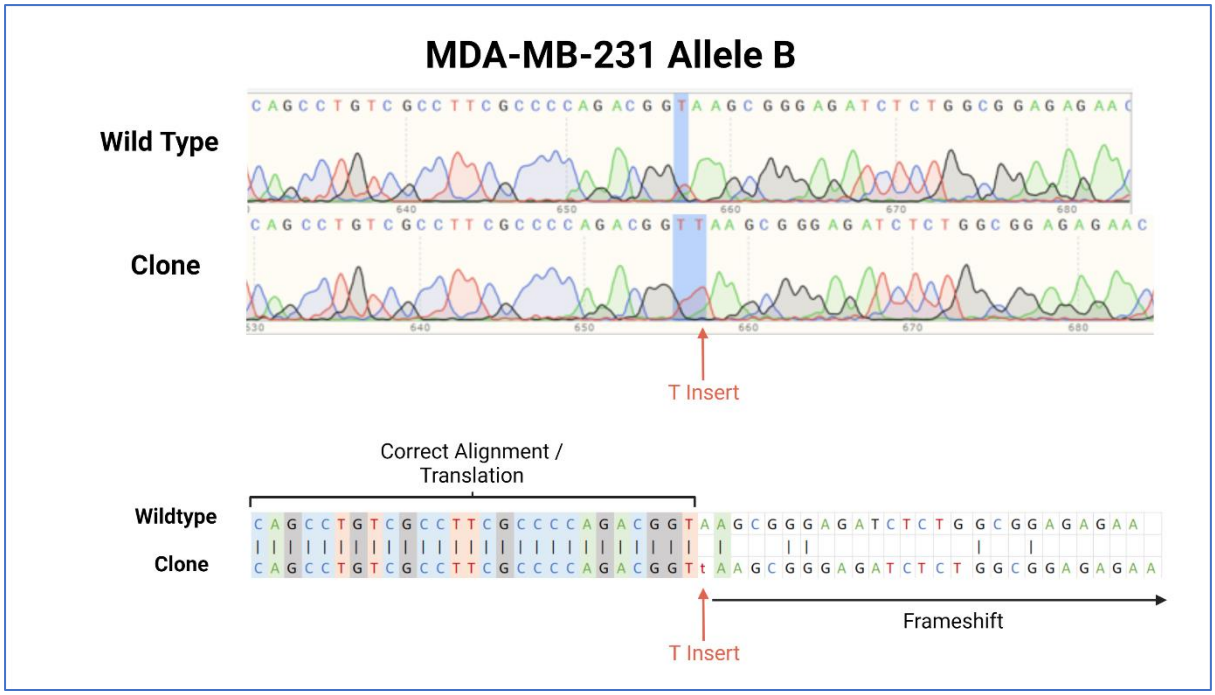

Figure 4.14: MDA-MB-231 Clone 3 Allele B Histogram Sequencing and Alignment with SPAG5 Wild-Type: Figure displays a comparison of MDA-MB-231 wildtype sequence and MDA-MB-231 clone 3 sequence histogram. A T indel is highlighted in MDA-MB-231 clone 3. The relative sequences are displayed in text, identifying the frameshift effect downstream from the T insert.

4.4.3 Western Blotting

Due to two COVID-19 lockdowns, and an unfortunate contamination of the incubator containing the clones, potential SPAG5-knockdown clones were lost on three occasions. Therefore, a Western Blot to confirm the successful disruption of SPAG5 in MDA-MB-231 and BT549 was unable to be performed within the time frame of this thesis.

Chapter 5: Discussion

5.1 DNA Preparation and Detection

5.1.1 Guide RNA and Donor Plasmid Confirmation

The restriction enzyme digestion of guide plasmids pCasGuide-SPAG5-RNA1 and donor plasmids pUC-SPAG5-DonorLuc successfully confirmed that the correct plasmids were used in the experiments.

Figure 5.1 depicts the expected band sizes when the relative restriction enzyme digests each plasmid are determined. When digested with *Hind*III, 8014 bp donor plasmid pUC-SPAG5-DonorLuc is cleaved in two locations where the palindromic DNA sequence A/AGCCT is present: at nt 3988 and 4549; This results in two linear DNA strands of 561 bp and 7453 bp in length. Similarly, when digested with *Eco*RI, 7998 bp pCasGuide-SPAG5-RNA1 is cleaved in two locations wherein the palindromic DNA sequence G/TTAAC at nt 1 and 1123; This results in two linear DNA strands of 1123bp and 6875bp in length.

The two expected band sizes for each digestion were present in the electrophoresis gel, indicating that guide plasmid pCasGuide-SPAG5-RNA1 and donor plasmid pUC-SPAG5-DonorLuc were correctly identified.

Donor plasmid pUC-SPAG5-GFPneo and guide plasmid pCasGuide-SPAG5-RNA2 were also utilised during this thesis work, and the confirmation of these plasmids completed prior to this thesis work. The binding location of these primers within the SPAG5 gene can be found in the supplementary materials.

5.2 Cell Maintenance

Throughout the study, four breast cancer cell lines were maintained. While each cell line shares similar basic requirements for growth and survival, some variations were necessary to provide optimal growth capacity for each cell line.

BT549 cell line is a triple-negative human breast cancer epithelial cell line obtained from a 72-year-old Caucasian woman in 1978. T47D is a luminal A human breast cancer epithelial cell line obtained from a 54-year-old Caucasian woman. MCF-7 is a luminal A human breast cancer epithelial cell line obtained from the breast tissue of a 69-year-old Caucasian woman. MDA-MB-231 is an epithelial triple-negative breast cancer cell line obtained from a 51-year-old Caucasian woman. As all cell lines originate from Caucasian women, there is cause for consideration to the restrictions in conclusions that may be drawn.

5.2.1 Media Selection and Provision

Human breast cancer cells require a consistent supply of complete media to maintain nutrient supply, pH level, and osmolality. Each of these contributes to providing the ideal environment for the cells to survive and proliferate.

Each cell culture media contains a mixture of amino acids to boost cell vitality and growth, vitamins for cellular growth and proliferation, carbohydrates such as glucose to provide an energy source for living cells, inorganic salts for membrane potential regulation and osmolality, and finally, basic trace elements required for growth, such as iron, potassium, zinc and magnesium can be provided in the base media. These provisions are considered when determining the best culture environment to deliver to your cell type.

Throughout this thesis, four breast cancer cell lines were maintained, and the best base cell media was selected considering these provisions, alongside previous successful growth by published studies. Cell lines BT549 and T47D were maintained in RMPI1640 media, with 10% heat-inactivated FBS, 1% L-glutamine, 100U/mL Penicillin and 100U/mL streptomycin, in a 37°C 5% CO_2 incubator. MCF-7 and MDA-MB-231 cell lines were maintained with DMEM media, with 10% heat-inactivated FBS, 1% L-glutamine, 100U/mL Penicillin and 100U/mL streptomycin, in a 37°C 5% CO_2 incubator. Regular media changes every 2-3 days ensure consistent and uninhibited access to their required needs.

5.2.2 Passaging Cells

Providing the cells with media does not finish with simply changing media frequently. All cells require space within their (artificial) environment to obtain access to the media provided. Thus, it is essential to ensure that the cells within the environment do not exceed 80% confluence. Overcrowding within any environment places the cells under stress, causing competition for space and resources within the flask. Such evolutionary pressure may cause cell death and changes within the cell line behaviour. Prevention of these changes is essential to ensure any results comparing wild-type to SPAG5-knockout cells result solely from SPAG5 knockdown, as opposed to environmental pressure. Consistent provision and access to resources must therefore be prioritised throughout the study. Thus, regular passaging allows cells to grow freely with enough space to access all required elements for growth and survival.

Washing cells with PBS allows for easy removal of dead cells, and cellular debris, ensuring a clean environment when the cells are transferred into the new solution. PBS provides a safe pH level for cells during exposure, and unlike water, PBS prevents cells from rupturing or shrivelling up due to osmosis.

Removing the cells from one flask to transfer into another requires exposure to trypsin. Trypsin, a protease, breaks down proteins such as integrin, which maintains the adhesion of the cells to the flask surface, thus allowing the cells to be collected within a pipette for transport. However, as all cells are comprised of proteins, it is essential to limit exposure to trypsin to minimise the probability of cell damage during exposure. For this reason, the incubation of cells submerged in trypsin should be limited to the minimum time required to dissociate the adhesion between the cells and the flask bottom. Once cells have been suspended within the flask, diluting trypsin with complete media to provide a healthy environment is necessary before centrifugation to separate the cells from the trypsin.

After centrifugation, the cells have formed pellets at the bottom of the 15 mL centrifuge tubes, the supernatant is removed, including all trypsin, and the cells are resuspended in 2mL of complete media for recovery. Finally, 400 µL of the cell suspension is transferred into a new 25 mL flask, containing 6 mL of complete media. This allows the cells enough room and access to complete media to grow and proliferate without stress factors.

5.2.3 Freezing Cells

Freezing cell lines not actively being utilised is an effective method of minimising manual labour and expenditure on long-term maintenance. Cryopreservation of cells was conducted across several COVID-19 lockdowns, and stock of both cell lines was preserved and frozen. Ideally, the target number of cells within a cryovial contains 2 x 10^5 cells/mL. Once cells had reached 80 – 90% confluency within a T25 flask, approximately six cryovials could be preserved in the cell medium. As described in 5.2.2, Washing the cells with PBS is essential to remove cellular debris and dead cells. Exposure to trypsin is also limited throughout this process to prevent cellular damage. However, cryopreservation places the cells under significant stress, and without intervention, exposing cells to temperatures below 0°C typically results in cell death. Unprotected, intracellular and extracellular crystallisation occurs rapidly at freezing temperatures due to the high percentage of water within human cells. Thus, protective actions were chosen to protect the cells from freezing injury or death.

The medium cells are stored in a solution containing dimethyl sulfoxide (DMSO), a cryoprotectant. When added to the complete media, DMSO prevents intracellular and extracellular crystallisation that otherwise forms throughout the freezing process. Furthermore, the cells are not immediately placed into the liquid nitrogen freezer but are first established in the -80°C freezer. This provided a slower, more controlled freezing environment before they were put into the much cooler liquid nitrogen freezer, effectively increasing viable cells' yield when revived.

5.2.4 Reviving Cells

Revival of cryopreserved cells stored in liquid nitrogen requires quick, attentive handling. Although not as critical as cooling, the speed at which cells are thawed and warmed is crucial in cell yield. To prevent ice recrystallisation, the cells should be heated rapidly as vitrified water exists in a higher-energy state than ice; as it is only semi-stable and can therefore rearrange itself into a more stable, lower-energy, crystallised state during thawing. This crystallisation is not compatible with life. Consequently, it is widely recommended that cells be warmed for 90-120 seconds in a 37°C water bath (Yokoyama et al., 2012). There is some debate as to whether this is the best protocol. However, at least one study suggests that warming cells at half the rate does not affect viability post-thaw (Baboo et al., 2019; Thorpe et al., 1976). If proven true, it could be possible to thaw cells at an even slower rate via air-thawing. This would provide the benefit of reducing water bath exposure, one of the most common sources of contamination within the laboratory. This method is not common practice, so it was not utilised during this thesis; however, it will be worth considering should further studies conclude similarly, as it could significantly increase sterility.

To maintain cell viability throughout the cryopreservation process, the cells are stored in cryoprotectant DMSO. However, in higher concentrations, cryopreservation agents decrease membrane thickness, increasing cellular permeability, cell death and reducing cell yields. Thus, the frozen cell mixture must be immediately transferred into pre-warmed complete media to minimise the DMSO concentration from 10% to 1% before centrifugation and complete removal.

Cryopreservation is a stressful and potentially fatal condition for cells. Therefore, the cells must receive adequate time and nutrition to recover from the state. Therefore, the cells should receive fresh media every 2 – 3 days for two weeks before undergoing further stresses, such as transfection. In this study, the cells were passaged for 3 weeks without intervention, to optimise conditions and decrease the stress on the cell lines.

5.3 Confirmation of Successful Disruption of SPAG5

5.3.1 PCR

The most used technique is polymerase chain reaction or PCR to obtain many copies of an area of DNA. Within just a few hours, PCR technology's three-step cycle can create billions of copies of the target DNA sequence. During each cycle, the reaction mixture is heated to denature the double-stranded DNA helix before being cooled to allow for the annealing of complementary DNA primers and dNTPs, creating a complementary sequence on each strand of the target sequence in a 5' to 3' direction. To achieve the complete separation of the DNA double helix, the reaction mixture must be heated to at least 90 ˚C. Taq polymerase is a heat-stable DNA polymerase utilised to automate the

repetitive amplification of the specific DNA target without being denatured by the cycling high temperatures.

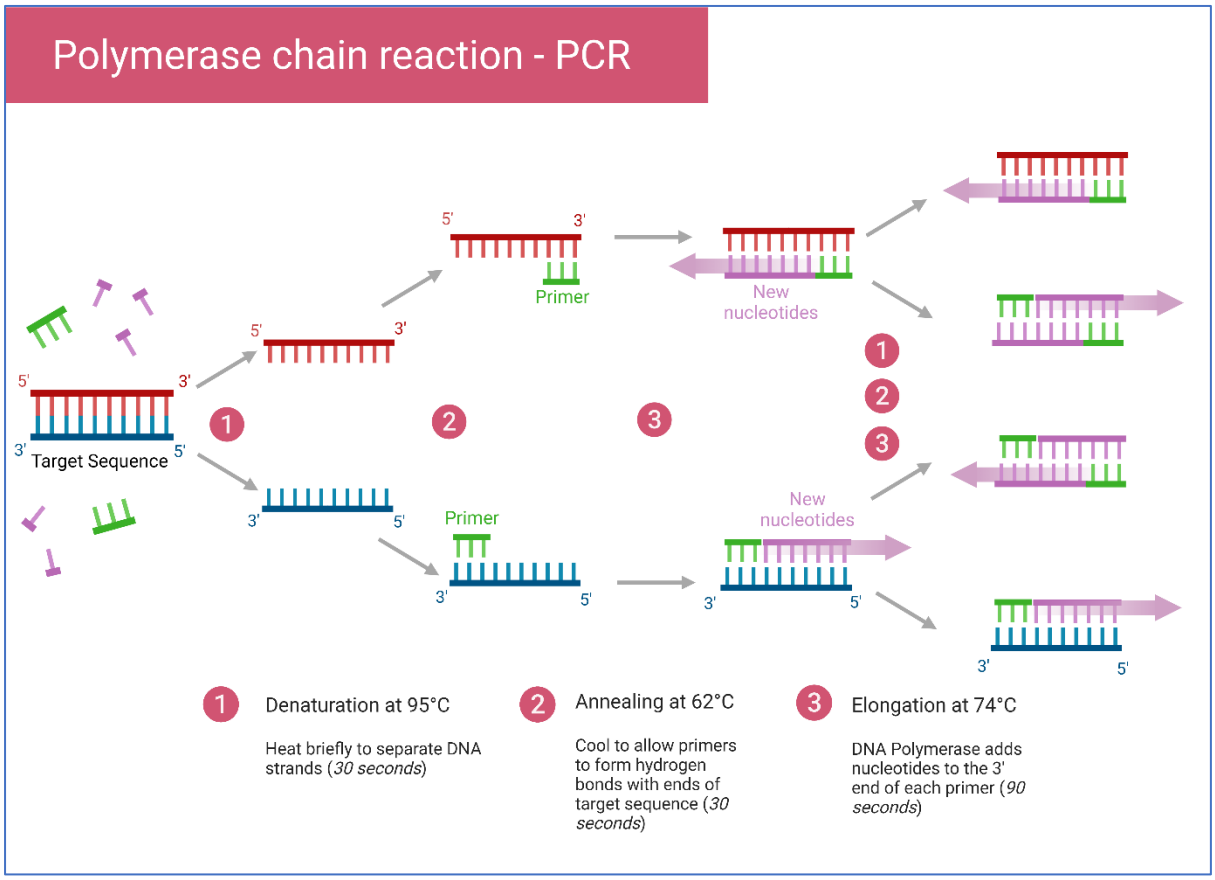

Figure 5.1: The Polymerase Chain Reaction. PCR requires double-stranded DNA containing the target sequence, Taq polymerase, dNTPs, and two specific primers. Each primer is complementary to one end of the target sequence on opposite strands. The first step of the cycle is denaturation, followed by annealing and elongation. With each successive cycle, the number of target sequence molecules increases exponentially; after 30 cycles, approximately one billion copies of the exact DNA target sequence are present. *Adapted from "Polymerase Chain Reaction (PCR)", by Biorender.com (2022). Retrieved from https://app.biorender.com/biorender-templates*

All fifteen BT549 and twenty-one MCF-7 clones were successfully lysed, the DNA was extracted, and PCR amplification of the SPAG5 knockout regions was conducted.

Three of the fourteen BT549 clones produced an expected band of 1071 bp, indicating the successful knockout of SPAG5 with the insertion of the donor plasmid SPAG5DonorLuc. These clones are BT549 clones 8, 12, and 14. Eight of the twenty-one MCF-7 clones produced the expected band of 1071 bp; These clones are 1, 3, 6, 10, 11, 13, 19 and 20. Therefore, we can conclude that the SPAG5 gene has been successfully disrupted in these clones.

The transfection efficiency of these clones is not as high as may be expected based on previous studies (Li et al., 2022; Luo et al., 2021). BT549 had a transfection efficiency of 20%, while MCF-7 had a transfection efficiency of 38%. However, in both cited sources, Lipofectamine 3000 was utilised. Lipofectamine™ 3000 reagent has superior transfection performance compared to the Turbofect™ transfection reagent, which was used in this round of genome editing. It is of note that BT549, a notably difficult-to-transfect cell line, did have a lower transfection efficiency, as expected.

No band exists in all other BT549 and MCF-7 clones, indicating that the SPAG5 gene had not been disrupted. This may be explained by the non-specific integration of the donor sequence, SPAG5DonorLuc, into the clones' genomes. This would account for their puromycin-resistant quality without the disruption of SPAG5.

However, the successful disruption of *SPAG5* in BT549 in three clones and MCF-7 in eight clones has provided the first positive steps towards determining the role of SPAG5 in chemotherapy drug response in breast cancer. Critical further steps may now be taken to confirm the suitability of these eleven clones for this thesis aim.

Unfortunately, due to the COVID-19 pandemic, these clones could not be used, as the results were achieved just days before the August 2021 lockdown period, and cryopreservation was not possible then. In January 2022, the entire methodology was repeated.

BT549 and MCF-7 wild-type cells were revived, maintained, seeded, transfected and selected in puromycin as previously conducted. However, having observed a lower-than-desired transfection efficiency in the previous clones, Lipofectamine™ 3000 was utilised as the transfection reagent to increase the yield of potential *SPAG5*-disrupted cells in both cell lines. Significantly more individual cell colonies were puromycin resistant in both cell lines. A total of 63 BT549 and 187 MCF-7 single-cell colonies were selected. This significant improvement may be attributed to the change in transfection reagents and increased confidence in laboratory techniques.

Unfortunately, contamination within the incubator resulted in these cell lines being unusable after selection. To complete this project within the time frame, PhD candidate Leo He provided BT549, and MDA-MD-231 clones confirmed by PCR that had not been contaminated. These clones were then prepared and sent for Sanger sequencing at Massey University.

5.3.2 Sequencing

Sanger sequencing is a technology in which the sequence of nucleotides within any DNA fragment up to 800 – 1000 bp in length can be determined and recorded. This method conducts

sequencing reactions and separates the identified nucleotide calls by length. The reaction mixture contains the DNA sample, specific primer, fluorescently labelled dNTPs and chain-terminating dideoxy nucleotides (ddNTPs). Similar to PCR, the reaction mixture is heated to denature the template DNA, then cooled for the primer to bind to the single-stranded template before being warmed again for DNA polymerase to synthesise from the primer. Single-stranded DNA provides a template for sequencing; the short oligonucleotide primer provides a free OH^- group for DNA synthesis utilising dNTPs for chain elongation by DNA polymerase. Each dNTP is tagged with a distinctive fluorescent label at its 3' end. DNA will continue until it happens to bind a chain-terminating ddNTP. The fragments are detected by separating the different sizes by capillary electrophoresis sequencing. This process is depicted in Figure 5.2 below.

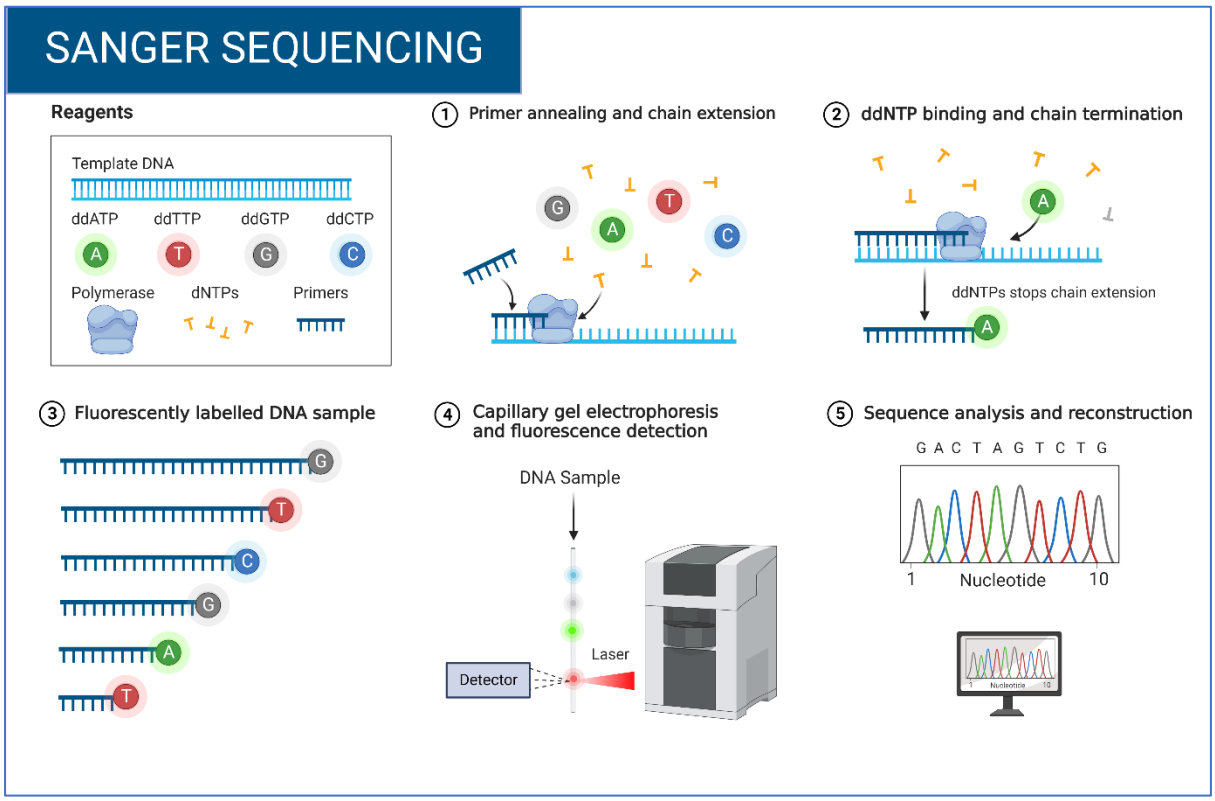

Figure 5.2: Sanger Sequencing: The figure displays the functional process of sanger sequencing in four main steps: 1) The primer first anneals to the template DNA, and DNA polymerase synthesis commences. 2) DNA polymerase binds a ddNTP, terminating the extension of the chain. 3) Fluorescently labelled DNA is now formed in chains. 4) DNA chains travel through the electrophoresis gel towards the laser, the shortest fragments arriving first. The nucleotides are recorded according to their fluorescent tags. 5) Sequencing order is determined, and a chromatogram is developed. *Adapted from "Sanger Sequencing", by BioRender.com (2022). Retrieved from https://app.biorender.com/biorender-templates*

Sanger sequencing, while limited in the nucleotide length of sequencing, is cost-effective and accurate. Single nucleotide polymorphisms can be accurately and quickly, which is a crucial advantage compared to next-generation sequencing, which is more appropriate for large genomic regions and

whole-genome analysis. This makes Sanger sequencing ideal for the purpose of this study, as less than 1000 bp is needed for analysis, and high accuracy is required to identify any single nucleotide polymorphisms.

Accurate assessment of the effect of SPAG5 on chemotherapy effectiveness in breast cancer cell lines BT549 and MDA-MB-231 requires a homozygous knockout of the *SPAG5* gene. This results in loss of function of the *SPAG5* gene within the cell line, ensuring a significantly more accurate analysis of the effect of SPAG5 on chemotherapy drug effectiveness in breast cancer compared to a heterozygous knockout and wild-type cells. The PCR results confirmed several successful clones in which the donor plasmid SPAG5DonorLuc was inserted into the genome, it does not confirm whether these clones are homozygous knockouts. DNA Sanger sequencing analysis was performed to determine the genotype of each of the clones identified via PCR.

5.3.2.1 BT549 Clone Sequencing Analysis

BT549 clones 1 and 2 were identified as homozygous knockout clones. However, *SPAG5* was not disrupted in identical ways. In allele "A", SPAG5DonorLuc was successfully knocked into the chromosome, replacing the DNA between the identified target sequences, and disrupting the SPAG5 gene allele. This was confirmed by the alignment of the sequenced BT549 clone with the SPAG5DonorLuc plasmid produced by BLASTn on the NCBI website (*BLASTn*). This alignment provided a 99% identical 589 bp comparison sequence, with 581 identical nucleotide matches, 2 gaps in the clone sequence, and 6 non-identical nucleotide alignments.

Analysis of the clone sequencing data and chromatogram suggests the gaps identified at positions 22 and 31 of the clone sequence were likely misread by the sequencing programme. Sanger sequencing is limited in quality for the first 15 to 40 bases, as this is the area in which the primer binds, resulting in lower coverage, and therefore lesser quality read. This is conclusion is supported by the poorly distinguished peaks in the chromatogram. In this sequence, high-quality base calls begin at base 33 and finish at approximately base 660. When the chromatogram is analysed as in Figure 4.9 (A), missing base 22 could be an identical A, as the adenine peak is non-distinctly forming. Similarly, missing base 31 is likely an adenine, not called due to insufficient coverage. While this cannot be confirmed without sequencing the clone, this does not alter the conclusion that SPAG5DonorLuc has been inserted into the BT549 genome, disrupting the SPAG5 gene.

While determining a base by human analysis of chromatogram peaks, it is not the only consideration when determining a likely base point. As we are familiar with the SPAG5DonorLuc sequence, we can also utilise the donor sequence to determine the most likely base call. Position 82 of BT549 Clone 1 is reported as an S – a shorthand utilised to indicate a base call that could be either

guanine or cytosine. Analysis of the peak reported in the chromatogram, in conjunction with the known expected base (guanine) provided by the known SPAG5DonorLuc sequence suggests this base is likely to be guanine.

Analysis of the chromatogram and the alignment across this sequence was conducted for all undetermined bases, and the most likely base is recorded in Table 5.1.

BT549 Clone 2 Allele "A" sequence consisted of 297 bp of these 278 bp were aligned in the nucleotide BLASTn alignment (*BLASTn*) with SPAG5DonorLuc DNA sequence. Of these, 276 bp were an identical match, only 20 bases were not aligned as a result of poor coverage in nt positions 1 – 20 in BT549 Clone 2 Allele A sequence. The gap identified at position 29 is likely the result of poor sequencing quality within the first 30 bp, as the three adenine peaks appear to merge into one another, resulting in an incorrect reading. At position 133, an undefined base call of "R" has been produced by the sequencing software, indicating guanine or adenine is present. The chromatogram (Figure 4.11) indicates a higher guanine peak, indicating guanine is the most likely base. This is supported by the alignment with the confirmed SPAG5DonorLuc sequence. It is likely that the number of adenine base calls is a result of adenine bases located on either side of the affected base. These conclusions are summarised in Table 5.1.

Table 5.1: Summary of BT549 Clone Sequence Unmatched Base Confirmation

Base Position	Unmatched Base Call	Base Call Interpretation	Highest Chromatogram Peak	SPAG5DonorLuc Base	Probable Base
BT549 Clone 1					
22	-	Gap	Guanine or Adenine	Adenine	Adenine
31	-	Gap	Adenine	Adenine	Adenine
82	S	Guanine or Cytosine	Guanine	Guanine	Guanine
129	Y	Cytosine or Thymine	Cytosine	Cytosine	Cytosine
135	R	Guanine or Adenine	Guanine	Guanine	Guanine
149	Y	Cytosine or Thymine	Cytosine	Cytosine	Cytosine
165	Y	Cytosine or Thymine	Cytosine	Cytosine	Cytosine
377	K	Guanine or Thymine	Thymine	Thymine	Thymine
BT549 Clone 2					
29	-	Gap	Adenine	Adenine	Adenine
133	R	Guanine or Adenine	Guanine	Guanine	Guanine

The variation in length of the sequencing results between BT549 Clones 1 and 2 is likely resultant of a pipetting error. When too high a quantity of primer DNA is included in the sequencing mixture, the template DNA is consumed binding to the primer, resulting in a short sequencing distance. Likewise, if too little template DNA is provided, the length of sequencing will reduce as the DNA templates are quickly consumed. It is likely that in preparation for BT549-14A sequencing, the ratio of primer and template DNA was inadequate for lengthened sequencing. To increase the sequencing length for future research, 200ng per 20µL of sequencing reaction is ideal for primers 22-24 nt in length.

An indel mutation is an insertion or deletion of nucleotide(s) into genomic DNA. Due to codons' triplet nature of DNA expression, inserting or deleting nucleotides in numbers not divisible by three will change the reading frame inside coding regions. Consequently, the translation of the encoded protein will be nonsensical. A frameshift mutation will also alter the first stop codon ("UAA", "UGA" or "UAG") translated in the coding sequence, resulting in a different length of translated polypeptide. Ultimately, the resultant protein will most likely be non-functional.

BT549 Clone 1 allele B contains a thymine nucleotide insertion, disrupting the mRNA splicing and resulting in a reading frame shift. In this allele, a "T" nucleotide has been inserted into *SPAG5* at the 18th codon of exon 1. This will therefore result in a reading frame shift and inaccurate translation of SPAG5 mRNA into amino acids. After just 22 codons, the protein translation is halted by a premature UGA stop codon. Thus, SPAG5 is functionally knocked out of this allele.

5.3.2.2 MDA-MB-231 Clone Sequencing Analysis

As was observed in BT549, MDA-MB-231 clones were identified as having SPAG5 functionally disrupted in both alleles. While several clones were sequenced, MDA-MB-231, Clone 3 was utilised as a representative result of each of the SPAG5 knockout MDA-MB-231 cells.

In Clone 3, allele "A", SPAG5DonorLuc was successfully knocked into the chromosome, replacing the DNA between the identified target sequences, and disrupting the SPAG5 gene. This was confirmed by the alignment of the sequenced MDA-MB-231 clone with the SPAG5DonorLuc plasmid produced by BLASTn on the NCBI website (*BLASTn*). This alignment provided a 98% identical, 593 bp comparison sequence, with 579 identical nucleotide matches, two gaps in the clone sequence, two additional bases and ten non-identical nucleotide alignments.

Analysis of the Clone 1 sequencing data and chromatogram suggests the sequencing programme likely miscalled the additional guanine identified at position 16 of the clone sequence. Sanger sequencing is limited in quality for the first 15 to 40 bases, as this is where the primer binds, resulting in lower coverage and, therefore, lesser quality read. This conclusion is supported by the

poorly distinguished peaks in the chromatogram. In this sequence, high-quality base calls begin at base 30 and finish at approximately base 602. Furthermore, this position is expected to be generally unchanged from the original *SPAG5* donor sequence. The gaps in the sequence at nt positions 24 and 29 also result from the limited quality of the first 30 bases, as supported by analysis of the chromatogram, which indicates unspecified peaks not identified by the programme of C and A in positions 24 and 29, respectively. While this cannot be confirmed without re-sequencing the clone, this does not alter the conclusion that SPAG5DonorLuc has been inserted into the BT549 genome, disrupting the *SPAG5* gene.

Several undetermined base calls in the MDA-MB-231 Allele A sequence were recorded as "Y" at nt positions 126, 146, 168 and 310. This indicates that the base at these positions is likely to be either a cytosine or a thymine. Cytosine and thymine are often miscalled as the other base due to their relatively similar molecular structure forming pyrimidines. When one base is not called significantly more than the other, the position is instead called as Y. Positions 126, 146, and 168 are likely cytosine, as indicated by the higher blue peak at each of these positions and the known corresponding base of SPAG5DonorLuc. Position 310 is expected to be thymine, following the same reasoning.

Positions 132, 224, and 335 are also undetermined base calls, identified as R, to indicate that the base is either a guanine or an adenine. These bases, like cytosine and thymine, are also often misinterpreted by the sequencing software due to their similar purine structure. All three positions are likely guanine, as supported by the alignment with SPAG5DonorLuc, and a slightly higher base call percentage is observed as a black peak in the chromatogram.

Position 296 is an undetermined base call, "S", indicating the programme could not determine whether the base present was a guanine or a cytosine. This is a less commonly occurring instance, as cytosine and guanine have significantly different sizes and structures. In this instance, guanine is more commonly called, and this is likely the correct base, as indicated when aligned with the SPAG5DonorLuc sequence. It is possible that the incorrect cytosine call was a result of several nearby cytosine bases, particularly the next base call 297. However, the cytosine peaks are defined between 296 and 297, so the miscall may result from random chance.

Position 320 is called "K", indicating the programme could not call either thymine or guanine. This instance is likely thymine due to the more significant red thymine peak. This conclusion is supported by the SPAG5DonorLuc sequence and the surrounding guanine bases at positions 318, 319 and 321, which likely resulted in the increased miscall of guanine at position 320.

Position 459 reports an additional cytosine in what is known as a soft-masked sequence. This repetitive sequence of seven cytosine calls increases the likelihood of an inaccurate number of distinct base calls. In this instance, it is difficult to determine which sequence is likely to be correct. However, it is unlikely to be a true indel like the thymine in BT549 Clone 2 allele B (Figure 4.10).

Ultimately, this sequencing analysis confirms that despite misidentified base calls, the donor plasmid, SPAG5DonorLuc, was successfully incorporated into the MDA-MB-231 allele A at the intended position, disrupting *SPAG5*. These conclusions are summarised in Table 5.2.

In MDA-MB-231 allele B, a thymine insertion was observed in the same position as in BT549 Clone 2 Allele A. This thymine insertion similarly results in a frameshift mutation resulting in a nonsensical translation downstream of the insertion and ultimately resulting in the disruption of SPAG5.

Table 5.2: Summary of MDA-MB-231 Clone Sequence Unmatched Base Confirmation

Base Position	Unmatched Base Call	Base Call Interpretation	Highest Chromatogram Peak	SPAG5DonorLuc Base	Probable Base
MDA-MB-231 Clone 3 Allele A					
16	G	Insertion	Guanine	-	-
24	-	Gap / Deletion	Cytosine	Cytosine	Cytosine
29	-	Gap / Deletion	Adenine	Adenine	Adenine
126	Y	Cytosine or Thymine	Cytosine	Cytosine	Cytosine
132	R	Guanine or Adenine	Guanine	Guanine	Guanine
146	Y	Cytosine or Thymine	Cytosine	Cytosine	Cytosine
162	Y	Cytosine or Thymine	Cytosine	Cytosine	Cytosine
222	R	Guanine or Adenine	Guanine	Guanine	Guanine
297	S	Guanine or Cytosine	Guanine	Guanine	Guanine
310	Y	Cytosine or Thymine	Thymine	Thymine	Thymine
320	K	Guanine or Thymine	Thymine	Thymine	Thymine
333	R	Guanine or Adenine	Guanine	Guanine	Guanine
356	W	Adenine or Thymine	Adenine	Adenine	Adenine
459	c	Cytosine or -	Cytosine	-	Cytosine or -

5.4 Future Directions

When considering the potential impact of these findings, there are several further steps I would have performed to confirm the findings presented in this thesis. I would conduct a western blot and an MTT Assay on the SPAG5-disrupted cell lines.

5.4.1 Western Blotting

Western blotting is an analytical technique used to separate and identify the presence of proteins based on weight through gel electrophoresis. The results are then transferred to a membrane, producing a band for each protein (Mahmood & Yang, 2012). The size of the protein is determined by the molecular standard. When analysing western blotting results, the thickness of the protein band indicates the amount of protein present. An analytical comparison of the presence and relative concentrations of SPAG5 present in wild-type BT549 and MDA-MB-231 cells compared to their respective clones would provide an indication of functional SPAG5 knockdown in the edited clones. If such results were achieved, a drug treatment MTT assay could then be performed to indicate the relationship between SPAG5 expression and chemotherapy drug efficacy in breast cancer.

Protein extraction collects the proteins in the cell cytosol during cell lysis. To prevent the denaturation of proteins during this extraction, the cell solution is kept on ice at a cool temperature. A protease inhibitor was not outlined in this methodology; however, it may also be utilised to prevent proteolysis and maintain protein phosphorylation. Extended agitation of the solution is necessary to extract proteins from the cells.

In western blots, the electrophoresis gel is made up of two types of agarose gels: stacking gel and separating gel. The stacking gel is a porous, slightly acidic gel, allowing thinner, more sharply defined bands. However, it does not adequately separate proteins due to its increase pore sizes. Comparatively, the lower layer of gel, the separating gel has significantly smaller pores, due to its higher polyacrylamide content. Thus, the separation of proteins through this gel is more effective, as the smaller proteins travel more quickly towards the positive electrode than larger proteins.

The loading (2X Laemmli) buffer contains glycerol, enabling the cells to sink cleanly into the wells of the stacking gel. The bromophenol blue component of this buffer also serves as a visual indication of how far the separation has progressed within the gel. Once the sample has been diluted in the loading buffer, the samples are heated in order to denature the higher order structure, ensuring

the negative charge of the amino acids is not neutralised by the high structure, thereby enabling the proteins to move in the electric field generated during gel electrophoresis.

By first applying a lower voltage (50V) for 10 minutes, the proteins will align evenly within the stacking gel. If the resultant bands are not consistent across the gel at the end of the run, it may be useful to increase the time that the proteins run at a low voltage to 30 minutes to improve the alignment and ensure the proteins have entered the separating gel. For larger proteins, such as SPAG5, the voltage should not be increased beyond 110 V for the remainder of the electrophoresis to ensure a more uniform conformation due to their slower diffusion through the gel.

After approximately 60 minutes, the proteins are usually adequately separated, and the proteins can be transferred to a membrane. An electrophoretic transfer can be performed in semi-dry, or wet conditions. Semi-dry conditions are more efficient, and rapidly transfer the negatively charged proteins to the membrane. A wet transfer requires more time and transfer buffer but can produce higher quality transfer. Both conditions require close contact of the gel and membrane to ensure a clear image. If the resultant image is unclear, repeat the process with extra attention to air bubbles and connection between the sandwich layers.

To reduce background noise, the membrane is then blocked using TBST and 5% milk to prevent non-specific binding of antibodies to the membrane. The membrane is also washed in TBST to reduce background noise. The primary antibody (RM112) is diluted 1:1000 within the blocking solution and is produces a signal captured on film for analysis.

Analysis of the film considers two attributes of each band. The size of the band as measured by the protein standard should be 135kDa, indicating the SPAG5 protein has been successfully detected. The thickness of the band indicates the relative quantity of the protein detected. In this instance, it is expected that the wild-type cell lines would produce thicker bands than the SPAG5 clones, as SPAG5 should be knocked down in the edited cells, resulting in less protein.

Unfortunately, due to time restrictions, a western blot was not completed during this project, and should be conducted in future to confirm the relative quantity of SPAG5 protein in both BT549 and MDA-MB-231 wild-type and *SPAG5* knockout clones.

However, data produced by a western blot, is semi-qualitative. While it provides a relative comparison of protein levels, the loading and transfer rates between lanes and blots can be variable, and therefore, a more specific experiment should also be conducted to support the findings of a future western blot. One such method is an MTT assay.

5.4.2 MTT Assay

SPAG5 has known inhibitory interactions with gefitinib (Li et al., 2021), olaparib (Li et al., 2019), and paclitaxel (Yuan et al., 2014). Therefore, it is logical to determine whether the cell viability and proliferation is less affected by these chemotherapy drugs in SPAG5-knockdown breast cancer clones when compared to their wildtype equivalent cell line.

An MTT assay measures the cell viability and proliferation of a cell population in response to external factors. For the purposes of this research, the first MTT assay would assist in confirming the SPAG5 gene had been successfully disrupted and the puromycin resistance gene provided by SPAG5DonorLuc had been successfully integrated into the genome. An analytical comparison of the cell viability and proliferation between wild-type BT549 and MDA-MB-231 cells over a period of seven days could evidence that SPAG5 expression has been reduced in the knockout clones.

To support this hypothesis, a significant decrease in cell viability and the rate of proliferation would be observed in BT549 clones when compared to BT549 wild-type cells. Similarly, MDA-MB-231 clones would be expected to have a significantly lower rate of proliferation. This is indicated by lower absorbance values over time, as a higher absorbance rate is indicative of an increase in cell proliferation and viability.

To obtain reliable results, the several conditions should be met during the MTT assay. The blanks should produce low absorbance readings. High absorbance readings in the blanks decreases the reliability of the results due to high background noise. Furthermore, it indicates there is likely contamination of the media by yeast or bacteria. In this instance, the plates should be discarded and the MTT assay should be repeated with fresh, sterile media. The cell density should be calculated to give an absorbance value between 0.75 and 1.25. This will allow for stimulation and inhibition of cell proliferation can be measured over time. If the cell density is too high, the absorbance readings will also be too high, and a significant data will not be recordable. The inverse is also true; if the cell density is too low, the absorbance readings will also be low. This will increase the difficulty to distinguish between background readings and true data. Furthermore, it will not be possible to determine the any decrease in population or inhibition of cell proliferation. Incubation and recovery times are also critical to obtain significant absorbance values. If the incubation period for the reduction of MTT is too short, this incubation period should be increased until the purple colour is evident. Similarly, the incubation period with for the solubilisation may also be increased to ensure no crystals remain. If the replications of this test are significantly different, accuracy of the cell plating should be increased. All

pipettes utilised should be calibrated, and the cells should be homogenously distributed in the medium before plating.

Once an MTT assay had been utilised to confirm the inhibition of SPAG5 in BT549 and MDA-MB-231 clones. To determine the effect on chemotherapy drug efficacy in breast cancer, another MTT assay should be performed to compare the cell viability and proliferation in wild-type and SPAG5 inhibited breast cancer cells when treated with commonly prescribed chemotherapies.

Although it is hypothesised that SPAG5 expression will inhibit the efficacy of several chemotherapy treatments in breast cancer cell lines, unfortunately, this test unable to be performed during this thesis. Consequently, no results may be analysed to confirm this hypothesis.

To determine the impact of SPAG5 expression on chemosensitivity within breast cancer cell lines, this project should be completed with extended parameters. At least two cell lines of each breast cancer subtype should be utilised to determine the role SPAG5 expression may have on efficacy of commonly prescribed chemotherapy drugs. Western blots for key cell signalling pathways can then be performed on chemotherapy drug treated cell lines, to determine the mechanism by which SPAG5 affects chemotherapy response in breast cancer. Key signalling pathways to investigate would include P53, PI3K/AKT/mTOR, Wnt3/β-catenin/TC4, and MYCBP/c-MYC, all of which have direct interactions with SPAG5, and are associated with proliferative and anti-apoptotic activity in various cancers. This information could lead to the development of SPAG5-targeted novel therapies.

To investigate the oncogenicity of SPAG5, breast cancer cell lines with functionally knocked-down SPAG5 expression could be assessed against wild-type breast cancer cell lines. Utilising functional assays, the proliferative and anti-apoptotic behaviours of each cell line could be analysed using quantitative analysis.

5.8 Therapeutic Potential

Despite many various therapies, and rapidly evolving research and tests to determine the most effective treatments, there are still many unexplained resistances to and adverse effects from several chemotherapies and endocrine therapies for breast cancer. Although many chemotherapies target mitotic spindles, due to a lack of specificity, many of such drugs have detrimental effects on cells not undergoing mitosis. Mitotic-spindle interference outside of mitosis damage to healthy cells. It is therefore critical that novel drug targets are identified, and SPAG5 presents as a promising contributor. SPAG5 regulates microtubule formation and chromosomal attachment during mitosis, and unlike other mitotic regulators, does not restrict microtubule function in non-replicating cells.

Thus, as a potential therapeutic target, a SPAG5 inhibiting drug could potentially compete with some of the most successful chemotherapeutic compounds worldwide.

Chemotherapy is too often inhibited by drug resistance in breast cancers. The majority of breast cancer patients are recommended chemotherapy, and yet, it is still limited in its efficacy by several unknown, and untreated inhibitory interactions. Downregulation of SPAG5 may increase chemotherapy sensitivity in several cancers, including drug-resistant breast cancers. By administering SPAG5 inhibitors, targeted inhibition of SPAG5 in conjunction with chemotherapy may improve the clinical outcome for breast cancer patients worldwide.

SPAG5 overexpression is associated with poorer clinical outcome, more aggressive and resistant cancer phenotypes, and increased risk of recurrence and decreased overall survival. SPAG5 amplification has been identified in 10% of breast cancer patients with more aggressive phenotypes (Abdel-Fatah et al., 2016). SPAG5 could therefore also serve as a biomarker to identify cancers requiring more aggressive treatments, and, in future, SPAG5-inhibiting agents to inhibit aggressive progression.

Further investigation into the downstream signalling pathways of SPAG5 should be conducted to determine potentially unknown adverse effects of targeting SPAG5. However, it is a promising novel target and potential biomarker that may be one key piece to the ever-changing puzzle that is the development of increasingly effective, rapid treatments for breast cancer.

5.9 Conclusion

Breast cancer is a highly prevalent cancer worldwide, and especially so in Aotearoa, New Zealand. As breast cancer is so heterogeneous, multiple therapeutic strategies are required to provide effective care for all ethnic, socio-economic groups, and patients of each breast cancer subtype globally. Certainly, the most promising upcoming therapy lies in personalised, targeted therapy. Targeted therapy promises to increase treatment efficacy and decrease adverse impact to the patient. To achieve this, not only is it essential that we identify novel biomarkers and new therapeutic targets such as SPAG5, but also to determine the interactions of the currently available chemotherapy drugs with these new targets. The aim of this thesis was to determine the impact of SPAG5 expression on the response of breast cancer cell lines to chemotherapy drugs. While this project was unable to be fulfilled to completion, our understanding of SPAG5 and its intracellular interactions and molecular pathways makes it a promising novel target for breast cancer therapy, and a propitious biomarker for

chemotherapy sensitivity. Further research to determine downstream pathways of SPAG5 in breast cancer should be conducted to determine the underlying correlation between SPAG5 and chemotherapy sensitivity. Future investigation into the potential use of SPAG5 as a biomarker and therapeutic target could lead to the development of novel therapies and improved patient outcomes in breast cancer, and many other cancers.

Supplementary Information

SPAG5 Sequence (Exon 1 and 2)

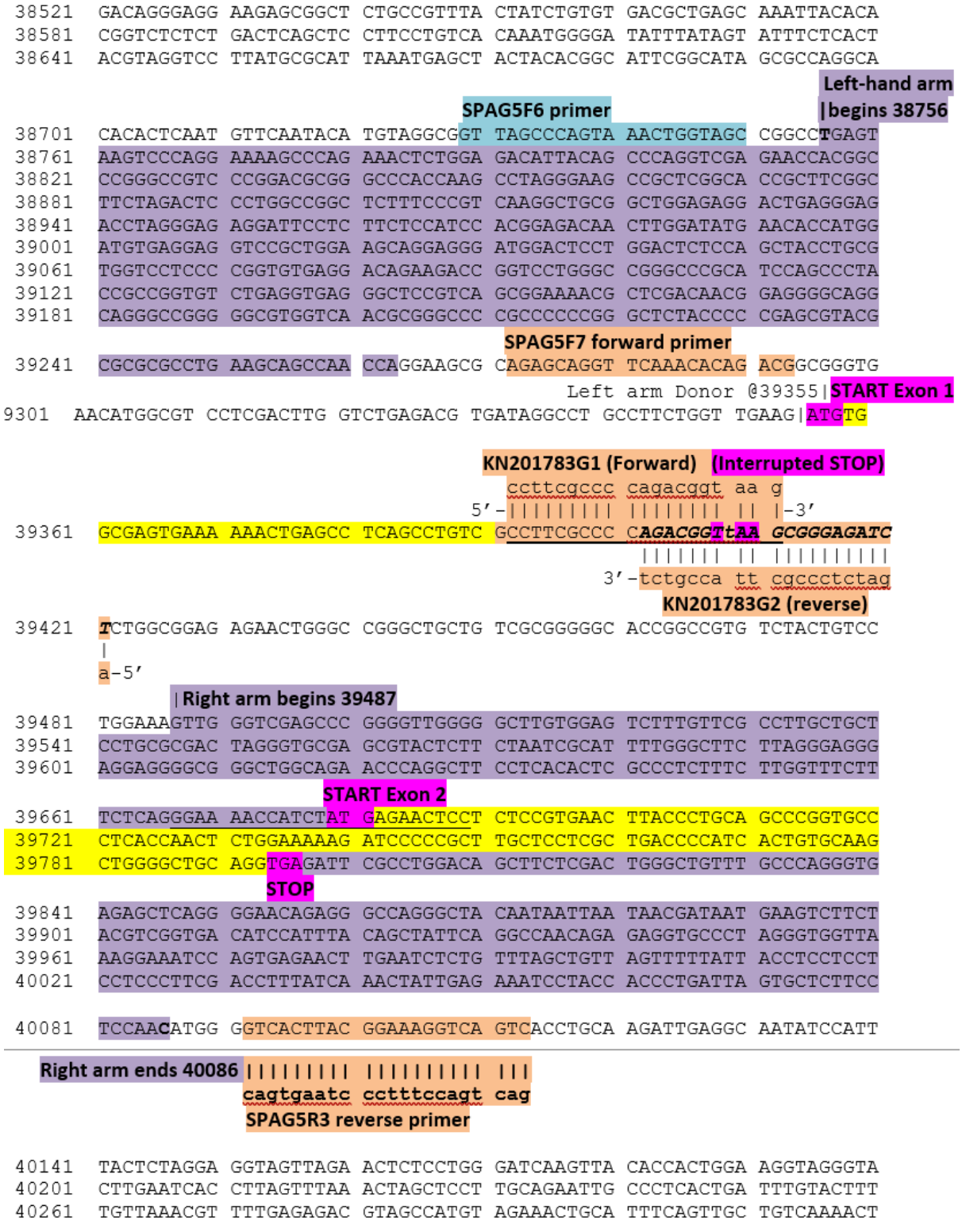


```
38521  GACAGGGAGG AAGAGCGGCT CTGCCGTTTA CTATCTGTGT GACGCTGAGC AAATTACACA
38581  CGGTCTCTCT GACTCAGCTC CTTCCTGTCA CAAATGGGGA TATTTATAGT ATTTCTCACT
38641  ACGTAGGTCC TTATGCGCAT TAAATGAGCT ACTACACGGC ATTCGGCATA GCGCCAGGCA

38701  CACACTCAAT GTTCAATACA TGTAGGCGGT TAGCCCAGTA AACTGGTAGC CGGCCTGAGT
38761  AAGTCCCAGG AAAAGCCCAG AAACTCTGGA GACATTACAG CCCAGGTCGA GAACCACGGC
38821  CCGGGCCGTC CCGGACGCGG GCCCACCAAG CCTAGGGAAG CCGCTCGGCA CCGCTTCGGC
38881  TTCTAGACTC CCTGGCCGGC TCTTTCCCGT CAAGGCTGCG GCTGGAGAGG ACTGAGGGAG
38941  ACCTAGGGAG AGGATTCCTC TTCTCCATCC ACGGAGACAA CTTGGATATG AACACCATGG
39001  ATGTGAGGAG GTCCGCTGGA AGCAGGAGGG ATGGACTCCT GGACTCTCCA GCTACCTGCG
39061  TGGTCCTCCC CGGTGTGAGG ACAGAAGACC GGTCCTGGGC CGGGCCCGCA TCCAGCCCTA
39121  CCGCCGGTGT CTGAGGTGAG GGCTCCGTCA GCGGAAAACG CTCGACAACG GAGGGGCAGG
39181  CAGGGCCGGG GGCGTGGTCA ACGCGGGCCC CGCCCCCCGG GCTCTACCCC CGAGCGTACG

39241  CGCGCGCCTG AAGCAGCCAA CCAGGAAGCG CAGAGCAGGT TCAAACACAG ACGGCGGGTG

9301  AACATGGCGT CCTCGACTTG GTCTGAGACG TGATAGGCCT GCCTTCTGGT TGAAG|ATGTG

                                    ccttcgcccc cagacggt aa g
                                5'-||||||||| |||||||| || |-3'
39361  GCGAGTGAAA AAACTGAGCC TCAGCCTGTC GCCTTCGCCC CAGACGGTTAA GCGGGAGATC
                                        ||||||| || ||||||||||
                                    3'-tctgcca tt cgccctctag

39421  TCTGGCGGAG AGAACTGGGC CGGGCTGCTG TCGCGGGGGC ACCGGCCGTG TCTACTGTCC
       |
       a-5'

39481  TGGAAAGTTG GGTCGAGCCC GGGGTTGGGG GCTTGTGGAG TCTTTGTTCG CCTTGCTGCT
39541  CCTGCGCGAC TAGGGTGCGA GCGTACTCTT CTAATCGCAT TTTGGGCTTC TTAGGGAGGG
39601  AGGAGGGGCG GGCTGGCAGA ACCCAGGCTT CCTCACACTC GCCCTCTTTC TTGGTTTCTT

39661  TCTCAGGGAA AACCATCTAT GAGAACTCCT CTCCGTGAAC TTACCCTGCA GCCCGGTGCC
39721  CTCACCAACT CTGGAAAAAG ATCCCCCGCT TGCTCCTCGC TGACCCCATC ACTGTGCAAG
39781  CTGGGGCTGC AGGTGAGATT CGCCTGGACA GCTTCTCGAC TGGGCTGTTT GCCCAGGGTG

39841  AGAGCTCAGG GGAACAGAGG GCCAGGGCTA CAATAATTAA TAACGATAAT GAAGTCTTCT
39901  ACGTCGGTGA CATCCATTTA CAGCTATTCA GGCCAACAGA GAGGTGCCCT AGGGTGGTTA
39961  AAGGAAATCC AGTGAGAACT TGAATCTCTG TTTAGCTGTT AGTTTTTATT ACCTCCTCCT
40021  CCTCCCTTCG ACCTTTATCA AACTATTGAG AAATCCTACC ACCCTGATTA GTGCTCTTCC

40081  TCCAACATGG GGTCACTTAC GGAAAGGTCA GTCACCTGCA AGATTGAGGC AATATCCATT

                    ||||||||| |||||||||| |||
                    cagtgaatc cctttccagt cag

40141  TACTCTAGGA GGTAGTTAGA ACTCTCCTGG GATCAAGTTA CACCACTGGA AGGTAGGGTA
40201  CTTGAATCAC CTTAGTTTAA ACTAGCTCCT TGCAGAATTG CCCTCACTGA TTTGTACTTT
40261  TGTTAAACGT TTTGAGAGAC GTAGCCATGT AGAAACTGCA TTTCAGTTGC TGTCAAAACT
```

Guide Plasmid (pCasGuide-SPAG5-RNA1)

EcoRI Cut Site (G/AATTC) Below (1bp)

```
  1    GAATTCCCCA GTGGAAAGAC GCGCAGGCAA AACGCACCAC GTGACGGAGC GTGACCGCGC
 61    GCCGAGCGCG CGCCAAGGTC GGGCAGGAAG AGGGCCTATT TCCCATGATT CCTTCATATT
121    TGCATATACG ATACAAGGCT GTTAGAGAGA TAATTAGAAT TAATTTGACT GTAAACACAA
```

```
 181  AGATATTAGT ACAAAATACG TGACGTAGAA AGTAATAATT TCTTGGGTAG TTTGCAGTTT
 241  TAAAATTATG TTTTAAAATG GACTATCATA TGCTTACCGT AACTTGAAAG TATTTCGATT
 301  TCTTGGGTTT ATATATCTTG TGGAAAGGAC GCGGGATCGC TTCGCCCCAG ACGGTAAGGT
 361  TTTAGAGCTA GAAATAGCAA GTTAAAATAA GGCTAGTCCG TTATCAACTT GAAAAAGTGG
 421  CACCGAGTCG GTGCTTTTTT TGGTGTACAT TTATATTGGC TCATGTCCAA TATGACCGCC
 481  ATGTTGACAT TGATTATTGA CTAGTTATTA ATAGTAATCA ATTACGGGGT CATTAGTTCA
 541  TAGCCCATAT ATGGAGTTCC GCGTTACATA ACTTACGGTA AATGGCCCGC CTGGCTGACC
 601  GCCCAACGAC CCCCGCCCAT TGACGTCAAT AATGACGTAT GTTCCCATAG TAACGCCAAT
 661  AGGGACTTTC CATTGACGTC AATGGGTGGA GTATTTACGG TAAACTGCCC ACTTGGCAGT
 721  ACATCAAGTG TATCATATGC CAAGTCCGCC CCCTATTGAC GTCAATGACG GTAAATGGCC
 781  CGCCTGGCAT TATGCCCAGT ACATGACCTT ACGGGACTTT CCTACTTGGC AGTACATCTA
 841  CGTATTAGTC ATCGCTATTA CCATGGTGAT GCGGTTTTGG CAGTACACCA ATGGGCGTGG
 901  ATAGCGGTTT GACTCACGGG GATTTCCAAG TCTCCACCCC ATTGACGTCA ATGGGAGTTT
 961  GTTTTGGCAC CAAAATCAAC GGGACTTTCC AAAATGTCGT AATAACCCCG CCCCGTTGAC
1021  GCAAATGGGC GGTAGGCGTG TACGGTGGGA GGTCTATATA AGCAGAGCTC GTTTAGTGAA
```

EcoRI Cut Site (G/AATTC) Below (1123bp)

```
1081  CCGTCAGAAT TTTGTAATAC GACTCACTAT AGGGCGGCCG GGAATTCGTC GACTGGAACC
1141  GGTACCGAGG AGATCTGCCG CCGCGATCGC CATGGATAAG AAATACTCAA TAGGACTGGA
1201  TATTGGCACA AATAGCGTCG GATGGGCTGT GATCACTGAT GAATATAAGG TTCCTTCTAA
1261  AAAGTTCAAG GTTCTGGGAA ATACAGACCG CCACAGTATC AAAAAAAATC TTATAGGGGC
1321  TCTTCTGTTT GACAGTGGAG AGACAGCCGA AGCTACTAGA CTCAAACGGA CAGCTAGGAG
1381  AAGGTATACA AGACGGAAGA ATAGGATTTG TTATCTCCAG GAGATTTTTT CAAATGAGAT
1441  GGCCAAAGTG GATGATAGTT TCTTTCATAG ACTTGAAGAG TCTTTTTTGG TGGAAGAAGA
1501  CAAGAAGCAT GAAAGACATC CTATTTTTGG AAATATAGTG GATGAAGTTG CTTATCACGA
1561  GAAATATCCA ACTATCTATC ATCTGAGAAA AAAATTGGTG GATTCTACTG ATAAAGCCGA
1621  TTTGCGCCTG ATCTATTTGG CCCTGGCCCA CATGATTAAG TTTAGAGGTC ATTTTTTGAT
1681  TGAGGGCGAT CTGAATCCTG ATAATAGTGA TGTGGACAAA CTGTTTATCC AGTTGGTGCA
1741  AACCTACAAT CAACTGTTTG AAGAAAACCC TATTAACGCA AGTGGAGTGG ATGCTAAAGC
1801  CATTCTTTCT GCAAGATTGA GTAAATCAAG AAGACTGGAA AATCTCATTG CTCAGCTCCC
1861  CGGTGAGAAG AAAAATGGCC TGTTTGGGAA TCTCATTGCT TTGTCATTGG GTTTGACCCC
1921  TAATTTTAAA TCAAATTTTG ATTTGGCAGA AGATGCTAAA CTCCAGCTTT CAAAAGATAC
1981  TTACGATGAT GATCTGGATA ATCTGTTGGC TCAAATTGGA GATCAATATG CTGATTTGTT
2041  TTTGGCAGCT AAGAATCTGT CAGATGCTAT TCTGCTTTCA GACATCCTGA GAGTGAATAC
2101  TGAAATAACT AAGGCTCCCC TGTCAGCTTC AATGATTAAA CGCTACGATG AACATCATCA
2161  AGACTTGACT CTTCTGAAAG CCCTGGTTAG ACAACAACTT CCAGAAAAGT ATAAAGAAAT
2221  CTTTTTTGAT CAATCAAAAA ACGGATATGC AGGTTATATT GATGGCGGCG CAAGCCAAGA
2281  AGAATTTTAT AAATTTATCA AACCAATTCT GGAAAAAATG GATGGTACTG AGGAACTGTT
2341  GGTGAAACTG AATAGAGAAG ATTTGCTGCG CAAGCAACGG ACCTTTGACA ACGGCTCTAT
2401  TCCCCATCAA ATTCACTTGG GTGAGCTGCA TGCTATTTTG AGAAGACAAG AAGACTTTTA
2461  TCCATTTCTG AAAGACAATA GAGAGAAGAT TGAAAAAATC TTGACTTTTA GGATTCCTTA
2521  TTATGTTGGT CCATTGGCCA GAGGCAATAG TAGGTTTGCA TGGATGACTC GGAAGTCTGA
2581  AGAAACAATT ACCCCATGGA ATTTTGAAGA AGTTGTCGAT AAAGGTGCTT CAGCTCAATC
2641  ATTTATTGAA CGCATGACAA ACTTTGATAA AAATCTTCCA AATGAAAAAG TGCTGCCAAA
2701  ACATAGTTTG CTTTATGAGT ATTTTACCGT TTATAACGAA TTGACAAAGG TCAAATATGT
2761  TACTGAAGGA ATGAGAAAAC CAGCATTTCT TTCAGGTGAA CAGAAGAAAG CCATTGTTGA
2821  TCTGCTCTTC AAAACAAATA GGAAAGTGAC CGTTAAGCAA CTGAAAGAAG ATTATTTCAA
2881  AAAAATAGAA TGTTTTGATA GTGTTGAAAT TTCAGGAGTT GAAGATAGAT TTAATGCTTC
2941  ACTGGGTACA TACCATGATT TGCTGAAAAT TATTAAAGAT AAAGATTTTT TGGATAATGA
3001  AGAAAATGAA GACATCCTGG AGGATATTGT TCTGACATTG ACCCTGTTTG AAGATAGGGA
3061  GATGATTGAG GAAAGACTTA AAACATACGC TCACCTCTTT GATGATAAGG TGATGAAACA
3121  GCTTAAAAGA CGCAGATATA CTGGTTGGGG AAGGTTGTCC AGAAAATTGA TTAATGGTAT
3181  TAGGGATAAG CAATCTGGCA AAACAATACT GGATTTTTTG AAATCAGATG GTTTTGCCAA
3241  TCGCAATTTT ATGCAGCTCA TCCATGATGA TAGTTTGACA TTTAAAGAAG ACATCCAAAA
3301  AGCACAAGTG TCTGGACAAG GCGATAGTCT GCATGAACAT ATTGCAAATC TGGCTGGTAG
3361  CCCTGCTATT AAAAAAGGTA TTCTCCAGAC TGTGAAAGTT GTTGATGAAT TGGTCAAAGT
3421  GATGGGGCGG CATAAGCCAG AAAATATCGT TATTGAAATG GCAAGAGAAA ATCAGACAAC
3481  TCAAAAGGGC CAGAAAAATT CCAGAGAGAG GATGAAAAGA ATCGAAGAAG GTATCAAAGA
3541  ACTGGGAAGT CAGATTCTTA AAGAGCATCC TGTTGAAAAT ACTCAATTGC AAAATGAAAA
3601  GCTCTATCTC TATTATCTCC AAAATGGAAG AGATATGTAT GTGGACCAAG AACTGGATAT
3661  TAATAGGCTG AGTGATTATG ATGTCGATCA CATTGTTCCA CAAAGTTTCC TTAAAGACGA
3721  TTCAATAGAC AATAAGGTCC TGACCAGGTC TGATAAAAAT AGAGGTAAAT CCGATAACGT
```

```
3781  TCCAAGTGAA GAAGTGGTCA AAAAGATGAA AAACTATTGG AGACAACTTC TGAACGCCAA
3841  GCTGATCACT CAAAGGAAGT TTGATAATCT GACCAAAGCT GAAAGAGGAG GTTTGAGTGA
3901  ACTTGATAAA GCTGGTTTTA TCAAACGCCA ATTGGTTGAA ACTCGCCAAA TCACTAAGCA
3961  TGTGGCACAA ATTTTGGATA GTCGCATGAA TACTAAATAC GATGAAAATG ATAAACTTAT
4021  TAGAGAGGTT AAAGTGATTA CCCTGAAATC TAAACTGGTT TCTGACTTCA GAAAAGATTT
4081  CCAATTCTAT AAAGTGAGAG AGATTAACAA TTACCATCAT GCCCATGATG CCTATCTGAA
4141  TGCCGTCGTT GGAACTGCTT TGATTAAGAA ATATCCAAAA CTTGAAAGCG AGTTTGTCTA
4201  TGGTGATTAT AAAGTTTATG ATGTTAGGAA AATGATTGCT AAGTCTGAGC AAGAAATAGG
4261  CAAAGCAACC GCAAAGTATT TCTTTTACTC TAATATCATG AACTTCTTCA AAACAGAAAT
4321  TACACTTGCA AATGGAGAGA TTCGCAAACG CCCTCTGATC GAAACTAATG GGGAAACTGG
4381  AGAAATTGTC TGGGATAAAG GGAGAGATTT TGCCACAGTG CGCAAAGTGT TGTCCATGCC
4441  CCAAGTCAAT ATCGTCAAGA AAACAGAAGT GCAGACAGGC GGATTCTCTA AGGAGTCAAT
4501  TCTGCCAAAA AGAAATTCCG ACAAGCTGAT TGCTAGGAAA AAAGACTGGG ACCCAAAAAA
4561  ATATGGTGGT TTTGATAGTC CAACCGTGGC TTATTCAGTC CTGGTGGTTG CTAAGGTGGA
4621  AAAAGGGAAA TCCAAGAAGC TGAAATCCGT TAAAGAGCTG CTGGGGATCA CAATTATGGA
4681  AAGAAGTTCC TTTGAAAAAA ATCCCATTGA CTTTCTGGAA GCTAAAGGAT ATAAGGAAGT
4741  TAAAAAAGAC CTGATCATTA AACTGCCTAA ATATAGTCTT TTTGAGCTGG AAAACGGTAG
4801  GAAACGGATG CTGGCTAGTG CCGGAGAACT GCAAAAAGGA AATGAGCTGG CTCTGCCAAG
4861  CAAATATGTG AATTTTCTGT ATCTGGCTAG TCATTATGAA AAGTTGAAGG GTAGTCCAGA
4921  AGATAACGAA CAAAAACAAT TGTTTGTGGA GCAGCATAAG CATTATCTGG ATGAGATTAT
4981  TGAGCAAATC AGTGAATTTT CTAAGAGAGT TATTCTGGCA GATGCCAATC TGGATAAAGT
5041  TCTTAGTGCA TATAACAAAC ATAGAGACAA ACCAATAAGA GAACAAGCAG AAAATATCAT
5101  TCATCTGTTT ACCTTGACCA ATCTTGGAGC ACCCGCTGCT TTTAAATACT TTGATACAAC
5161  AATTGATAGG AAAAGATATA CCTCTACAAA AGAAGTTCTG GATGCCACTC TTATCCATCA
5221  ATCCATCACT GGTCTTTATG AAACACGCAT TGATTTGAGT CAGCTGGGAG GTGACCCCAA
5281  GAAAAAACGC AAGGTGGAAG ATCCTAAGAA AAAGCGGAAA GTGGACACGC GTACGCGGCC
5341  GCTCGAGCAG AAACTCATCT CAGAAGAGGA TCTGGCAGCA AATGATATCC TGGATTACAA
5401  GGATGACGAC GATAAGGTTT AAACGGCCGG CCGCGGTCAT AGCTGTTTCC TGAACAGATC
5461  CCGGGTGGCA TCCCTGTGAC CCCTCCCCAG TGCCTCTCCT GGCCCTGGAA GTTGCCACTC
5521  CAGTGCCCAC CAGCCTTGTC CTAATAAAAT TAAGTTGCAT CATTTTGTCT GACTAGGTGT
5581  CCTTCTATAA TATTATGGGG TGGAGGGGGG TGGTATGGAG CAAGGGGCAA GTTGGGAAGA
5641  CAACCTGTAG GGCCTGCGGG GTCTATTGGG AACCAAGCTG GAGTGCAGTG GCACAATCTT
5701  GGCTCACTGC AATCTCCGCC TCCTGGGTTC AAGCGATTCT CCTGCCTCAG CCTCCCGAGT
5761  TGTTGGGATT CCAGGCATGC ATGACCAGGC TCAGCTAATT TTTGTTTTTT TGGTAGAGGC
5821  GGGGTTTCAC CATATTGGCC AGGCTGGTCT CCAACTCCTA ATCTCAGGTG ATCTACCCAC
5881  CTTGGCCTCC CAAATTGCTG GGATTACAGG CGTGAACCAC TGCTCCCTTC CCTGTCCTTC
5941  TGATTTTAAA ATAACTATAC CAGCAGGAGG ACGTCCAGAC ACAGCATAGG CTACCTGGCC
6001  ATGCCCAACC GGTGGGACAT TTGAGTTGCT TGCTTGGCAC TGTCCTCTCA TGCGTTGGGT
6061  CCACTCAGTA GATGCCTGTT GAATTGGGTA CGCGGCCAGC GGCGAGCGGT ATCAGCTCAC
6121  TCAAAGGCGG TAATACGGTT ATCCACAGAA TCAGGGGATA ACGCAGGAAA GAACATGTCC
6181  GTAAAAAGGC CGCGTTGCTG GCGTTTTTCC ATAGGCTCCG CCCCCCTGAC GAGCATCACA
6241  AAAATCGACG CTCAAGTCAG AGGTGGCGAA ACCCGACAGG ACTATAAAGA TACCAGGCGT
6301  TTCCCCCTGG AAGCTCCCTC GTGCGCTCTC CTGTTCCGAC CCTGCCGCTT ACCGGATACC
6361  TGTCCGCCTT TCTCCCTTCG GGAAGCGTGG CGCTTTCTCA TAGCTCACGC TGTAGGTATC
6421  TCAGTTCGGT GTAGGTCGTT CGCTCCAAGC TGGGCTGTGT GCACGAACCC CCCGTTCAGC
6481  CCGACCGCTG CGCCTTATCC GGTAACTATC GTCTTGAGTC CAACCCGGTA AGACACGACT
6541  TATCGCCACT GGCAGCAGCC ACTGGTAACA GGATTAGCAG AGCGAGGTAT GTAGGCGGTG
6601  CTACAGAGTT CTTGAAGTGG TGGCCTAACT ACGGCTACAC TAGAAGAACA GTATTTGGTA
6661  TCTGCGCTCT GCTGAAGCCA GTTACCTTCG GAAAAAGAGT TGGTAGCTCT TGATCCGGCA
6721  AACAAACCAC CGCTGGTAGC GGTGGTTTTT TTGTTTGCAA GCAGCAGATT ACGCGCAGAA
6781  AAAAAGGATC TCAAGAAGAT CCTTTGATCT TTTCTACGGG GTCTGACGCT CAGTGGAACG
6841  ACGCGTAACT CACGTTAAGG GATTTTGGTC ATGAGATTAT CAAAAAGGAT CTTCACCTAG
6901  ATCCTTTTGC GGCCGCAAAT CAATCTAAAG TATATATGAG TAAACTTGGT CTGACAGTTA
6961  CCAATGCTTA ATCAGTGAGG CACCTATCTC AGCGATCTGT CTATTTCGTT CATCCATAGT
7021  TGCCTGACTC CCCGTCGTGT AGATAACTAC GATACGGGAG GGCTTACCAT CTGGCCCCAG
7081  TGCTGCAATG ATACCGCGAG ACCCACGCTC ACCGGCTCCA GATTTATCAG CAATAAACCA
7141  GCCAGCCGGA AGGGCCGAGC GCAGAAGTGG TCCTGCAACT TTATCCGCCT CCATCCAGTC
7201  TATTAATTGT TGCCGGGAAG CTAGAGTAAG TAGTTCGCCA GTTAATAGTT TGCGCAACGT
7261  TGTTGCCATT GCTACAGGCA TCGTGGTGTC ACGCTCGTCG TTTGGTATGG CTTCATTCAG
7321  CTCCGGTTCC CAACGATCAA GGCGAGTTAC ATGATCCCCC ATGTTGTGCA AAAAAGCGGT
7381  TAGCTCCTTC GGTCCTCCGA TCGTTGTCAG AAGTAAGTTG GCCGCAGTGT TATCACTCAT
```

```
7441  GGTTATGGCA GCACTGCATA ATTCTCTTAC TGTCATGCCA TCCGTAAGAT GCTTTTCTGT
7501  GACTGGTGAG TACTCAACCA AGTCATTCTG AGAATAGTGT ATGCGGCGAC CGAGTTGCTC
7561  TTGCCCGGCG TCAATACGGG ATAATACCGC GCCACATAGC AGAACTTTAA AAGTGCTCAT
7621  CATTGGAAAA CGTTCTTCGG GGCGAAAACT CTCAAGGATC TTACCGCTGT TGAGATCCAG
7681  TTCGATGTAA CCCACTCGTG CACCCAACTG ATCTTCAGCA TCTTTTACTT TCACCAGCGT
7741  TTCTGGGTGA GCAAAAACAG GAAGGCAAAA TGCCGCAAAA AAGGGAATAA GGGCGACACG
7801  GAAATGTTGA ATACTCATAC TCTTCCTTTT TCAATATTAT TGAAGCATTT ATCAGGGTTA
7861  TTGTCTCATG ATGATATATT TTTATCTTGT GCAATGTAAC ATCAGAGATT TTGAGACACG
7921  GGCCAGAGCT GCCAGGAAAC AGCTATGACC ATGTAATACG ACTCACTATA GGGGATATCA
7981  GCTGGATGGC AGTTAAC
```

References

Aaronson, S. A. (1991). Growth Factors and Cancer. *Science, 254*(5035), 1146-1153. http://www.jstor.org.ezproxy.aut.ac.nz/stable/2879323

Abdel-Fatah, Agarwal, D., Liu, D. X., Russell, R., Rueda, O. M., Liu, K., Xu, B., Moseley, P. M., Green, A. R., Pockley, A. G., Rees, R. C., Caldas, C., Ellis, I. O., Ball, G. R., & Chan, S. Y. T. (2016, Jul). SPAG5 as a prognostic biomarker and chemotherapy sensitivity predictor in breast cancer: a retrospective, integrated genomic, transcriptomic, and protein analysis. *Lancet Oncol, 17*(7), 1004-1018. https://doi.org/10.1016/s1470-2045(16)00174-1

Acheampong, T., Kehm, R. D., Terry, M. B., Argov, E. L., & Tehranifar, P. (2020, Aug 3). Incidence Trends of Breast Cancer Molecular Subtypes by Age and Race/Ethnicity in the US From 2010 to 2016. *JAMA Netw Open, 3*(8), e2013226. https://doi.org/10.1001/jamanetworkopen.2020.13226

Aita, V. M., Liang, X. H., Murty, V. V., Pincus, D. L., Yu, W., Cayanis, E., Kalachikov, S., Gilliam, T. C., & Levine, B. (1999, Jul 1). Cloning and genomic organization of beclin 1, a candidate tumor suppressor gene on chromosome 17q21. *Genomics, 59*(1), 59-65. https://doi.org/10.1006/geno.1999.5851

Baboo, J., Kilbride, P., Delahaye, M., Milne, S., Fonseca, F., Blanco, M., Meneghel, J., Nancekievill, A., Gaddum, N., & Morris, G. J. (2019, 2019/03/04). The Impact of Varying Cooling and Thawing Rates on the Quality of Cryopreserved Human Peripheral Blood T Cells. *Scientific Reports, 9*(1), 3417. https://doi.org/10.1038/s41598-019-39957-x

Badowska-Kozakiewicz, A. M., & Budzik, M. P. (2016). Immunohistochemical characteristics of basal-like breast cancer. *Contemp Oncol (Pozn), 20*(6), 436-443. https://doi.org/10.5114/wo.2016.56938

Bates, D. O. (2010, Jul 15). Vascular endothelial growth factors and vascular permeability. *Cardiovasc Res, 87*(2), 262-271. https://doi.org/10.1093/cvr/cvq105

Belzile-Dugas, E., & Eisenberg, M. J. (2021, Sep 21). Radiation-Induced Cardiovascular Disease: Review of an Underrecognized Pathology. *J Am Heart Assoc, 10*(18), e021686. https://doi.org/10.1161/jaha.121.021686

Bertucci, F., Viens, P., & Birnbaum, D. (2016, 06/13). SPAG5: the ultimate marker of proliferation in early breast cancer? *The Lancet. Oncology, 17*. https://doi.org/10.1016/S1470-2045(16)30092-4

Bhowmick, N. A., Neilson, E. G., & Moses, H. L. (2004). Stromal fibroblasts in cancer initiation and progression. *Nature, 432*(7015), 332-337.

Bhushan, A., Gonsalves, A., & Menon, J. U. (2021, May 14). Current State of Breast Cancer Diagnosis, Treatment, and Theranostics. *Pharmaceutics, 13*(5). https://doi.org/10.3390/pharmaceutics13050723

BLASTn. (14/9/2022). National Center for Biotechnology Information (NCBI). https://blast.ncbi.nlm.nih.gov/Blast.cgi?PROGRAM=blastn&PAGE_TYPE=BlastSearch&LINK_LOC=blasthome

Bonnell, E., Pasquier, E., & Wellinger, R. J. (2021). Telomere Replication: Solving Multiple End Replication Problems. *Front Cell Dev Biol, 9*, 668171. https://doi.org/10.3389/fcell.2021.668171

Breast cancer in New Zealand. Breast Cancer Foundation New Zealand. Retrieved 19/09/2022 from https://www.breastcancerfoundation.org.nz/breast-awareness/breast-cancer-facts/breast-cancer-in-nz

Breast cancer treatment. (2023). Breast Cancer Foundation NZ. Retrieved 12-03-2023 from https://www.breastnet.nz/topic/breast-cancer-treatment

Carmeliet, P. (2005, Dec 15). Angiogenesis in life, disease and medicine. *Nature, 438*(7070), 932-936. https://doi.org/10.1038/nature04478

Chang, M. S., Huang, C. J., Chen, M. L., Chen, S. T., Fan, C. C., Chu, J. M., Lin, W. C., & Yang, Y. C. (2001, Sep 14). Cloning and characterization of hMAP126, a new member of mitotic spindle-associated proteins. *Biochem Biophys Res Commun, 287*(1), 116-121. https://doi.org/10.1006/bbrc.2001.5554

Chen, Y., Wei, H., Liu, F., & Guan, J. L. (2014, Jan 10). Hyperactivation of mammalian target of rapamycin complex 1 (mTORC1) promotes breast cancer progression through enhancing glucose starvation-induced autophagy and Akt signaling. *J Biol Chem, 289*(2), 1164-1173. https://doi.org/10.1074/jbc.M113.526335

Cheng, K., Samimi, R., Xie, G., Shant, J., Drachenberg, C., Wade, M., Davis, R. J., Nomikos, G., & Raufman, J.-P. (2008). Acetylcholine release by human colon cancer cells mediates autocrine stimulation of cell proliferation. *American Journal of Physiology-Gastrointestinal and Liver Physiology, 295*(3), G591-G597.

Chung, H. J., Park, J. E., Lee, N. S., Kim, H., & Jang, C. Y. (2016, Aug 19). Phosphorylation of Astrin Regulates Its Kinetochore Function. *J Biol Chem, 291*(34), 17579-17592. https://doi.org/10.1074/jbc.M115.712745

Cicenas, J. (2008, Jan-Mar). The potential role of Akt phosphorylation in human cancers. *Int J Biol Markers, 23*(1), 1-9. https://doi.org/10.5301/jbm.2008.618

Cilibrasi, C., Papanastasopoulos, P., Samuels, M., & Giamas, G. (2021, Nov 6). Reconstituting Immune Surveillance in Breast Cancer: Molecular Pathophysiology and Current Immunotherapy Strategies. *Int J Mol Sci, 22*(21). https://doi.org/10.3390/ijms222112015

Collins, A., & Politopoulos, I. (2011). The genetics of breast cancer: risk factors for disease. *Appl Clin Genet, 4*, 11-19. https://doi.org/10.2147/tacg.S13139

Conti, D., Gul, P., Islam, A., Martin-Duran, J. M., Pickersgill, R. W., & Draviam, V. M. (2019, Dec 6). Kinetochores attached to microtubule-ends are stabilised by Astrin bound PP1 to ensure proper chromosome segregation. *Elife, 8*. https://doi.org/10.7554/eLife.49325

Darby, S., McGale, P., Correa, C., Taylor, C., Arriagada, R., Clarke, M., Cutter, D., Davies, C., Ewertz, M., Godwin, J., Gray, R., Pierce, L., Whelan, T., Wang, Y., & Peto, R. (2011, Nov 12). Effect of radiotherapy after breast-conserving surgery on 10-year recurrence and 15-year breast cancer death: meta-analysis of individual patient data for 10,801 women in 17 randomised trials. *Lancet, 378*(9804), 1707-1716. https://doi.org/10.1016/s0140-6736(11)61629-2

Dastmalchi, N., Safaralizadeh, R., Hosseinpourfeizi, M. A., Baradaran, B., & Khojasteh, S. M. B. (2021, Feb). MicroRNA-424-5p enhances chemosensitivity of breast cancer cells to Taxol and regulates cell cycle, apoptosis, and proliferation. *Mol Biol Rep, 48*(2), 1345-1357. https://doi.org/10.1007/s11033-021-06193-4

de Regt, A. K., Asbury, C. L., & Biggins, S. (2018). Tension on kinetochore substrates is insufficient to prevent Aurora-triggered detachment. *bioRxiv*, 415992. https://doi.org/10.1101/415992

DeSantis, C. E., Bray, F., Ferlay, J., Lortet-Tieulent, J., Anderson, B. O., & Jemal, A. (2015, Oct). International Variation in Female Breast Cancer Incidence and Mortality Rates. *Cancer Epidemiol Biomarkers Prev, 24*(10), 1495-1506. https://doi.org/10.1158/1055-9965.Epi-15-0535

Easton, J. B., & Houghton, P. J. (2006, Oct 16). mTOR and cancer therapy. *Oncogene, 25*(48), 6436-6446. https://doi.org/10.1038/sj.onc.1209886

Ferlay J, E. M., Lam F, Laversanne M, Colombet M, Mery L, Piñeros M, Znaor A, Soerjomataram I, Bray F. (2024). *BREAST*. Global Cancer Observatory: Cancer Today. Lyon, France: International Agency for Research on Cancer. Retrieved 5/03/2024 from https://gco.iarc.who.int/media/globocan/factsheets/cancers/20-breast-fact-sheet.pdf

Gholkar, A. A., Senese, S., Lo, Y. C., Vides, E., Contreras, E., Hodara, E., Capri, J., Whitelegge, J. P., & Torres, J. Z. (2016, Jan 12). The X-Linked-Intellectual-Disability-Associated Ubiquitin Ligase Mid2 Interacts with Astrin and Regulates Astrin Levels to Promote Cell Division. *Cell Rep, 14*(2), 180-188. https://doi.org/10.1016/j.celrep.2015.12.035

Gonzalez, H., Hagerling, C., & Werb, Z. (2018, Oct 1). Roles of the immune system in cancer: from tumor initiation to metastatic progression. *Genes Dev, 32*(19-20), 1267-1284. https://doi.org/10.1101/gad.314617.118

Gruber, J., Harborth, J., Schnabel, J., Weber, K., & Hatzfeld, M. (2002). The mitotic-spindle-associated protein astrin is essential for progression through mitosis. *Journal of Cell Science, 115*(21), 4053-4059. https://doi.org/10.1242/jcs.00088

Gu, L., & Sun, W. (2015, Sep 4). MiR-539 inhibits thyroid cancer cell migration and invasion by directly targeting CARMA1. *Biochem Biophys Res Commun, 464*(4), 1128-1133. https://doi.org/10.1016/j.bbrc.2015.07.090

Gu, X. (2002). Helix 12 in the human estrogen receptor (hER) is essential for the hER function by overcoming nucleosome repression in yeast. *J Cell Biochem, 86*(2), 224-238. https://doi.org/10.1002/jcb.10229

Guan, X. (2015, Sep). Cancer metastases: challenges and opportunities. *Acta Pharm Sin B, 5*(5), 402-418. https://doi.org/10.1016/j.apsb.2015.07.005

Guertin, D. A., & Sabatini, D. M. (2007, Jul). Defining the role of mTOR in cancer. *Cancer Cell, 12*(1), 9-22. https://doi.org/10.1016/j.ccr.2007.05.008

Guidolin, K., Lock, M., Vogt, K., McClure, J. A., Winick-Ng, J., Vinden, C., & Brackstone, M. (2019, Dec). Recurrence and mortality after breast-conserving surgery without radiation. *Curr Oncol, 26*(6), 380-388. https://doi.org/10.3747/co.26.5225

Gunaldi, M., Isiksacan, N., Kocoglu, H., Okuturlar, Y., Gunaldi, O., Topcu, T. O., & Karabulut, M. (2018, Apr-Jun). The value of serum survivin level in early diagnosis of cancer. *J Cancer Res Ther, 14*(3), 570-573. https://doi.org/10.4103/0973-1482.171369

Hanahan, & Weinberg. (2011, Mar 4). Hallmarks of cancer: the next generation. *Cell, 144*(5), 646-674. https://doi.org/10.1016/j.cell.2011.02.013

Hanahan, D., & Folkman, J. (1996, Aug 9). Patterns and emerging mechanisms of the angiogenic switch during tumorigenesis. *Cell, 86*(3), 353-364. https://doi.org/10.1016/s0092-8674(00)80108-7

Hanahan, D., & Weinberg, R. A. (2000, Jan 7). The hallmarks of cancer. *cell, 100*(1), 57-70. https://doi.org/10.1016/s0092-8674(00)81683-9

Hapach, L. A., Mosier, J. A., Wang, W., & Reinhart-King, C. A. (2019). Engineered models to parse apart the metastatic cascade. *NPJ Precis Oncol, 3*, 20. https://doi.org/10.1038/s41698-019-0092-3

Harris, C. C. (1996). p53 tumor suppressor gene: From the basic research laboratory to the clinic - An abridged historical perspective [Review]. *Carcinogenesis, 17*(6), 1187-1198. https://doi.org/10.1093/carcin/17.6.1187

Hass, R., von der Ohe, J., & Ungefroren, H. (2019, Sep 25). Potential Role of MSC/Cancer Cell Fusion and EMT for Breast Cancer Stem Cell Formation. *Cancers (Basel), 11*(10). https://doi.org/10.3390/cancers11101432

Hayashi, M. T., & Karlseder, J. (2013, Sep 26). DNA damage associated with mitosis and cytokinesis failure. *Oncogene, 32*(39), 4593-4601. https://doi.org/10.1038/onc.2012.615

Heitz, F., Harter, P., Lueck, H. J., Fissler-Eckhoff, A., Lorenz-Salehi, F., Scheil-Bertram, S., Traut, A., & du Bois, A. (2009, Nov). Triple-negative and HER2-overexpressing breast cancers exhibit an elevated risk and an earlier occurrence of cerebral metastases. *Eur J Cancer, 45*(16), 2792-2798. https://doi.org/10.1016/j.ejca.2009.06.027

Ho, C. M., Huang, C. J., Huang, S. H., Chang, S. F., & Cheng, W. F. (2015, Oct 24). Demethylation of HIN-1 reverses paclitaxel-resistance of ovarian clear cell carcinoma through the AKT-mTOR signaling pathway. *BMC Cancer, 15*, 789. https://doi.org/10.1186/s12885-015-1744-5

Huang, J., Chan, P. S., Lok, V., Chen, X., Ding, H., Jin, Y., Yuan, J., Lao, X. Q., Zheng, Z. J., & Wong, M. C. (2021, Feb 11). Global incidence and mortality of breast cancer: a trend analysis. *Aging (Albany NY), 13*(4), 5748-5803. https://doi.org/10.18632/aging.202502

Huang, R., & Li, A. (2020, 2020/11/01). SPAG5 is associated with unfavorable prognosis in patients with lung adenocarcinoma and promotes proliferation, motility and autophagy in A549 cells. *Exp Ther Med, 20*(5), 77. https://doi.org/10.3892/etm.2020.9205

Itoh, N., Semba, S., Ito, M., Takeda, H., Kawata, S., & Yamakawa, M. (2002, Jun 15). Phosphorylation of Akt/PKB is required for suppression of cancer cell apoptosis and tumor progression in human colorectal carcinoma. *Cancer, 94*(12), 3127-3134. https://doi.org/10.1002/cncr.10591

Jaiswal, P. K., Goel, A., & Mittal, R. D. (2015, Apr). Survivin: A molecular biomarker in cancer. *Indian J Med Res, 141*(4), 389-397. https://doi.org/10.4103/0971-5916.159250

Jiang, J., Wang, J., He, X., Ma, W., Sun, L., Zhou, Q., Li, M., & Yu, S. (2019, Jun). High expression of SPAG5 sustains the malignant growth and invasion of breast cancer cells through the activation of Wnt/beta-catenin signalling. *Clin Exp Pharmacol Physiol, 46*(6), 597-606. https://doi.org/10.1111/1440-1681.13082

Johnson, S. M., Gulhati, P., Arrieta, I., Wang, X., Uchida, T., Gao, T., & Evers, B. M. (2009, Aug). Curcumin inhibits proliferation of colorectal carcinoma by modulating Akt/mTOR signaling. *Anticancer Res, 29*(8), 3185-3190. https://www.ncbi.nlm.nih.gov/pubmed/19661333

Joo, W. D., Visintin, I., & Mor, G. (2013, Dec). Targeted cancer therapy--are the days of systemic chemotherapy numbered? *Maturitas, 76*(4), 308-314. https://doi.org/10.1016/j.maturitas.2013.09.008

Kampan, N. C., Madondo, M. T., McNally, O. M., Quinn, M., & Plebanski, M. (2015). Paclitaxel and Its Evolving Role in the Management of Ovarian Cancer. *Biomed Res Int, 2015*, 413076. https://doi.org/10.1155/2015/413076

Klos, K. S., Zhou, X., Lee, S., Zhang, L., Yang, W., Nagata, Y., & Yu, D. (2003, Oct 1). Combined trastuzumab and paclitaxel treatment better inhibits ErbB-2-mediated angiogenesis in breast carcinoma through a more effective inhibition of Akt than either treatment alone. *Cancer, 98*(7), 1377-1385. https://doi.org/10.1002/cncr.11656

Kreisberg, J. I., Malik, S. N., Prihoda, T. J., Bedolla, R. G., Troyer, D. A., Kreisberg, S., & Ghosh, P. M. (2004, Aug 1). Phosphorylation of Akt (Ser473) is an excellent predictor of poor clinical outcome in prostate cancer. *Cancer Res, 64*(15), 5232-5236. https://doi.org/10.1158/0008-5472.CAN-04-0272

Kroemer, G., Senovilla, L., Galluzzi, L., André, F., & Zitvogel, L. (2015, Oct). Natural and therapy-induced immunosurveillance in breast cancer. *Nat Med, 21*(10), 1128-1138. https://doi.org/10.1038/nm.3944

Kumari, R., & Jat, P. (2021). Mechanisms of Cellular Senescence: Cell Cycle Arrest and Senescence Associated Secretory Phenotype. *Front Cell Dev Biol, 9*, 645593. https://doi.org/10.3389/fcell.2021.645593

Kunter, I., Erdal, E., Nart, D., Yilmaz, F., Karademir, S., Sagol, O., & Atabey, N. (2014, Feb). Active form of AKT controls cell proliferation and response to apoptosis in hepatocellular carcinoma. *Oncol Rep, 31*(2), 573-580. https://doi.org/10.3892/or.2013.2932

Lawrenson, R., Seneviratne, S., Scott, N., Peni, T., Brown, C., & Campbell, I. (2016, Mar). Breast cancer inequities between Māori and non-Māori women in Aotearoa/New Zealand. *Eur J Cancer Care (Engl), 25*(2), 225-230. https://doi.org/10.1111/ecc.12473

Le, X. F., Lammayot, A., Gold, D., Lu, Y., Mao, W., Chang, T., Patel, A., Mills, G. B., & Bast, R. C., Jr. (2005, Jan 21). Genes affecting the cell cycle, growth, maintenance, and drug sensitivity are preferentially regulated by anti-HER2 antibody through phosphatidylinositol 3-kinase-AKT signaling. *J Biol Chem, 280*(3), 2092-2104. https://doi.org/10.1074/jbc.M403080200

Li, M., Li, A., Zhou, S., Lv, H., & Yang, W. (2019, Feb 8). SPAG5 upregulation contributes to enhanced c-MYC transcriptional activity via interaction with c-MYC binding protein in triple-negative breast cancer. *J Hematol Oncol, 12*(1), 14. https://doi.org/10.1186/s13045-019-0700-2

Li, Q., Wang, Y., & He, J. (2021, Jul). MiR-133a-3p attenuates resistance of non-small cell lung cancer cells to gefitinib by targeting SPAG5. *J Clin Lab Anal, 35*(7), e23853. https://doi.org/10.1002/jcla.23853

Li, X., Zhao, G., Mi, X., Xu, T., Li, X., & Liu, B. (2022). Ajuba Overexpression Promotes Breast Cancer Chemoresistance and Glucose Uptake through TAZ-GLUT3/Survivin Pathway. *BioMed Research International*, 1-13. https://doi.org/10.1155/2022/3321409

Li, Z., Li, H., Chen, J., Luo, H., Zeng, J., Yao, Y., & Duan, M. (2020, Sep). SPAG5 promotes osteosarcoma metastasis via activation of FOXM1/MMP2 axis. *Int J Biochem Cell Biol, 126*, 105797. https://doi.org/10.1016/j.biocel.2020.105797

Liang, X. H., Jackson, S., Seaman, M., Brown, K., Kempkes, B., Hibshoosh, H., & Levine, B. (1999, Dec 9). Induction of autophagy and inhibition of tumorigenesis by beclin 1. *Nature, 402*(6762), 672-676. https://doi.org/10.1038/45257

Lim, P. T., Goh, B. H., & Lee, W.-L. (2022). 3 - Taxol: Mechanisms of action against cancer, an update with current research. In M. K. Swamy, T. Pullaiah, & Z.-S. Chen (Eds.), *Paclitaxel* (pp. 47-71). Academic Press. https://doi.org/https://doi.org/10.1016/B978-0-323-90951-8.00007-2

Liu, Hu, Wei, R., Zhou, L., Pan, H., Zhu, H., Huang, M., Luo, J., & Xu, W. (2018, Sep 18). SPAG5 promotes hepatocellular carcinoma progression by downregulating SCARA5 through modifying β-catenin degradation. *J Exp Clin Cancer Res, 37*(1), 229. https://doi.org/10.1186/s13046-018-0891-3

Liu, Zeng, Q. H., Cao, P. G., Xie, D., Yang, F., He, L. Y., Dai, Y. B., Li, J. J., Liu, X. M., Zeng, H. L., Fan, X. J., Liu, L., Zhu, Y. X., Gong, L., Cheng, Y., Zhou, J. D., Hu, J., Bo, H., Xu, Z. Z., & Cao, K. (2018, Jul). SPAG5 promotes proliferation and suppresses apoptosis in bladder urothelial carcinoma by upregulating Wnt3 via activating the AKT/mTOR pathway and predicts poorer survival. *Oncogene, 37*(29), 3937-3952. https://doi.org/10.1038/s41388-018-0223-2

Liu, D., Vader, G., Vromans, M. J., Lampson, M. A., & Lens, S. M. (2009, Mar 6). Sensing chromosome bi-orientation by spatial separation of aurora B kinase from kinetochore substrates. *Science, 323*(5919), 1350-1353. https://doi.org/10.1126/science.1167000

Liu, G., Liu, S., Cao, G., Luo, W., Li, P., Wang, S., & Chen, Y. (2019, Jun 1). SPAG5 contributes to the progression of gastric cancer by upregulation of Survivin depend on activating the wnt/beta-catenin pathway. *Exp Cell Res, 379*(1), 83-91. https://doi.org/10.1016/j.yexcr.2019.03.024

Liu, H., Hu, J., Wei, R., Zhou, L., Pan, H., Zhu, H., Huang, M., Luo, J., & Xu, W. (2018, Sep 18). SPAG5 promotes hepatocellular carcinoma progression by downregulating SCARA5 through modifying β-catenin degradation. *J Exp Clin Cancer Res, 37*(1), 229. https://doi.org/10.1186/s13046-018-0891-3

Liu, J., Zhang, Y., Zeng, H., Wang, L., Zhang, Q., Wu, P., Liu, X., Xie, H., Xiang, W., Liu, B., Liu, J., Liu, X., Xie, J., Tang, J., Long, Z., He, L., Xiao, M., Xiang, L., & Cao, K. (2021, Jun 23). Fe-doped chrysotile nanotubes containing siRNAs to silence SPAG5 to treat bladder cancer. *J Nanobiotechnology, 19*(1), 189. https://doi.org/10.1186/s12951-021-00935-z

Liu, J. Y., Zeng, Q. H., Cao, P. G., Xie, D., Yang, F., He, L. Y., Dai, Y. B., Li, J. J., Liu, X. M., Zeng, H. L., Fan, X. J., Liu, L., Zhu, Y. X., Gong, L., Cheng, Y., Zhou, J. D., Hu, J., Bo, H., Xu, Z. Z., & Cao, K. (2018, Jul). SPAG5 promotes proliferation and suppresses apoptosis in bladder urothelial carcinoma by upregulating Wnt3 via activating the AKT/mTOR pathway and predicts poorer survival. *Oncogene, 37*(29), 3937-3952. https://doi.org/10.1038/s41388-018-0223-2

Liu, P., Begley, M., Michowski, W., Inuzuka, H., Ginzberg, M., Gao, D., Tsou, P., Gan, W., Papa, A., Kim, B. M., Wan, L., Singh, A., Zhai, B., Yuan, M., Wang, Z., Gygi, S. P., Lee, T. H., Lu, K. P., Toker, A., Pandolfi, P. P., Asara, J. M., Kirschner, M. W., Sicinski, P., Cantley, L., & Wei, W. (2014, Apr 24). Cell-cycle-regulated activation of Akt kinase by phosphorylation at its carboxyl terminus. *Nature, 508*(7497), 541-545. https://doi.org/10.1038/nature13079

López-Otín, C., Blasco, M. A., Partridge, L., Serrano, M., & Kroemer, G. (2013, Jun 6). The hallmarks of aging. *Cell, 153*(6), 1194-1217. https://doi.org/10.1016/j.cell.2013.05.039

Lugano, R., Ramachandran, M., & Dimberg, A. (2020, May). Tumor angiogenesis: causes, consequences, challenges and opportunities. *Cell Mol Life Sci, 77*(9), 1745-1770. https://doi.org/10.1007/s00018-019-03351-7

Łukasiewicz, S., Czeczelewski, M., Forma, A., Baj, J., Sitarz, R., & Stanisławek, A. (2021, Aug 25). Breast Cancer-Epidemiology, Risk Factors, Classification, Prognostic Markers, and Current Treatment Strategies-An Updated Review. *Cancers (Basel), 13*(17). https://doi.org/10.3390/cancers13174287

Luo, W., Wang, F., Luo, H., & Liu, H. (2021, Jun). Arctigenin inhibits human breast cancer cell proliferation, migratory and invasive abilities and epithelial to mesenchymal transition by targeting 4EBP1. *Exp Ther Med, 21*(6), 547. https://doi.org/10.3892/etm.2021.9979

Mack, G. J., & Compton, D. A. (2001, Dec 4). Analysis of mitotic microtubule-associated proteins using mass spectrometry identifies astrin, a spindle-associated protein. *Proc Natl Acad Sci U S A, 98*(25), 14434-14439. https://doi.org/10.1073/pnas.261371298

Mahmood, T., & Yang, P. C. (2012, Sep). Western blot: technique, theory, and trouble shooting. *N Am J Med Sci, 4*(9), 429-434. https://doi.org/10.4103/1947-2714.100998

Manning, A. L., Bakhoum Sf Fau - Maffini, S., Maffini S Fau - Correia-Melo, C., Correia-Melo C Fau - Maiato, H., Maiato H Fau - Compton, D. A., & Compton, D. A. (2010). CLASP1, astrin and Kif2b form a molecular switch that regulates kinetochore-microtubule dynamics to promote mitotic progression and fidelity. (1460-2075 (Electronic)).

Manning, B. D., & Cantley, L. C. (2007, Jun 29). AKT/PKB signaling: navigating downstream. *Cell, 129*(7), 1261-1274. https://doi.org/10.1016/j.cell.2007.06.009

Mansoori, B., Mohammadi, A., Davudian, S., Shirjang, S., & Baradaran, B. (2017, Sep). The Different Mechanisms of Cancer Drug Resistance: A Brief Review. *Adv Pharm Bull, 7*(3), 339-348. https://doi.org/10.15171/apb.2017.041

Marinello, J., Delcuratolo, M., & Capranico, G. (2018, Nov 6). Anthracyclines as Topoisomerase II Poisons: From Early Studies to New Perspectives. *Int J Mol Sci, 19*(11). https://doi.org/10.3390/ijms19113480

Mayor, P. C., Eng, K. H., Singel, K. L., Abrams, S. I., Odunsi, K., Moysich, K. B., Fuleihan, R., Garabedian, E., Lugar, P., Ochs, H. D., Bonilla, F. A., Buckley, R. H., Sullivan, K. E., Ballas, Z. K., Cunningham-Rundles, C., & Segal, B. H. (2018, Mar). Cancer in primary immunodeficiency diseases: Cancer incidence in the United States Immune Deficiency Network Registry. *J Allergy Clin Immunol, 141*(3), 1028-1035. https://doi.org/10.1016/j.jaci.2017.05.024

McElligott, R., & Wellinger, R. J. (1997, Jun 16). The terminal DNA structure of mammalian chromosomes. *Embo j, 16*(12), 3705-3714. https://doi.org/10.1093/emboj/16.12.3705

McLaughlin, M., Florida-James, G., & Ross, M. (2021). Breast cancer chemotherapy vascular toxicity: a review of mediating mechanisms and exercise as a potential therapeutic. *Vasc Biol, 3*(1), R106-r120. https://doi.org/10.1530/vb-21-0013

Miller, D. M., Thomas, S. D., Islam, A., Muench, D., & Sedoris, K. (2012, Oct 15). c-Myc and cancer metabolism. *Clin Cancer Res, 18*(20), 5546-5553. https://doi.org/10.1158/1078-0432.CCR-12-0977

Mitra, A., Raychaudhuri, S. K., & Raychaudhuri, S. P. (2012, Oct). IL-22 induced cell proliferation is regulated by PI3K/Akt/mTOR signaling cascade. *Cytokine, 60*(1), 38-42. https://doi.org/10.1016/j.cyto.2012.06.316

Montisci, A., Palmieri, V., Liu, J. E., Vietri, M. T., Cirri, S., Donatelli, F., & Napoli, C. (2021). Severe Cardiac Toxicity Induced by Cancer Therapies Requiring Intensive Care Unit Admission. *Front Cardiovasc Med, 8*, 713694. https://doi.org/10.3389/fcvm.2021.713694

Nakashima, N., Liu, D., Huang, C. L., Ueno, M., Zhang, X., & Yokomise, H. (2012, May). Wnt3 gene expression promotes tumor progression in non-small cell lung cancer. *Lung Cancer, 76*(2), 228-234. https://doi.org/10.1016/j.lungcan.2011.10.007

Nie, X., Liu, H., Liu, L., Wang, Y. D., & Chen, W. D. (2020). Emerging Roles of Wnt Ligands in Human Colorectal Cancer. *Front Oncol, 10*, 1341. https://doi.org/10.3389/fonc.2020.01341

Nitulescu, G. M., Van De Venter, M., Nitulescu, G., Ungurianu, A., Juzenas, P., Peng, Q., Olaru, O. T., Gradinaru, D., Tsatsakis, A., Tsoukalas, D., Spandidos, D. A., & Margina, D. (2018, Dec). The Akt pathway in oncology therapy and beyond (Review). *Int J Oncol, 53*(6), 2319-2331. https://doi.org/10.3892/ijo.2018.4597

O'Reilly, K. E., Rojo, F., She, Q.-B., Solit, D., Mills, G. B., Smith, D., Lane, H., Hofmann, F., Hicklin, D. J., Ludwig, D. L., Baselga, J., & Rosen, N. (2006). mTOR inhibition induces upstream receptor tyrosine kinase signaling and activates Akt. *Cancer research, 66*(3), 1500-1508. https://doi.org/10.1158/0008-5472.CAN-05-2925

Padmanaban, V., Krol, I., Suhail, Y., Szczerba, B. M., Aceto, N., Bader, J. S., & Ewald, A. J. (2019, Sep). E-cadherin is required for metastasis in multiple models of breast cancer. *Nature, 573*(7774), 439-444. https://doi.org/10.1038/s41586-019-1526-3

Park, S. Y., & Nam, J. S. (2020, Apr). The force awakens: metastatic dormant cancer cells. *Exp Mol Med, 52*(4), 569-581. https://doi.org/10.1038/s12276-020-0423-z

Patel, H. K., & Bihani, T. (2018, Jun). Selective estrogen receptor modulators (SERMs) and selective estrogen receptor degraders (SERDs) in cancer treatment. *Pharmacol Ther, 186*, 1-24. https://doi.org/10.1016/j.pharmthera.2017.12.012

Petrova, Y. I., Schecterson, L., & Gumbiner, B. M. (2016, Nov 1). Roles for E-cadherin cell surface regulation in cancer. *Mol Biol Cell, 27*(21), 3233-3244. https://doi.org/10.1091/mbc.E16-01-0058

Qu, F., Wang, L., Wang, C., Yu, L., Zhao, K., & Zhong, H. (2021, May 22). Circular RNA circ_0006168 enhances Taxol resistance in esophageal squamous cell carcinoma by regulating miR-194-5p/JMJD1C axis. *Cancer Cell Int, 21*(1), 273. https://doi.org/10.1186/s12935-021-01984-y

Radiation Therapy. (2022). Breast Cancer Foundation New Zealand. Retrieved 15/6/2022 from https://www.breastcancerfoundation.org.nz/breast-cancer/treatment-options/radiation-therapy

Ravi, R., Mookerjee, B., Bhujwalla, Z. M., Sutter, C. H., Artemov, D., Zeng, Q., Dillehay, L. E., Madan, A., Semenza, G. L., & Bedi, A. (2000, Jan 1). Regulation of tumor angiogenesis by p53-induced degradation of hypoxia-inducible factor 1alpha. *Genes Dev, 14*(1), 34-44.

Redman, M., King, A., Watson, C., & King, D. (2016, Aug). What is CRISPR/Cas9? *Arch Dis Child Educ Pract Ed, 101*(4), 213-215. https://doi.org/10.1136/archdischild-2016-310459

Reusser, N. M., Downing, C., Guidry, J., & Tyring, S. K. (2015, Jan 29). HPV Carcinomas in Immunocompromised Patients. *J Clin Med, 4*(2), 260-281. https://doi.org/10.3390/jcm4020260

Reymond, N., d'Água, B. B., & Ridley, A. J. (2013, Dec). Crossing the endothelial barrier during metastasis. *Nat Rev Cancer, 13*(12), 858-870. https://doi.org/10.1038/nrc3628

Rozengurt, E., Soares, H. P., & Sinnet-Smith, J. (2014). Suppression of feedback loops mediated by PI3K/mTOR induces multiple overactivation of compensatory pathways: an unintended consequence leading to drug resistance. *Molecular cancer therapeutics, 13*(11), 2477-2488. https://doi.org/10.1158/1535-7163.MCT-14-0330

Saha, M., & Das, S. (2021, Aug). Free radical induced activity of an anthracycline analogue and its Mn(II) complex on biological targets through in situ electrochemical generation of semiquinone. *Heliyon, 7*(8), e07746. https://doi.org/10.1016/j.heliyon.2021.e07746

Samarin, J., Laketa, V., Malz, M., Roessler, S., Stein, I., Horwitz, E., Singer, S., Dimou, E., Cigliano, A., Bissinger, M., Falk, C. S., Chen, X., Dooley, S., Pikarsky, E., Calvisi, D. F., Schultz, C.,

Schirmacher, P., & Breuhahn, K. (2016, Mar). PI3K/AKT/mTOR-dependent stabilization of oncogenic far-upstream element binding proteins in hepatocellular carcinoma cells. *Hepatology, 63*(3), 813-826. https://doi.org/10.1002/hep.28357

Saxton, R. A., & Sabatini, D. M. (2017, Apr 6). mTOR Signaling in Growth, Metabolism, and Disease. *Cell, 169*(2), 361-371. https://doi.org/10.1016/j.cell.2017.03.035

Schoemmel, M., Loeser, H., Kraemer, M., Wagener-Ryczek, S., Hillmer, A., Bruns, C., Thelen, M., Schröder, W., Zander, T., Lechner, A., Buettner, R., Schlösser, H., Gebauer, F., & Quaas, A. (2021, Aug). Distribution of tumor-infiltrating-T-lymphocytes and possible tumor-escape mechanisms avoiding immune cell attack in locally advanced adenocarcinomas of the esophagus. *Clin Transl Oncol, 23*(8), 1601-1610. https://doi.org/10.1007/s12094-021-02556-2

Siu, M. K., Tsai, Y. C., Chang, Y. S., Yin, J. J., Suau, F., Chen, W. Y., & Liu, Y. N. (2015, Sep 3). Transforming growth factor-beta promotes prostate bone metastasis through induction of microRNA-96 and activation of the mTOR pathway. *Oncogene, 34*(36), 4767-4776. https://doi.org/10.1038/onc.2014.414

Slomovitz, B. M., & Coleman, R. L. (2012, Nov 1). The PI3K/AKT/mTOR pathway as a therapeutic target in endometrial cancer. *Clin Cancer Res, 18*(21), 5856-5864. https://doi.org/10.1158/1078-0432.Ccr-12-0662

Song, L., Dai, Z., Zhang, S., Zhang, H., Liu, C., Ma, X., Liu, D., Zan, Y., & Yin, X. (2018, Sep 26). MicroRNA-1179 suppresses cell growth and invasion by targeting sperm-associated antigen 5-mediated Akt signaling in human non-small cell lung cancer. *Biochem Biophys Res Commun, 504*(1), 164-170. https://doi.org/10.1016/j.bbrc.2018.08.149

Sosa, V., Moline, T., Somoza, R., Paciucci, R., Kondoh, H., & ME, L. L. (2013, Jan). Oxidative stress and cancer: an overview. *Ageing Res Rev, 12*(1), 376-390. https://doi.org/10.1016/j.arr.2012.10.004

Spoerke, J. M., O'Brien, C., Huw, L., Koeppen, H., Fridlyand, J., Brachmann, R. K., Haverty, P. M., Pandita, A., Mohan, S., Sampath, D., Friedman, L. S., Ross, L., Hampton, G. M., Amler, L. C., Shames, D. S., & Lackner, M. R. (2012, Dec 15). Phosphoinositide 3-kinase (PI3K) pathway alterations are associated with histologic subtypes and are predictive of sensitivity to PI3K inhibitors in lung cancer preclinical models. *Clin Cancer Res, 18*(24), 6771-6783. https://doi.org/10.1158/1078-0432.CCR-12-2347

Strilic, B., & Offermanns, S. (2017, Sep 11). Intravascular Survival and Extravasation of Tumor Cells. *Cancer Cell, 32*(3), 282-293. https://doi.org/10.1016/j.ccell.2017.07.001

Sudarsanam, S., & Johnson, D. E. (2010, Jan). Functional consequences of mTOR inhibition. *Curr Opin Drug Discov Devel, 13*(1), 31-40.

Sun, J. M., Kim, J. R., Do, I. G., Lee, S. Y., Lee, J., Choi, Y. L., Ahn, J. S., Ahn, M. J., & Park, K. (2013, Sep 17). A phase-1b study of everolimus plus paclitaxel in patients with small-cell lung cancer. *Br J Cancer, 109*(6), 1482-1487. https://doi.org/10.1038/bjc.2013.467

Tan, E. P., Duncan, F. E., & Slawson, C. (2017). The sweet side of the cell cycle. *Biochemical Society transactions, 45*(2), 313-322. https://doi.org/10.1042/BST20160145

Tauriello, D. V. F., Palomo-Ponce, S., Stork, D., Berenguer-Llergo, A., Badia-Ramentol, J., Iglesias, M., Sevillano, M., Ibiza, S., Cañellas, A., Hernando-Momblona, X., Byrom, D., Matarin, J. A., Calon, A., Rivas, E. I., Nebreda, A. R., Riera, A., Attolini, C. S.-O., & Batlle, E. (2018, 2018/02/01). TGFβ drives immune evasion in genetically reconstituted colon cancer metastasis. *Nature, 554*(7693), 538-543. https://doi.org/10.1038/nature25492

Thedieck, K., Holzwarth, B., Prentzell, M. T., Boehlke, C., Kläsener, K., Ruf, S., Sonntag, A. G., Maerz, L., Grellscheid, S. N., Kremmer, E., Nitschke, R., Kuehn, E. W., Jonker, J. W., Groen, A. K., Reth, M., Hall, M. N., & Baumeister, R. (2013, Aug 15). Inhibition of mTORC1 by astrin and stress granules prevents apoptosis in cancer cells. *Cell, 154*(4), 859-874. https://doi.org/10.1016/j.cell.2013.07.031

Thein, K. H., Kleylein-Sohn, J., Nigg, E. A., & Gruneberg, U. (2007, Jul 30). Astrin is required for the maintenance of sister chromatid cohesion and centrosome integrity. *J Cell Biol, 178*(3), 345-354. https://doi.org/10.1083/jcb.200701163

Thorpe, P. E., Knight, S. C., & Farrant, J. (1976, Apr). Optimal conditions for the preservation of mouse lymph node cells in liquid nitrogen using cooling rate techniques. *Cryobiology, 13*(2), 126-133. https://doi.org/10.1016/0011-2240(76)90123-1

Tolaney, S. M., Tayob, N., Dang, C., Yardley, D. A., Isakoff, S. J., Valero, V., Faggen, M., Mulvey, T., Bose, R., Hu, J., Weckstein, D., Wolff, A. C., Reeder-Hayes, K., Rugo, H. S., Ramaswamy, B., Zuckerman, D., Hart, L., Gadi, V. K., Constantine, M., Cheng, K., Briccetti, F., Schneider, B., Garrett, A. M., Marcom, K., Albain, K., DeFusco, P., Tung, N., Ardman, B., Nanda, R., Jankowitz, R. C., Rimawi, M., Abramson, V., Pohlmann, P. R., Van Poznak, C., Forero-Torres, A., Liu, M., Ruddy, K., Zheng, Y., Rosenberg, S. M., Gelber, R. D., Trippa, L., Barry, W., DeMeo, M., Burstein, H., Partridge, A., Winer, E. P., & Krop, I. (2021, Jul 20). Adjuvant Trastuzumab Emtansine Versus Paclitaxel in Combination With Trastuzumab for Stage I HER2-Positive Breast Cancer (ATEMPT): A Randomized Clinical Trial. *J Clin Oncol, 39*(21), 2375-2385. https://doi.org/10.1200/jco.20.03398

Toulany, M., Maier, J., Iida, M., Rebholz, S., Holler, M., Grottke, A., Juker, M., Wheeler, D. L., Rothbauer, U., & Rodemann, H. P. (2017). Akt1 and Akt3 but not Akt2 through interaction with DNA-PKcs stimulate proliferation and post-irradiation cell survival of K-RAS-mutated cancer cells. *Cell Death Discov, 3*, 17072. https://doi.org/10.1038/cddiscovery.2017.72

Trieu, P. D. Y., Mello-Thoms, C. R., Barron, M. L., & Lewis, S. J. (2022). Look how far we have come: BREAST cancer detection education on the international stage. *Front Oncol, 12*, 1023714. https://doi.org/10.3389/fonc.2022.1023714

Trybek, T., Kowalik, A., Góźdź, S., & Kowalska, A. (2020, Aug). Telomeres and telomerase in oncogenesis. *Oncol Lett, 20*(2), 1015-1027. https://doi.org/10.3892/ol.2020.11659

Vajdic, C. M., & van Leeuwen, M. T. (2009, Oct 15). Cancer incidence and risk factors after solid organ transplantation. *Int J Cancer, 125*(8), 1747-1754. https://doi.org/10.1002/ijc.24439

Välk, K., Vooder, T., Kolde, R., Reintam, M. A., Petzold, C., Vilo, J., & Metspalu, A. (2010). Gene expression profiles of non-small cell lung cancer: survival prediction and new biomarkers. *Oncology, 79*(3-4), 283-292. https://doi.org/10.1159/000322116

Vinay, D. S., Ryan, E. P., Pawelec, G., Talib, W. H., Stagg, J., Elkord, E., Lichtor, T., Decker, W. K., Whelan, R. L., Kumara, H., Signori, E., Honoki, K., Georgakilas, A. G., Amin, A., Helferich, W. G., Boosani, C. S., Guha, G., Ciriolo, M. R., Chen, S., Mohammed, S. I., Azmi, A. S., Keith, W. N., Bilsland, A., Bhakta, D., Halicka, D., Fujii, H., Aquilano, K., Ashraf, S. S., Nowsheen, S., Yang, X., Choi, B. K., & Kwon, B. S. (2015, Dec). Immune evasion in cancer: Mechanistic basis and therapeutic strategies. *Semin Cancer Biol, 35 Suppl*, S185-s198. https://doi.org/10.1016/j.semcancer.2015.03.004

Vousden, K. H., & Lane, D. P. (2007, Apr). p53 in health and disease. *Nat Rev Mol Cell Biol, 8*(4), 275-283. https://doi.org/10.1038/nrm2147

Waks, A. G., & Winer, E. P. (2019, Jan 22). Breast Cancer Treatment: A Review. *Jama, 321*(3), 288-300. https://doi.org/10.1001/jama.2018.19323

Wang, G., Jiang, Y., Lu, C., Jiang, W., Wu, S., & Hua, Y. (2021, Dec 13). CircFOXM1 promotes proliferation and metastasis of hepatocellular carcinoma via regulating miR-1179/SPAG5 axis. *Sci Rep, 11*(1), 23890. https://doi.org/10.1038/s41598-021-03285-w

Wang, H. S., Nie, X., Wu, R. B., Yuan, H. W., Ma, Y. H., Liu, X. L., Zhang, J. Y., Deng, X. L., Na, Q., Jin, H. Y., Bian, Y. C., Gao, Y. M., Wang, Y. D., & Chen, W. D. (2016). Downregulation of human Wnt3 in gastric cancer suppresses cell proliferation and induces apoptosis. *Onco Targets Ther, 9*, 3849-3860. https://doi.org/10.2147/ott.S101782

Wang, L., Cao, L., Wen, C., Li, J., Yu, G., & Liu, C. (2020, Jan). LncRNA LINC00857 regulates lung adenocarcinoma progression, apoptosis and glycolysis by targeting miR-1179/SPAG5 axis. *Hum Cell, 33*(1), 195-204. https://doi.org/10.1007/s13577-019-00296-8

Wang, T., Li, K., Song, H., Xu, D., Liao, Y., Jing, B., Guo, W., Hu, M., Kuang, Y., Sun, B., Ling, J., Zhang, T., Xu, J., Yao, F., & Deng, J. (2019, May 28). p53 suppression is essential for oncogenic SPAG5 upregulation in lung adenocarcinoma. *Biochem Biophys Res Commun, 513*(2), 319-325. https://doi.org/10.1016/j.bbrc.2019.03.198

Weigelt, B., Mackay, A., A'Hern, R., Natrajan, R., Tan, D. S., Dowsett, M., Ashworth, A., & Reis-Filho, J. S. (2010, Apr). Breast cancer molecular profiling with single sample predictors: a

retrospective analysis. *Lancet Oncol, 11*(4), 339-349. https://doi.org/10.1016/s1470-2045(10)70008-5

Wong, C. H., Loong, H. H., Hui, C. W., Lau, C. P., Hui, E. P., Ma, B. B., & Chan, A. T. (2013, Dec). Preclinical evaluation of the PI3K-mTOR dual inhibitor PF-04691502 as a novel therapeutic drug in nasopharyngeal carcinoma. *Invest New Drugs, 31*(6), 1399-1408. https://doi.org/10.1007/s10637-013-0007-z

Wu, Y., Ginther, C., Kim, J., Mosher, N., Chung, S., Slamon, D., & Vadgama, J. V. (2012, Dec). Expression of Wnt3 activates Wnt/beta-catenin pathway and promotes EMT-like phenotype in trastuzumab-resistant HER2-overexpressing breast cancer cells. *Mol Cancer Res, 10*(12), 1597-1606. https://doi.org/10.1158/1541-7786.MCR-12-0155-T

Xue, J., Tarnasky, H. A., Rancourt, D. E., & van Der Hoorn, F. A. (2002, Apr). Targeted disruption of the testicular SPAG5/deepest protein does not affect spermatogenesis or fertility. *Mol Cell Biol, 22*(7), 1993-1997. https://doi.org/10.1128/mcb.22.7.1993-1997.2002

Yan, H., Wang, S., Yu, H., Zhu, J., & Chen, C. (2013). Molecular pathways and functional analysis of miRNA expression associated with paclitaxel-induced apoptosis in hepatocellular carcinoma cells. *Pharmacology, 92*(3-4), 167-174. https://doi.org/10.1159/000354585

Yang, T., Tian, S., Wang, L., Wang, Y., & Zhao, J. (2020, Apr). MicroRNA-367-3p overexpression represses the proliferation and invasion of cervical cancer cells through downregulation of SPAG5-mediated Wnt/beta-catenin signalling. *Clin Exp Pharmacol Physiol, 47*(4), 687-695. https://doi.org/10.1111/1440-1681.13222

Yang, Y. C., Hsu, Y. T., Wu, C. C., Chen, H. T., & Chang, M. S. (2006, May 5). Silencing of astrin induces the p53-dependent apoptosis by suppression of HPV18 E6 expression and sensitizes cells to paclitaxel treatment in HeLa cells. *Biochem Biophys Res Commun, 343*(2), 428-434. https://doi.org/10.1016/j.bbrc.2006.02.166

Yang, Y. F., Zhang, M. F., Tian, Q. H., Fu, J., Yang, X., Zhang, C. Z., & Yang, H. (2018, Aug 8). SPAG5 interacts with CEP55 and exerts oncogenic activities via PI3K/AKT pathway in hepatocellular carcinoma. *Mol Cancer, 17*(1), 117. https://doi.org/10.1186/s12943-018-0872-3

Yersal, O., & Barutca, S. (2014, Aug 10). Biological subtypes of breast cancer: Prognostic and therapeutic implications. *World J Clin Oncol, 5*(3), 412-424. https://doi.org/10.5306/wjco.v5.i3.412

Ying, Z., Yang, J., Li, W., Wang, X., Zhu, Z., Jiang, W., Li, C., & Sha, O. (2020, 2020-August-28). Astrin: A Key Player in Mitosis and Cancer [Mini Review]. *Frontiers in Cell and Developmental Biology, 8*. https://doi.org/10.3389/fcell.2020.00866

Yokoyama, W. M., Thompson, M. L., & Ehrhardt, R. O. (2012, Nov). Cryopreservation and thawing of cells. *Curr Protoc Immunol, Appendix 3*, 3g. https://doi.org/10.1002/0471142735.ima03gs99

Yousefi, H., Vatanmakanian, M., Mahdiannasser, M., Mashouri, L., Alahari, N. V., Monjezi, M. R., Ilbeigi, S., & Alahari, S. K. (2021, Feb). Understanding the role of integrins in breast cancer invasion, metastasis, angiogenesis, and drug resistance. *Oncogene, 40*(6), 1043-1063. https://doi.org/10.1038/s41388-020-01588-2

Yuan, L. J., Li, J. D., Zhang, L., Wang, J. H., Wan, T., Zhou, Y., Tu, H., Yun, J. P., Luo, R. Z., Jia, W. H., & Zheng, M. (2014, May 22). SPAG5 upregulation predicts poor prognosis in cervical cancer patients and alters sensitivity to taxol treatment via the mTOR signaling pathway. *Cell Death Dis, 5*(5), e1247. https://doi.org/10.1038/cddis.2014.222

Zakrzewski, W., Dobrzyński, M., Szymonowicz, M., & Rybak, Z. (2019, 2019/02/26). Stem cells: past, present, and future. *Stem Cell Research & Therapy, 10*(1), 68. https://doi.org/10.1186/s13287-019-1165-5

Zhang, C., Awasthi, N., Schwarz, M. A., & Schwarz, R. E. (2013, Nov). The dual PI3K/mTOR inhibitor NVP-BEZ235 enhances nab-paclitaxel antitumor response in experimental gastric cancer. *Int J Oncol, 43*(5), 1627-1635. https://doi.org/10.3892/ijo.2013.2099

Zhang, H., Li, S., Yang, X., Qiao, B., Zhang, Z., & Xu, Y. (2016, Apr 1). miR-539 inhibits prostate cancer progression by directly targeting SPAG5. *J Exp Clin Cancer Res, 35*, 60. https://doi.org/10.1186/s13046-016-0337-8

Zhang, H., Lin, X., Huang, Y., Wang, M., Cen, C., Tang, S., Dique, M. R., Cai, L., Luis, M. A., Smollar, J., Wan, Y., & Cai, F. (2021). Detection Methods and Clinical Applications of Circulating Tumor Cells in Breast Cancer. *Front Oncol, 11*, 652253. https://doi.org/10.3389/fonc.2021.652253

Zhang, M., Sha, L., Hou, N., Shi, C., & Tan, L. (2020, Feb 28). High expression of sperm-associated antigen 5 correlates with poor survival in ovarian cancer. *Biosci Rep, 40*(2). https://doi.org/10.1042/bsr20193087

Zhang, M., Zhang, L., Hei, R., Li, X., Cai, H., Wu, X., Zheng, Q., & Cai, C. (2021). CDK inhibitors in cancer therapy, an overview of recent development. *Am J Cancer Res, 11*(5), 1913-1935.

Zhao, G. X., Pan, H., Ouyang, D. Y., & He, X. H. (2015, Jun). The critical molecular interconnections in regulating apoptosis and autophagy. *Ann Med, 47*(4), 305-315. https://doi.org/10.3109/07853890.2015.1040831

Zhao, Y., Sfeir, A. J., Zou, Y., Buseman, C. M., Chow, T. T., Shay, J. W., & Wright, W. E. (2009, Aug 7). Telomere extension occurs at most chromosome ends and is uncoupled from fill-in in human cancer cells. *Cell, 138*(3), 463-475. https://doi.org/10.1016/j.cell.2009.05.026